A GEOLOGICAL STUDY OF THE RIVER RANCH KIMBERLITE PIPE AND ASSOCIATED DIAMONDS AND MANTLE MINERALS: LIMPOPO MOBILE BELT, ZIMBABWE

by
MIRACLE MUUSHA

Thesis submitted in fulfilment
of the requirements for the degree of
Master of Science

Department of Geological Sciences
University of Cape Town
South Africa

December, 1997

DECLARATION

I hereby declare that, apart from the normal guidance from my supervisor, the work presented in this thesis is my own, except where otherwise stated in the text.

Signed by candidate
Signature Removed

Miracle Muusha
December, 1997.

CONTENTS

FIGURES

TABLES

PLATES

APPENDICES

CHAPTER 4:

Appendix 4.1 River Ranch diamonds, morphology and colour distributions per size fraction
Appendix 4.2 Diamond colour intensity variations
Appendix 4.3 Diamond inclusion and fracture intensity variations

CHAPTER 5:

Appendix 5.1 The Electron Microprobe: conditions, standards and detection limits
Appendix 5.2 River Ranch concentrate garnet analyses
Appendix 5.3 Concentrate low-Cr garnet macrocryst analyses
Appendix 5.4 Concentrate chromite analyses
Appendix 5.5 Concentrate clinopyroxene analyses
Appendix 5.6 Concentrate megacryst analyses

CHAPTER 6:

Appendix 6.1 River Ranch xenolith mineral analyses

ABSTRACT

The River Ranch kimberlite is a 5.2 hectare diatreme from which the original surficial crater facies material has been removed by erosion. Proof of the prior existence of such a feature is provided by down rafted blocks of epiclastic and pyroclastic rocks exposed in the diatreme during open pit mining operations.

Six intrusive kimberlite phases have been recognised in the diatreme by careful mapping and confirmed by petrographic observations, particularly variations in groundmass mineralogy. Subsequent to emplacement, the diatreme has been cut by intrusive tholeitic dolerites of apparently Karoo age.

The River Ranch occurrence is classified as a Group I kimberlite although the definitive isotopic evidence is lacking due to pervasive alteration of the exposed rocks. The absence of megacrystic and groundmass ilmenite and the presence of groundmass diopside are unusual for the group of rocks. However the presence of monticellite and the low abundance of phlogopite argue against a Group II classification.

The overwhelmingly peridotitic nature of the mantle mineral macrocrysts in the kimberlite is consistent with the observations of Kopylova et al (1995) that the diamonds at River Ranch are predominantly peridotitic and are likely to have formed in a single process. The approximate equilibration temperature for a small suite of coarse grained lherzolite from the kimberlites is 1200°C, suggesting a geothermal gradient rather higher than seen in the Kaap-Vaal craton.

The diamonds at River Ranch are predominantly brown, strongly resorbed and have less than average value. It is predicted that a combination of kimberlite petrography, micro-diamond measurements and mantle macrocryst studies should be a valuable aid to grade control and mine planning.

1. INTRODUCTION

1.1 BACKGROUND

The River Ranch kimberlite pipe was discovered in 1974. An alluvial diamond discovered in a stream draining the kimberlite in 1972 by Kimberlitic Searches (a wholly owned subsidiary of De Beers) was followed up and eventually led to the discovery of the pipe two years later. The pipe is situated about 12.5km west-north-west of Beitbridge town in Zimbabwe (Figure 1.1). The pipe was briefly sampled but not developed at that time.

Ownership of the whole prospect changed hands in 1991. Auridiam Zimbabwe (Pvt) Ltd has now developed the deposit into an operating mine under a Special Grant awarded by the Zimbabwe Government. River Ranch Mine has undergone a three phase development stage under Auridiam Zimbabwe (Pvt) Ltd. The Phase I stage was the commissioning in February 1992 of a 30 tonnes per hour (tph) pan plant consisting of three 10 ft. rotary pans. The Phase II stage saw the commissioning of a 120 tph Heavy Media Separation (HMS) plant in March 1994. Phase III, which was the upgrading of the Phase II plant into a 200 tph plant consisting of an HMS and a rotary pan section, was commissioned in September 1995. The kimberlite is a medium grade ore body with a lower than average value diamond production.

1.2 GEOLOGICAL SETTING

The pipe is situated in the Central Zone of the Limpopo Mobile Belt, a zone of high grade metamorphism between the Zimbabwean and the Kaapvaal cratons. Clifford (1966) noted that economically diamondiferous kimberlites occur within old cratons, that is, areas that have been tectonically stable for at least 1500 Ma. The Limpopo Mobile Belt has been tectonically stable for more than 1800 Ma. The well mineralised Venetia kimberlites in South Africa and other diamondiferous bodies such as The Oaks and Martins Drift also intrude the Limpopo Mobile Belt. (Figure 1.1). Further interest in this area has been generated by the recent discovery by De Beers of a 17 hectare pipe about 100km north-east of River Ranch.

Fig 1.1 **Southern African Kimberlites and Alluvial Diamond Deposits**

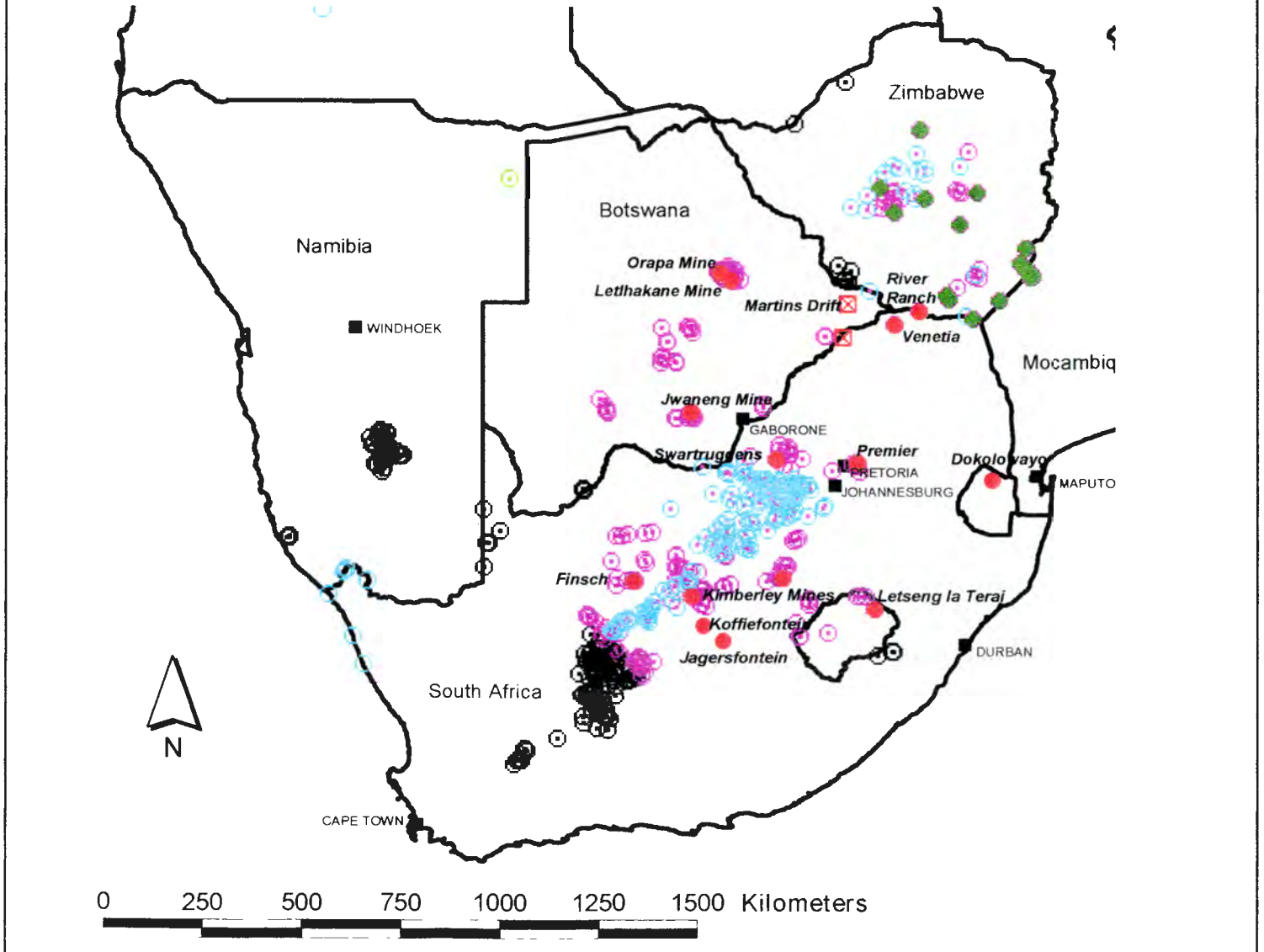

LEGEND:

- Country Borders
- Mined Kimberlite
- Diamondiferous Alluvial Deposits
- Miscellaneous Diamond Recoveries
- Non Diamondiferous Kimberlite
- Diamondiferous Kimberlite
- Kimberlite (Status Unknown)
- Kimberlite Prospect

Produced on the Mineral Services GIS
Date: 21 August 1996
Projection Geographic
Datum WGS84

The River Ranch pipe intrudes Archean metasediments of the Beitbridge Group (Watkeys, 1979) and a diabase of at least Waterberg (c. 1800 Ma) in age. It is in turn intruded by Karoo dolerite dykes (c. 170 Ma). The earliest attempts to date the kimberlite (Kramers and Smith, 1983) using U-Pb and Pb-Pb isotopes produced discrepant ages: 430 +/- 6 Ma and 740 + 260 /- 310 Ma respectively. It is apparent the agreement between the two dating methods is poor. The Pb-Pb age, although subject to inherently large experimental errors was considered by Kramers and Smith as the most reliable. Mica suitable for Rb-Sr dating has not been found. The Venetia cluster which occurs approximately 60km away from River Ranch has a Rb-Sr phlogopite whole rock age of 533 +/- 4 Ma (Allsopp et al, 1995). It is considered likely that the pre-Karoo River Ranch kimberlite is similar in age to the Venetia kimberlites.

1.3 SCOPE AND AIMS OF THIS SUDY

Compared to other diamond operations worldwide, River Ranch is a medium sized operation. The mine processes about one and half million tonnes of ore and produces about half a million (500 000) carats of diamonds per annum.

For a medium size and grade kimberlite ore body like River Ranch which has a lower than average value diamond production, efficient planning of the mining operation is absolutely essential if meaningful returns are to be realised. This can be achieved by putting in place a sound database from which variations in grade, size distribution and value of the diamonds can be predicted within the whole kimberlite. The main aim of this project is to set up the framework for such a database that could be used for future planning and optimisation of the whole mining operation.

Routine mining and a bulk sampling exercise carried out in June/July 1995 has shown that there is a variation in the diamond content amongst the different intrusive phases. Changes in lateral extent with depth of the phases would have an impact on the overall grade of the pipe. In working towards building the necessary reference framework for the future, this project aims to identify and describe all the discrete intrusive phases that comprise the kimberlite pipe and to establish their inter-relationships through surface mapping and petrographic studies.

A further aim of the project is to study the physical characteristics (i.e. mass, size, morphology and colour) of the diamonds and to investigate any trends that might be apparent in the entire diamond population.

Within the same framework, the project also aims at establishing the range in mineral chemistry of the garnets and chromites associated with the diamonds. The chemistry of these garnets and chromites often reflect the diamond potential of the source (eg. Gurney, 1984).

1.4 RESTRICTIVE CONDITIONS

The main problem encountered in the study was the weathered nature of the kimberlite. The freshest available samples for petrographic studies were selected from borehole cores. However a limited number of boreholes have been drilled and all the intrusive phases were not intersected by drilling. All the xenoliths found were extensively altered. No fresh olivine or orthopyroxene could be obtained for analysis, either from xenoliths or as macrocrysts.

2. REGIONAL GEOLOGY AND FIELD DESCRIPTION

2.1 INTRODUCTION

The Limpopo Mobile Belt has been subdivided into three zones (Cox et al, 1965; Mason, 1973,) namely:

1. The Northern Marginal Zone (NMZ)
2. The Central Zone (CZ)
3. The Southern Marginal Zone (SMZ)

The Mobile Belt is an ENE - WSW trending zone of late Archean granulite-facies tectonites separating the low grade granitoid -greenstone terranes of the Zimbabwe and Kaapvaal Cratons (Figure 2.1). The fault bounded Central Zone is of particular interest to this study as it hosts several known intrusive diamondiferous kimberlite localities in the Limpopo Mobile Belt including River Ranch.

The Limpopo Mobile Belt has a long and complex deformational history. Several theories and models relating to this history have been put forward (eg. Watkeys, 1984; McCourt and Vearncombe, 1987; Barton et al, 1990; Roering et al, 1992 and Treloar et al, 1992). Although some of the theories and models differ in detail, the general picture can be deciphered. In this chapter, the regional geology of the mobile belt is reviewed in the context of some of these theories. An attempt is made to focus into the local geology around the River Ranch kimberlite from this regional picture.

2.2 DEFORMATIONAL HISTORY OF THE LIMPOPO MOBILE BELT

The NMZ which is composed of granite-greenstone rocks at granulite grade of metamorphism, is separated from the granite-greenstone terrane of the Zimbabwe Craton by a southerly dipping shear zone with down-dip lineations (Coward, 1983). To the south the NMZ is separated from the supracrustal meta-sedimentary sequence of the CZ by a southerly - dipping Tuli - Sabi/Triangle Shear Zone (Figure 2.1). The CZ is in turn separated from granulite grade, granite-greenstone rocks of the SMZ by the Palala Shear Zone (McCourt and Vearncombe,

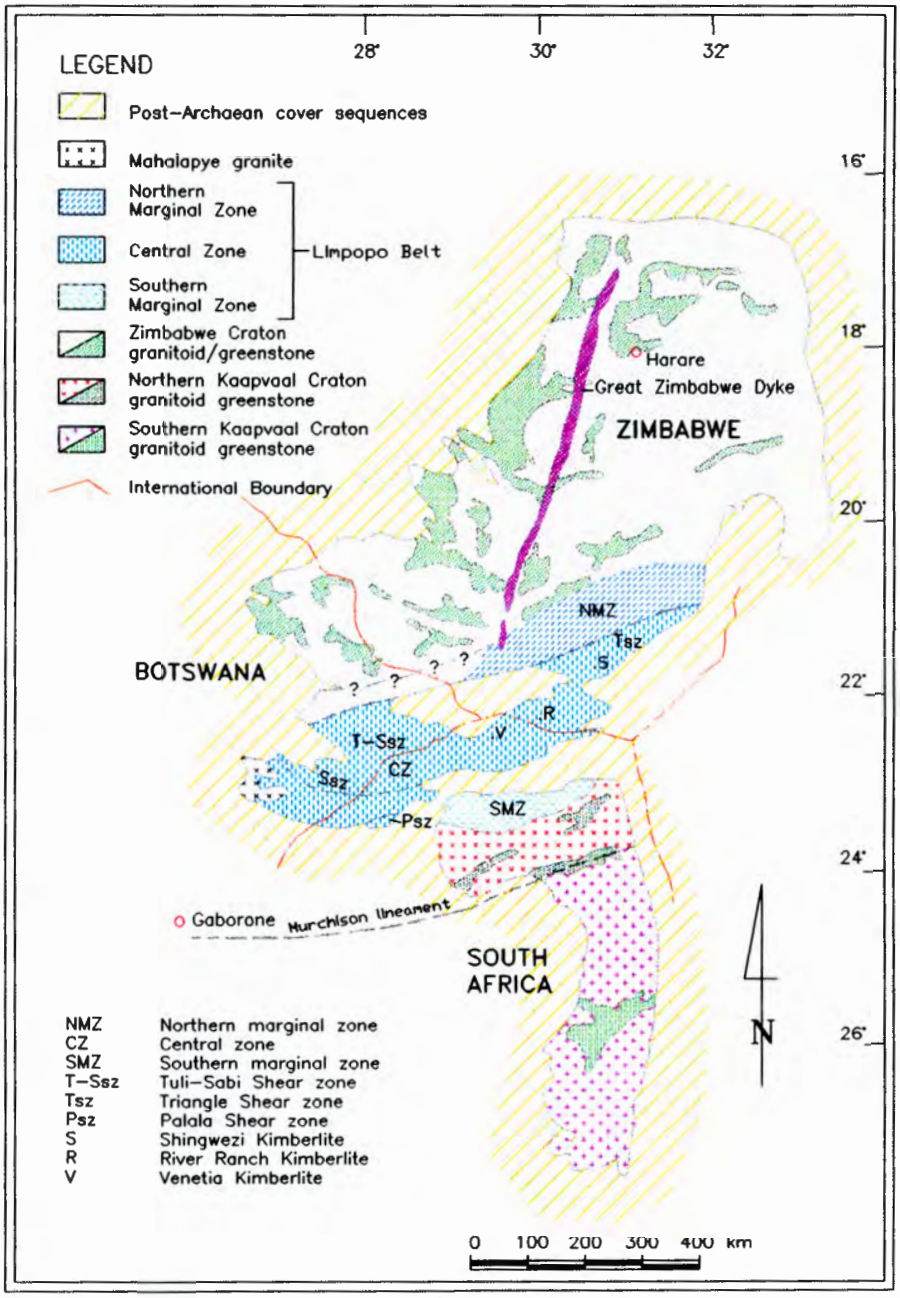

Fig 2.1 Geological outline of the Limpopo Mobile Belt and adjoining Cratons (after McCourt and Vearncombe, 1992)

1987).

MacGregor (1953) defined the Limpopo Mobile Belt as the deeply eroded roots of a mountain, chain and termed the process responsible for the deformation and metamorphism to be the Limpopo Orogeny.

Watkeys (1984) proposed that the CZ was an exotic crustal block which first collided with the Zimbabwe Craton at 2700 Ma and that these two crustal blocks were subsequently juxtaposed adjacent to the Kaapvaal Craton along the Palala Shear Zone at c. 1900 Ma. This was subsequently supported by Barton et al (1990) on the basis of anomalously large $^{238}U/^{204}Pb$ ratios and the presence of 3000 Ma deformed mafic dykes. The 3000 Ma mafic dykes show evidence that they were emplaced at upper crustal levels between at least two orogenic events. The first event involved metamorphism at at least amphibolite grade conditions. The second event was probably the 2700 Ma Limpopo orogeny. This implies that the rocks of the CZ have evolved along at least two P-T-time loops. This deformational history together with the Pb isotopic evidence is not recorded in the adjacent NMZ and SMZ granulite rocks and makes the CZ a unique exotic block.

Alternatively McCourt and Vearncombe (1987) proposed that the Limpopo Orogeny was a result of one crustal block, the CZ, colliding with the combined Zimbabwe and Kaapvaal Cratons and that the Palala and the Tuli-Sabi/Triangle Shear Zones acted as lateral ramps during this collision. Roering et al (1992) argued that the Tuli-Sabi/Triangle Shear Zone dips underneath the CZ and is a structure on which the CZ was thrust over the Zimbabwe Craton.

From this it is therefore not certain whether the CZ was an independent crustal block caught up in the collision event of the two Cratons or whether it was already attached to the Kaapvaal Craton by an earlier tectonic event.

Treloar et al (1992) noted that the Tuli-Sabi/Triangle Shear Zone and the Palala Shear Zone both have sub-horizontal stretching lineations and show a dextral and sinistral strike-slip movement respectively. They noted that the CZ must have moved west-south-west relative to

adjacent terrains during at least two periods of deformation and that there was general continental accretion and migration north-westward over a long period of time from the Kaapvaal Craton to the Zimbabwe Craton. Both Cratons and the CZ were accreted into a single tectonic unit by 2850 Ma. In this sense the CZ therefore fits in with Clifford's rule (1966) which recognizes that all economically diamondiferous kimberlites occur within old cratons, ie. areas that have been tectonically stable for at least 1500 Ma.

2.3 GEOLOGY OF THE AREA AROUND RIVER RANCH

The oldest rocks in the region around River Ranch are banded migmatitic gneisses of early Precambrian age. Overlying these old gneisses are formations of metasediments which were deposited in shallow sedimentary basins between 3600 Ma and 3200 Ma (Watkeys, 1979). These formations constitute the Beitbridge Group. The Beitbridge Group rocks are in turn intruded by the Bulai gneiss (c. 2690 Ma.), amphibolite and diabase dykes (c. 1800 Ma), (Watkeys, 1979) and the kimberlites (c. 533 Ma, Allsopp et al, 1995). This was followed by a major period of erosion, the unconformable deposition of Karoo sediments and later intrusion by dolerite dykes (c. 170 Ma). Since then a major period of erosion has taken place and there are no signs of relict Karoo sediments in the immediate vicinity of River Ranch. Table 2.1 summarises the geological formations and events. In the vicinity of the River Ranch kimberlite, the Diti Formation is widely exposed while the Nulli Formation lithologies are absent (see Table 2.1).

2.3.1 The Diti Formation

The Diti Formation is the basal unit of the Beitbridge Group and is comprised of garnetiferous gneisses, feldspathic gneisses, biotite-rich gneisses, calc-silicate rocks and thin bands of quartzites that are developed within the paragneisses. Lithological field mapping of these paragneisses has shown that contacts between the different gneisses are often gradational and certain lithologies, may be difficult to distinguish. The calc-silicate rocks have formed conspicuously erosion resistant hills around River Ranch. The Diti Formation is intruded by the River Ranch kimberlite and by at least three ages of dykes (Figure 2.2).

LITHOLOGY	AGE
RECENT	
Soils, alluvium, calcrete and ferricrete	
KAROO SYSTEM Dolerite: feeder dykes along fractures Forest Sandstone 80 - 100m thick Red Beds ~ 300m Escarpment Grit up to 15m	Upper Carb-Triassic
---------- minor unconformity Fulton's Drift Mudstone 50 - 120m Basal Beds	
----------major unconformity	
KIMBERLITE	~ 500 m.y.
DIABASE AND AMPHIBOLITIES Intrusive contacts	~ 1850 - 1800 m.y.
BULAI GNEISS Intrusive contacts	~ 2690 m.y.
BEITBRIDGE GROUP Nulli Formation: quartzites, calc silicates and ultramafics Diti Formation : paragneisses, quartzites, calc silicates	Early Precambrian
MACUVILLE GROUP Banded migmatitic gneisses	Early Precambrian

Table 2.1 Summary of geological formations and Events (After Watkeys, 1979)

2.3.2 The Bulai Gneisses

The Bulai gneiss is an intrusive granitic body which generally occupies an antiformal structure in the Beitbridge Group rocks. In the vicinity of River Ranch it occurs to the east of the kimberlite pipe (Figure 2.2). The granite body has formed a contact metamorphic aureole within the enclosing paragneisses which has resulted in the development of quartz and plagioclase aggregates from partial melting.

2.3.3 The Dykes

Dolerite dykes have intruded the extensive fracture system in the region (Figure 2.2). The dykes range in age from Waterberg (c. 1800 Ma) to post kimberlite emplacement, probably Karoo (c. 170 Ma). There are two types of older dykes which pre-date the kimberlite. One set is an older amphibolite dyke which is probably a metamorphosed dolerite while the other seems to be younger than the amphibolite and is an unmetamorphosed diabase. Both these sets fall within the Waterberg age of emplacement. The youngest dykes have intruded the kimberlite. At least two of these have been exposed so far during mining of the kimberlite (Plate 2.10).

2.3.4 Karoo Sediments

No Karoo sediments exist in the immediate vicinity of River Ranch. Karoo sediments have been mapped about 40km west of River Ranch in what has been interpreted as down-faulted synclines (Watkeys, 1979). The Karoo sequence in this area is about 400-500m thick.

2.3.5 Structure

There are two dominant fracture trends in the area, the 050°-060° trend and the 095°- 110° trend along which the dolerite dykes have been intruded. A stereoplot of the foliation measurements taken around River Ranch (Figure 2.3) shows that most foliation trends are steeply dipping to the south and southeast. Few trends have a northerly dip. The kimberlite pipe was emplaced at the intersection of the two dominant trends with the long axis on the 095° trend.

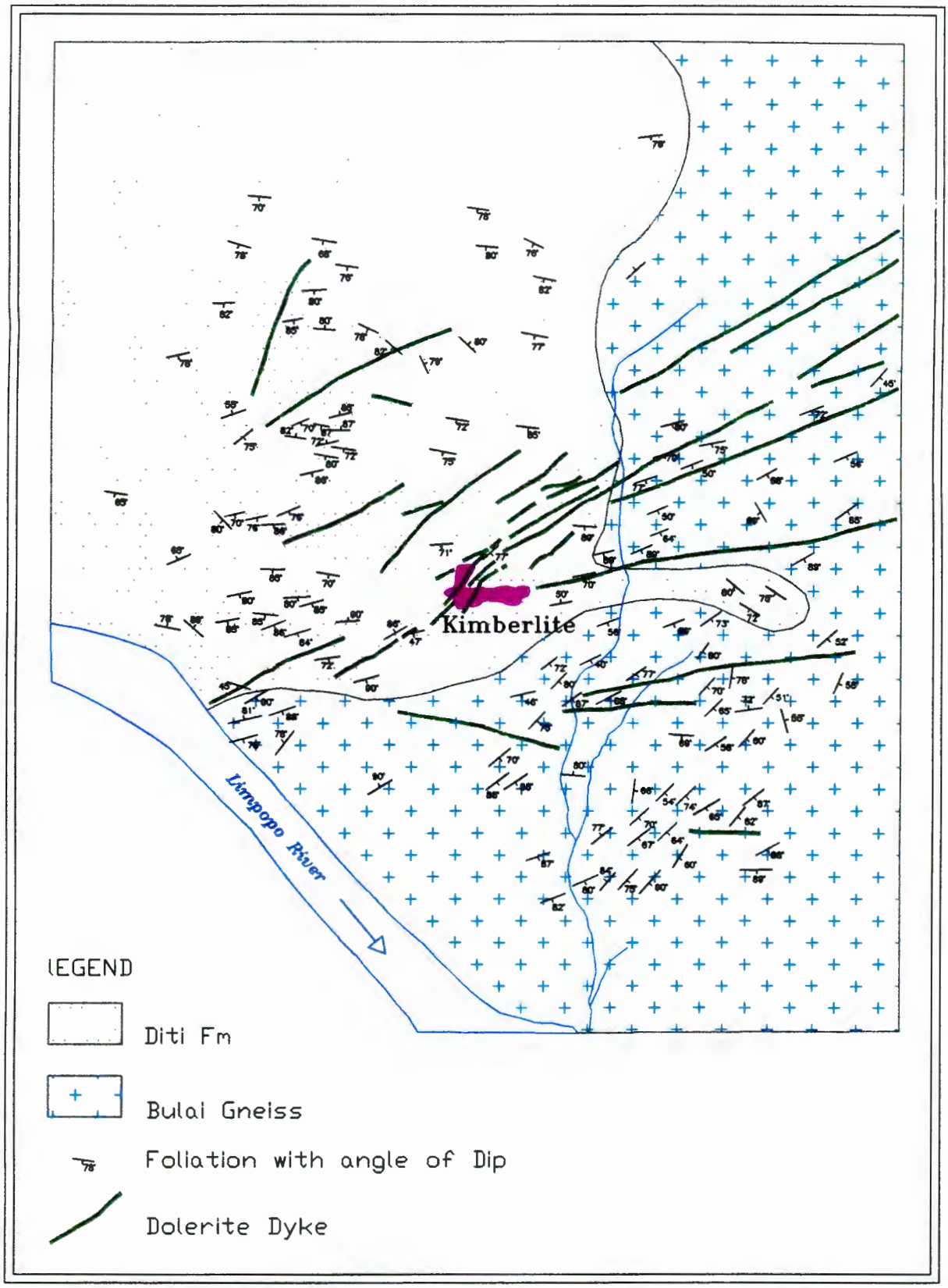

Fig 2.2 Structural Map of the area around River Ranch Kimberlite

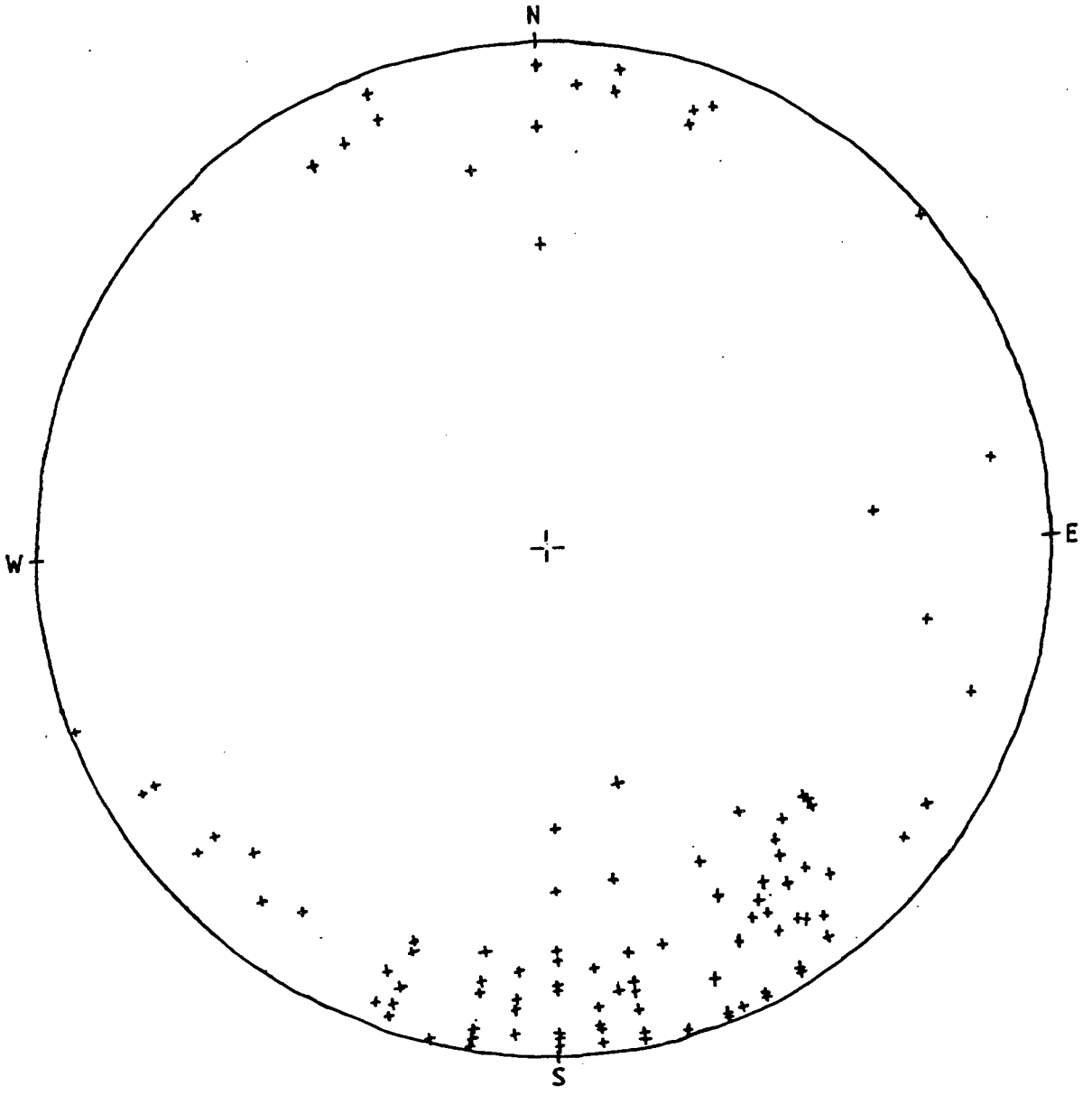

Figure 2.3 Stereoplot for foliation taken around River Ranch.

The paragneiss appears to have retained its sedimentary foliation enhanced by metamorphism. A deformational foliation also developed. From structural measurements taken, the dominant trend is along 095°-110° with a minor trend along 075°-085° (Figure 2.2). In both trends, folding of the foliation was observed at some localities.

The Bulai Gneiss to the east of the River Ranch kimberlite (Figure 2.2) has a mineral foliation trending at 050°-060°. Some feldspar porphyroblasts observed in the gneiss indicate a sinistral sense of rotation.

2.4 FIELD DESCRIPTIONS OF THE KIMBERLITE

The River Ranch Kimberlite pipe is lobate in shape (Figure 2.4). It measures approximately 500 m long by 100m wide with a north-east trending limb extending from the western end of the main body. The north-east trending limb is separated from the main pipe by a Karoo age dolerite dyke. Evidence from core drilling done by Kimberlitic Searches (Pvt) Ltd shows that the north-east trending limb resulted from displacement from the main pipe along a fault zone (E.M.W Skinner, pers. comm.) which was subsequently exploited by the Karoo dolerite dyke (Figure 2.4). The kimberlite is weathered at sub-surface and precludes observation of any kinematic indicators of the movement.

Two small kimberlite pipes were found within hundred metres east of the main pipe. They measure approximately 32 by 19 metres and 10 by 8 metres. No connecting dyke with the main pipe has been observed at surface.

The main kimberlite pipe is now eroded down to the diatreme level. It is not clear how much erosion has actual taken place. The ideal model of an uneroded kimberlite pipe with the crater zone, the diatreme zone and the root zone is illustrated in Figure 2.5. The total surface area of the diatreme is approximately 5.2 hectares (or 12.8 acres). The margins of the diatreme dip inwards at steep angles of around 88°. The whole pipe has a slight northerly dip. The margins of the pipe have sharp contacts with the country rock.

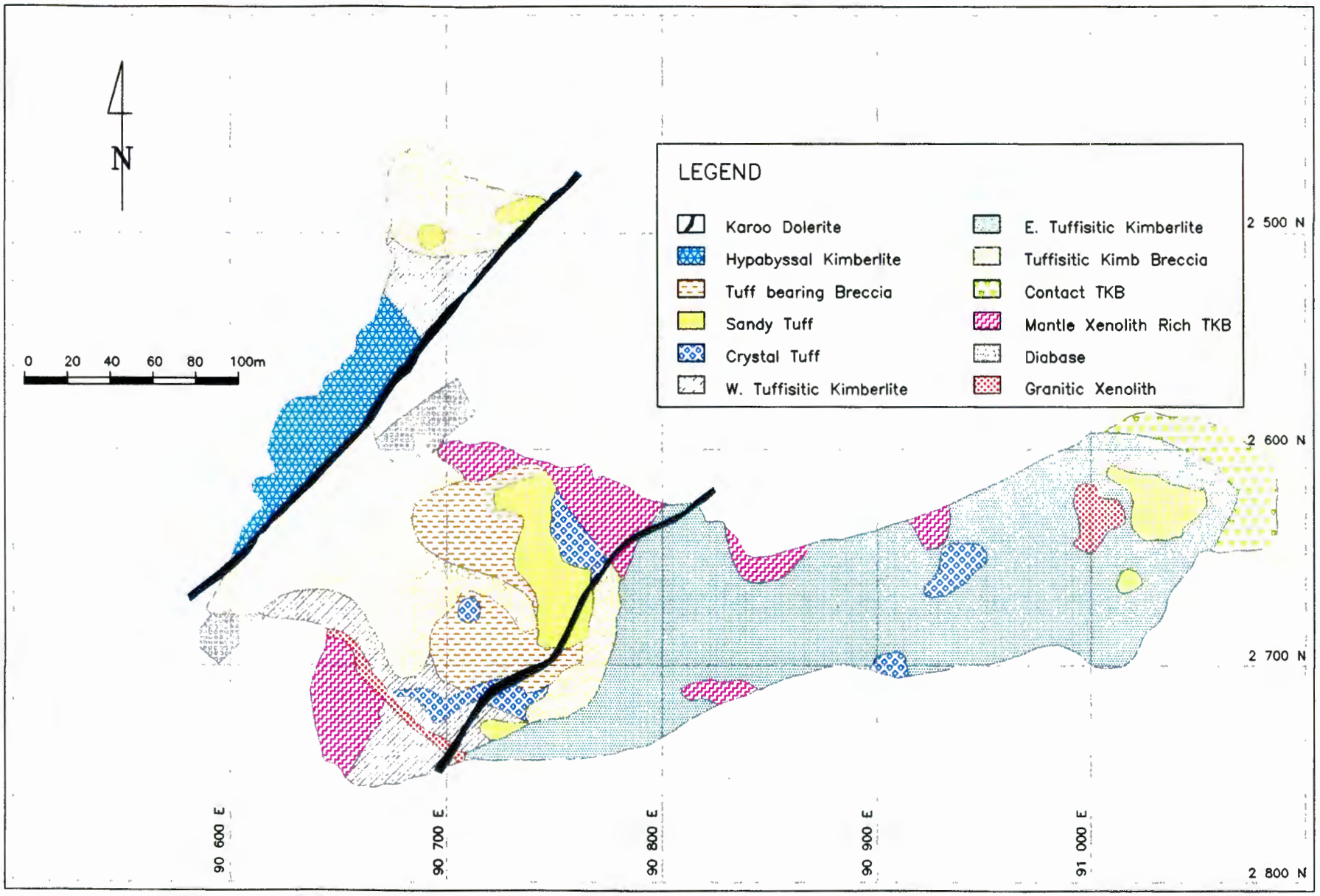

Figure 2.4 Geological Map of the River Ranch Kimberlite Pipe

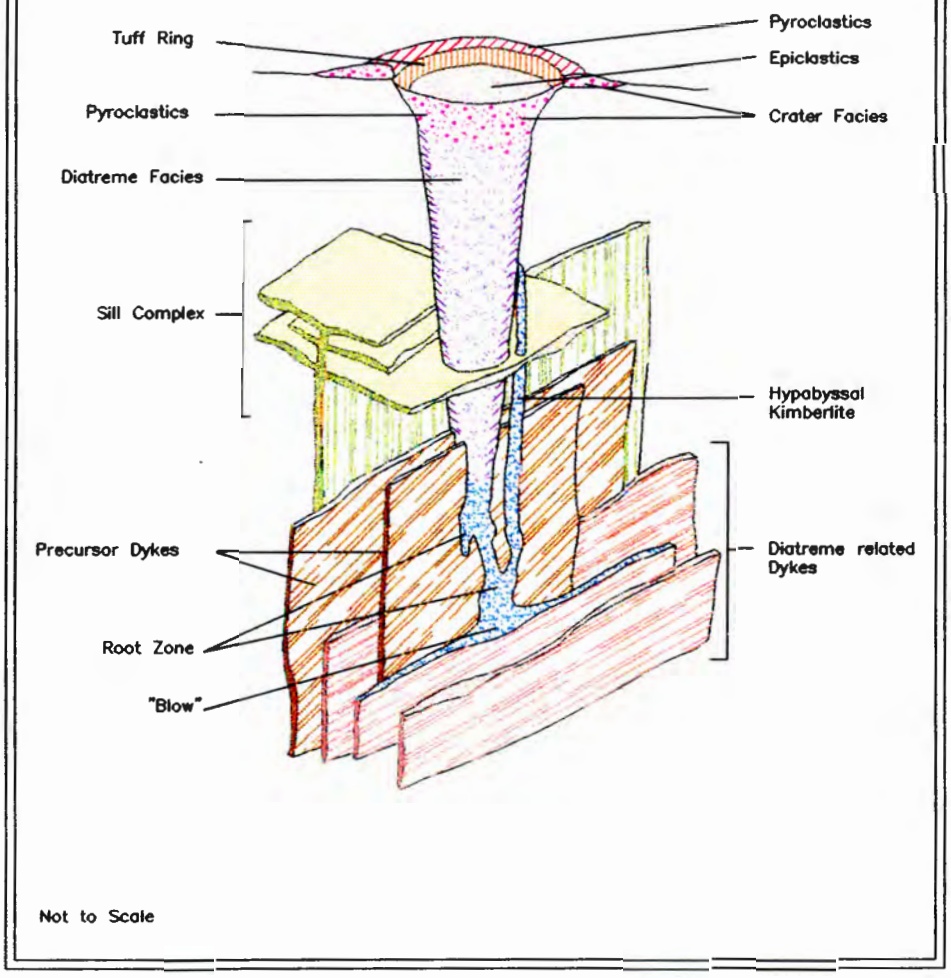

Fig 2.5 Idealized model of a kimberlite pipe (Mitchell, 1991) illustrating the relationship between crater, diatreme and hypabyssal facies (root zone) rocks.

The shape of the pipe can be described in terms of a western and eastern lobe. The western lobe is comprised of a variety of phases while the eastern lobe is fairly homogeneous and dominated by one phase with minor blocks of a second phase scattered throughout the eastern end of the pipe.

At least six intrusive phases and two crater facies phases have been identified at the current level of the diatreme. The high degree of weathering of the kimberlite at the current level of mining is a deterrent factor inhibiting accurate physical recognition of the different phases. The intrusive phases in the western lobe are generally ochrous yellow in colour while the kimberlite in the eastern lobe is blueish-green.

2.4.1 The Kimberlite Phases

The different phases were characterised in the field by a combination of texture, quantity of xenoliths, type of xenoliths and colour. Whenever possible, the textural classification of Clement and Skinner (1985) was utilised. In certain instances, descriptive terms were used to name some of the rock types. The age relationships between some of the phases is not easy to decipher but xenolith composition and contact relationships of some of the phases have made it possible to determine the sequence of intrusion in these phases.

Although the pipe has been eroded to the diatreme level, blocks of crater facies material have been identified and these have been interpreted as floating rafts that have fallen back into the diatreme through successive eruptions, as has been widely recorded elsewhere (eg. Wagner, 1914; Clement, 1982).
The diatreme kimberlite and crater facies phases identified are:

1. Mantle xenolith-rich tuffisitic kimberlite
2. Western tuffisitic kimberlite
3. Tuffisitic kimberlite breccia
4. Eastern tuffisitic kimberlite
5. Sandy/Crystal tuff

6. Tuff-bearing breccia
7. Hypabyssal kimberlite

2.4.1.1 Mantle Xenolith-Rich TKB

This is a TKB variety characterised by an unusual abundance of garnet-bearing mantle xenoliths occurring together with crustal xenoliths. It occurs at the margins of the diatreme and was identified at five localities (Figure 2.4). This phase is interpreted as the oldest among all the intrusive phases. Only relics of it still remain on the diatreme margins after successive eruptions of the younger phases have replaced it in the central areas of the pipe. The kimberlite itself is khaki-green in colour. It contains altered olivine macrocrysts which average less than 10mm in diameter.

2.4.1.2 Western Tuffisitic Kimberlite (WTK)

The WTK occurs in the western lobe of the diatreme. This kimberlite is khaki- green in colour and contains very little crustal and mantle xenoliths. The kimberlite satisfies the textural classification scheme adopted by Clement and Skinner (1985) in which the incorporated xenoliths comprise less than 15 volume per cent of the whole kimberlite. The altered olivine macrocrysts within the kimberlite are on average less than 10mm in diameter and normally give the rock its overall hue.

2.4.1.3 Tuffisitic Kimberlite Breccia (TKB)

The TKB is characterised by an abundance of crustal xenoliths which include granite, paragneiss, dolerite and/or amphibolite and cognate fragments of kimberlite (Plate 2.1). Mantle xenoliths are very rare. All the incorporated fragments constitute more than 15 volume per cent of the kimberlite, thereby falling into the TKB classification of Clement and Skinner (1985). The altered olivine macrocrysts are similar to those observed in WTK (less than 10mm in diameter) and also give the rock its overall hue.

2.1

2.2

PLATE 2.1 Tuffisitic kimberlite breccia (TKB) in the western section of the kimberlite pipe. The TKB is characterised by an abundance (> 15% by volume) of crustal xenoliths which are on average 5cm in diameter. The red or pink coloured xenoliths are the country rock paragneiss and granite. The dark coloured xenoliths are amphibolite or dolerite.

(The pen provides the scale).

PLATE 2.2 Core section through the eastern tuffisitic kimberlite (ETK). The ETK is characterised by mainly doleritic or amphibolitic xenoliths and is devoid of any paragneissic or granitic fragments.

2.4.1.4 Eastern Tuffisitic Kimberlite (ETK)

The Eastern tuffisitic kimberlite constitutes the largest single phase in the diatreme at surface (Figure 2.4). It is blueish-green in colour and is distinctly different to the rest of the phases in the western lobe (Plates 2.2 and 2.3). It is also devoid of any granitic or paragneissic xenoliths which are often observed in other phases in the western lobe. The minor crustal xenoliths within it are mainly doleritic and/or amphibolitic. The ETK is further characterised by an abundance of highly altered xenocrystic olivines which may be up to 50mm in diameter and are normally pale brown to khaki-green in colour. Mantle xenoliths are rarely observed.

2.4.1.5 Sandy/Crystal Tuff

These two phases can be distinguished from each other by one aspect, the crystal tuff is pyroclastic and has got numerous pelletal lapilli and highly altered olivines which are set in a clay matrix (Plate 2.4). The pellets can be cored by either country rock fragments or altered olivines. The altered olivines are generally less than 3mm in diameter and comprise 30-40% of the rock. On the other hand, the sandy tuff is epiclastic and possibly represents reworked crystal tuff. It has a poorly consolidated gritty sandstone appearance (Plate 2.4). Flat and rounded small pieces (less than 15mm) of lithified shale material have been identified in the sandy tuff. There are very few pelletal lapilli and olivines in the sandy tuff. Both graded bedding and cross-bedding have also been identified (Plate 2.4). Both phases occur as scattered blocks within the other diatreme phases (Plate 2.6). They have been inferred to be `floating reef' blocks from the crater facies that have subsided down the diatreme during or between successive eruptions of the younger intrusive phases.

2.4.1.6 Tuff-Bearing Breccia (TBB)

This phase occurs on the western lobe of the pipe in close association with the sandy and crystal tuff (Figure 2.4, Plate 2.7). It incorporates fragments of the sandy and crystal tuff together with the granitic, paragneissic, amphibolitic and/or doleritic fragments found in the other TKs and TKBs (Plate 2.7). The tuff xenoliths can be in excess of one metre in diameter. The TBB contains extensively altered light brown olivines in a groundmass of clay. The groundmass

2.3

2.4

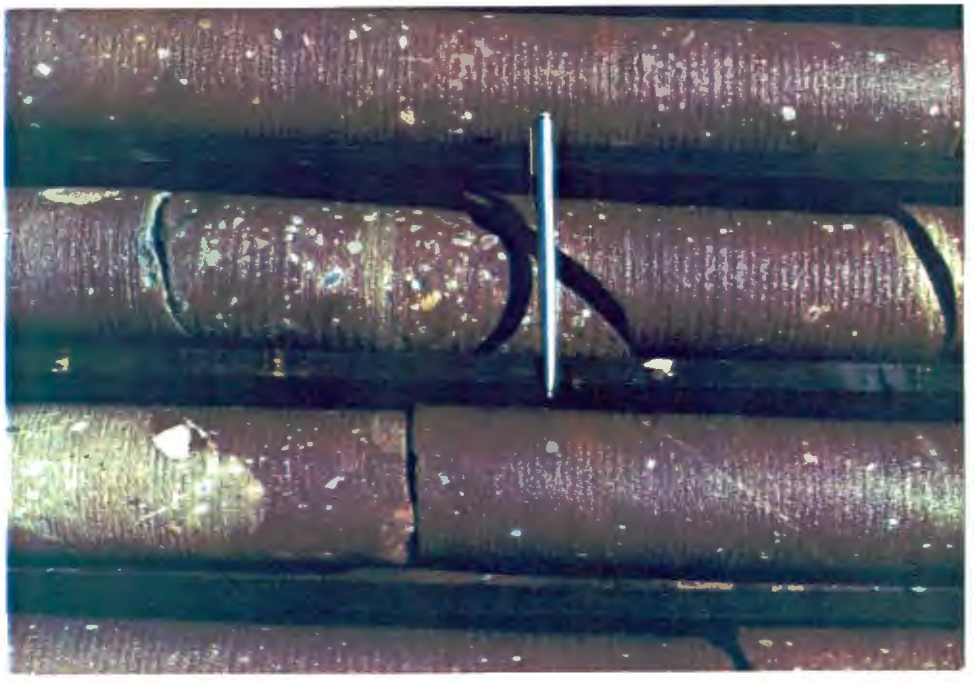

PLATE 2.3 The ETK in the eastern section of the pipe showing large khaki-green altered xenocrysts of olivine pseudomorphs.

PLATE 2.4 Section of core through the crystal tuff. The numerous pelletal lapilli are cored by either olivine pseudomorphs or lithic country rock fragments.

2.5

2.6

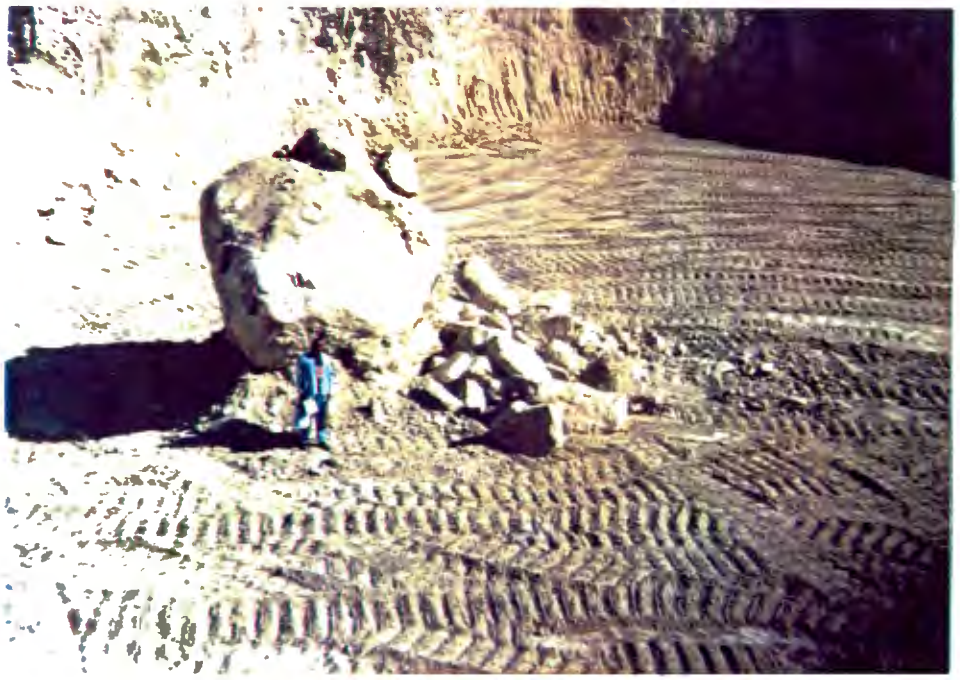

PLATE 2.5 Section of core through the sandy tuff. The light green and brown and the dark brown bands which are about 45 to the core axis show graded bedding in the sandy tuff. The graded bedding shows the reworked epiclastic nature of the sandy tuff.

PLATE 2.6 A block of sandy tuff within the TKB (north-east trending limb). The block is already totally exposed and is an indication of the 'floating' nature of the crater facies blocks within the diatreme.

2.7

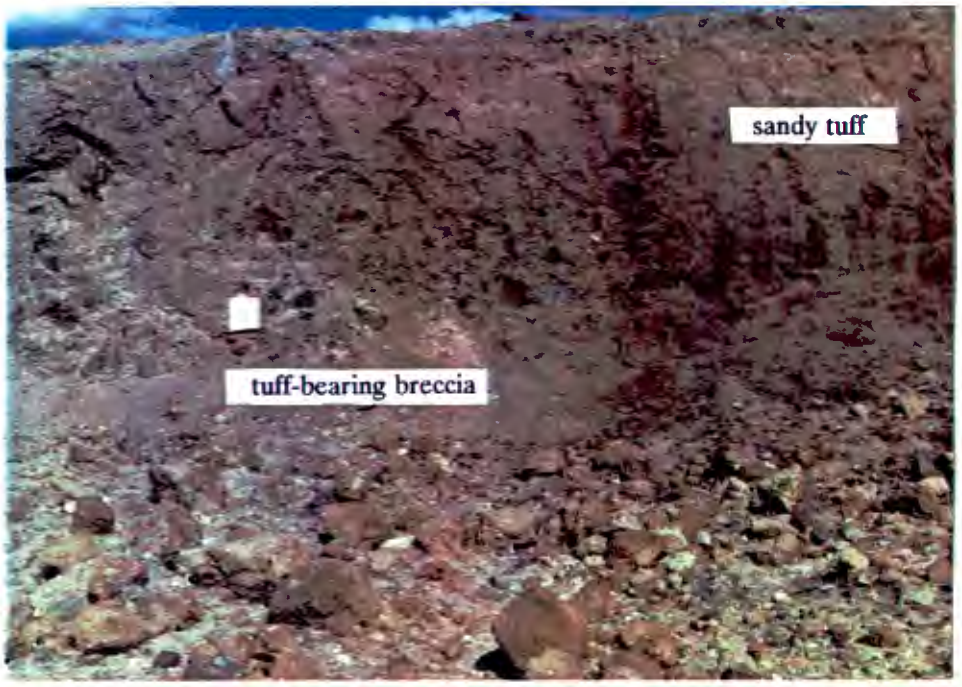

2.8

PLATE 2.7 A section of the kimberlite pipe showing the tuff-bearing breccia (left) occuring next to a block of sandy tuff (right). The tuff-bearing breccia is characterised by the occurence together of sandy/crystal tuff fragments (reddish- brown) and crustal xenoliths (dark green).

PLATE 2.8 The hypabyssal kimberlite in the north-west corner of the kimberlite pipe. The hypabyssal kimberlite is characterised by numerous dark green coloured olivine pseudomorph macrocrysts. The white patches are altered crustal xenoliths.

kimberlite has a light brown to ochrous yellow colour. This phase is younger than the rest of the diatreme phases since it contains xenoliths of the older phases.

2.4.1.7 Hypabyssal Kimberlite

This phase is localised at the north-west corner where the extended limb of the pipe joins the rest of the diatreme. It is demarcated to the south by the Karoo dyke (Figure 2.4) and has got sharp vertical contact. Its margin with country rock dips negatively into the country rock to the west. The hypabyssal phase is thought to have come up through a zone of weakness at the margins of the pipe at a very late stage. The kimberlite is almost devoid of mantle or crustal xenoliths and of any precursor kimberlites. It is characterised by abundant olivine macrocrysts (Plate 2.8). The few crustal xenoliths that have been observed are completely altered (Plate 2.8) and this further distinguishes the hypabyssal facies from the diatreme facies where such incorporated xenoliths are much less thermally affected. The relatively high temperature and volatile-rich environment of the hypabyssal facies is apparently responsible for altering the xenoliths (Clement, 1982).

2.4.2 Other Geological Features

2.4.2.1 Consequent Dyke

A consequent dyke has been intruded along the southern contact of the hypabyssal kimberlite and the rest of the diatreme. This same contact was subsequently exploited by a Karoo dolerite dyke (Plate 2.10, Figure 2.4). The kimberlite dyke is approximately one metre in width. It is highly altered and has a conspicuous blue-green colour.

2.4.2.2 Contact Breccia

A characteristic narrow zone of breccia occurs at the contact of the diatreme and country rock to the east (Figure 2.4, Plate 2.11). The contact breccia results from local incorporation of country rock fragments at the margins of the pipe during emplacement.

2.9

2.10

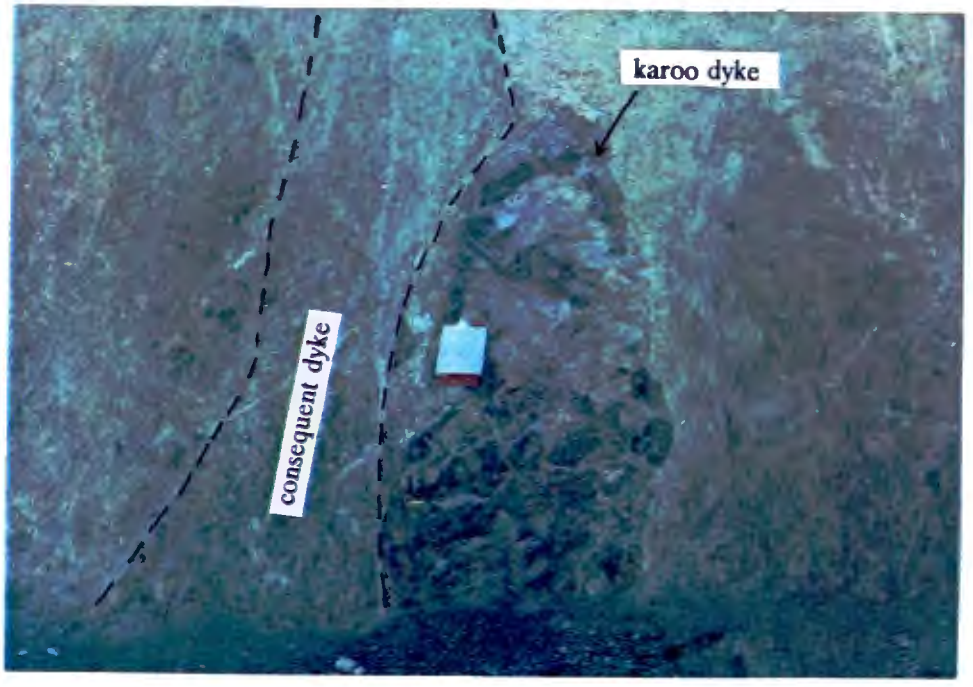

PLATE 2.9 Section of core through hypabyssal kimberlite with an abundance of calcite crystals (white). The calcite is primary in nature and this type of hypabyssal kimberlite is termed "snow storm".

PLATE 2.10 A consequent dyke that has been intruded along the contact of the hypabyssal kimberlite (right) and the tuff-bearing breccia (left). The karoo dyke subsequently exploited the same contact.

2.11

PLATE 2.11 The contact breccia zone on the eastern contact of the diatreme with the surrounding country rock. The numerous dark coloured xenoliths are mainly amphibolite .

3. PETROGRAPHY

3.1 INTRODUCTION

Petrographic classification of the different kimberlite phases was done on both a textural and mineralogical basis. The textural classification sub-divides the phases into facies (eg. hypabyssal, diatreme or crater), rock type (eg. tuffisitic kimberlite or tuffisitic kimberlite breccia) and lastly into the different macroscopic textures (Table 3.1, Clement and Skinner, 1985). The facies divisions usually correspond to the major depth zones of the kimberlite pipes namely root, diatreme and crater zones (Hawthorne, 1975). The mineralogical classification is based on the relative abundance of five primary minerals namely diopside, monticellite, phlogopite, calcite and serpentine (Table 3.2, Skinner and Clement, 1979 ; Clement, 1982). Further sub-divisions can be made if one or more of the five minerals, or any other mineral, is present to the extent of, or exceeding, two-thirds of the volumetric abundance of the dominant mineral. In cases where the total opaque mineral content of the matrix is at least two-thirds of the modal percentage of the dominant mineral, the kimberlite is qualified as opaque-mineral-rich (Skinner and Clement, 1979).

3.2 PETROGRAPHIC DESCRIPTIONS OF THE DIFFERENT PHASES

3.2.1 Western Tuffisitic Kimberlite (WTK)

3.2.1.1 Macroscopic Description

The WTK is identified by the presence (in very small proportions) of lithic angular to sub-angular country rock fragments. It is dark green in colour and contains macrocrysts of olivine pseudomorphed by serpentine (but hereafter referred as "olivine pseudomorphs" following Clement, 1982) which are generally less than 5mm in size. When country rock fragments are present they are usually granitic and/or doleritic. These xenoliths can vary in size up to about 5cm.

FACIES	ROCK TYPE	MACROSCOPIC TEXTURE
HYPABYSSAL-FACIES KIMBERLITE	KIMBERLITE	MACROCRYSTIC KIMBERLITE
		SEGREGATIONARY KIMBERLITE
		APHANITIC KIMBERLITE
	KIMBERLITE BRECCIA	MACROCRYSTIC KIMBERLITE BRECCIA
		SEGREGATIONARY KIMBERLITE BRECCIA
		APHANITIC KIMBERLITE BRECCIA
DIATREME-FACIES KIMBERLITE	TUFFISITIC KIMBERLITE	PELLETAL-TUFFISITIC KIMBERLITE
		LITHIC-TUFFISITIC KIMBERLITE
		CRYSTAL-TUFFISITIC KIMBERLITE
	TUFFISITIC KIMBERLITE BRECCIA	PELLETAL-TUFFISITIC KIMBERLITE BRECCIA
		LITHIC-TUFFISITIC KIMBERLITE BRECCIA
CRATER-FACIES KIMBERLITE	PYROCLASTIC KIMBERLITE	FURTHER SUBDIVISION ACCORDING TO STANDARD GRADE SCALES AND/OR IN TERMS OF LITHOLOGICAL-GENETIC FACIES CONCEPTS
	EPICLASTIC KIMBERLITE	

Table 3.1 A textural-genetic classification of kimberlites proposed by Clement and Skinner (1985).

KIMBERLITE						
STAGE 1	STAGE 2					STAGE 3
ESSENTIAL MINERAL	POTENTIAL CHARACTERIZING ACCESSORY MINERALS					OPAQUE MINERALS
DIOPSIDE	Monticellite	Phlogopite	Calcite	Serpentine	Apatite	Qualify as opaque-rich
MONTICELLITE	Diopside	Phlogopite	Calcite	Serpentine	Apatite	if opaque minerals = 2/3
PHLOGOPITE	Diopside	Monticellite	Calcite	Serpentine	Apatite	modal % of essential mineral
CALCITE	Diopside	Monticellite	Phlogopite	Serpentine	Apatite	
SERPENTINE	Diopside	Monticellite	Phlogopite	Calcite	Apatite	

Table 3.2. A mineralogical classification of kimberlites proposed by Skinner and Clement (1979).

3.2.1.2 Microscopic Description

In thin section, the WTK is comprised of macrocrysts of olivine pseudomorphs and lithic country rock fragments, which are mainly quartz and feldspar, all set in a groundmass of fine grained serpentine, altered monticellite, perovskite and spinels. [Plates 3.1, 3.2, 3.3 and 3.4].

The macrocrysts of olivine pseudomorphs are usually completely altered to serpentine and some exhibit "cores" of secondary carbonate (calcite) [Plates 3.1 and 3.2]. Some of the macrocrysts are irregularly shaped with edges that appear to have been corroded [Plate 3.3]. Notable in some sections are numerous small pieces of serpentinised olivines that are angular and appear to have been broken off from larger macrocrysts [Plates 3.1 and 3.2]. Phenocrysts of olivine pseudomorphs can also be observed. There are a few irregular shaped pelletal lapilli [Plate 3.4] but these are generally not well developed. Olivine pseudomorphs comprise about 60-70% of the kimberlite.

Quartz and feldspar grains together with granitic and doleritic rock fragments make up the lithic components. The quartz and feldspar grains are generally angular to sub-angular and less than 2mm. Together the lithic fragments constitute about 5-10% of the kimberlite.

The groundmass minerals are fine grained serpentine, altered monticellite, minor perovskite, very rare bleached phlogopite spinels (normally less than 0.02mm) and fine grained clays. The groundmass in some of the pellet rims shows replacement of olivine phenocrysts by diopside and monticellite shows replacement by calcite.

In summary the WTK is a perovskite-bearing monticellite kimberlite.

3.2.2 Tuffisitic Kimberlite Breccia (TKB)

When incorporated xenoliths and cognate kimberlite fragments, 4mm or more in size, make up at least 15 volume per cent in the tuffisitic kimberlite, it then becomes a tuffisitic kimberlite breccia (Clement and Skinner, 1985).

3.1

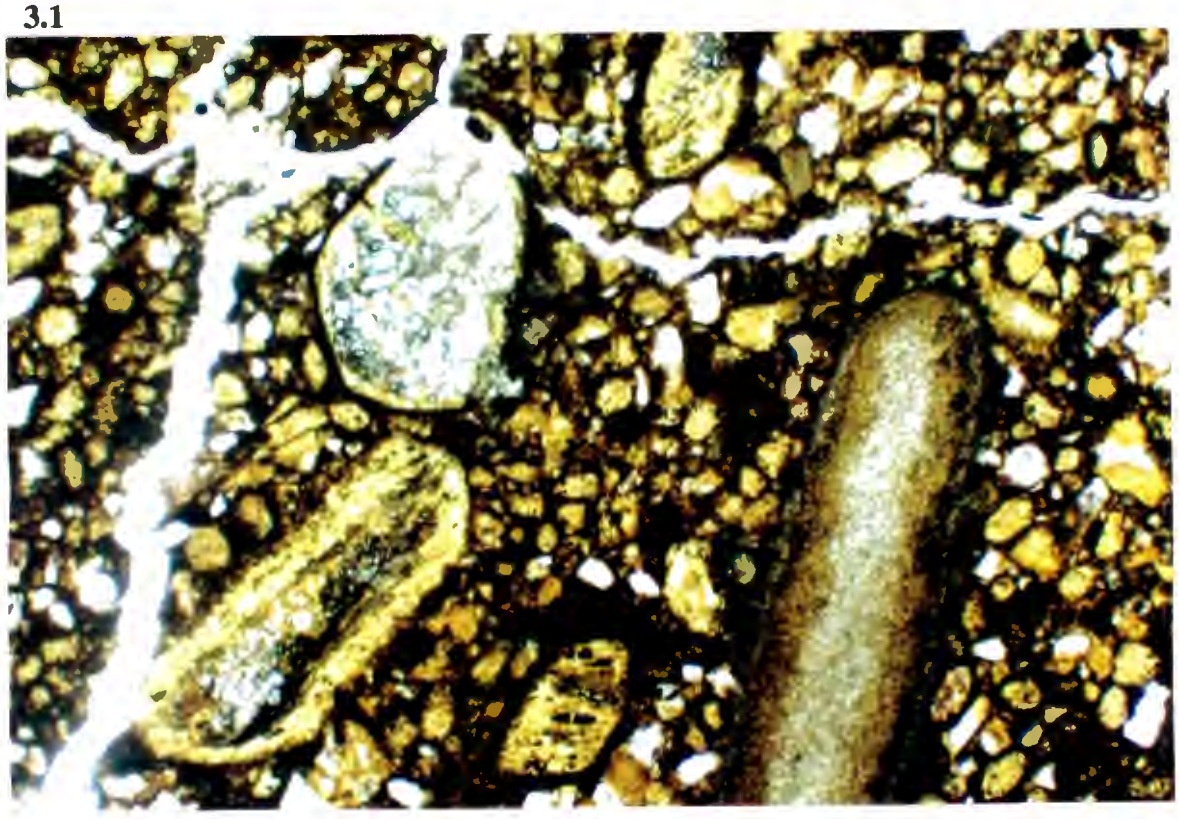

3.2

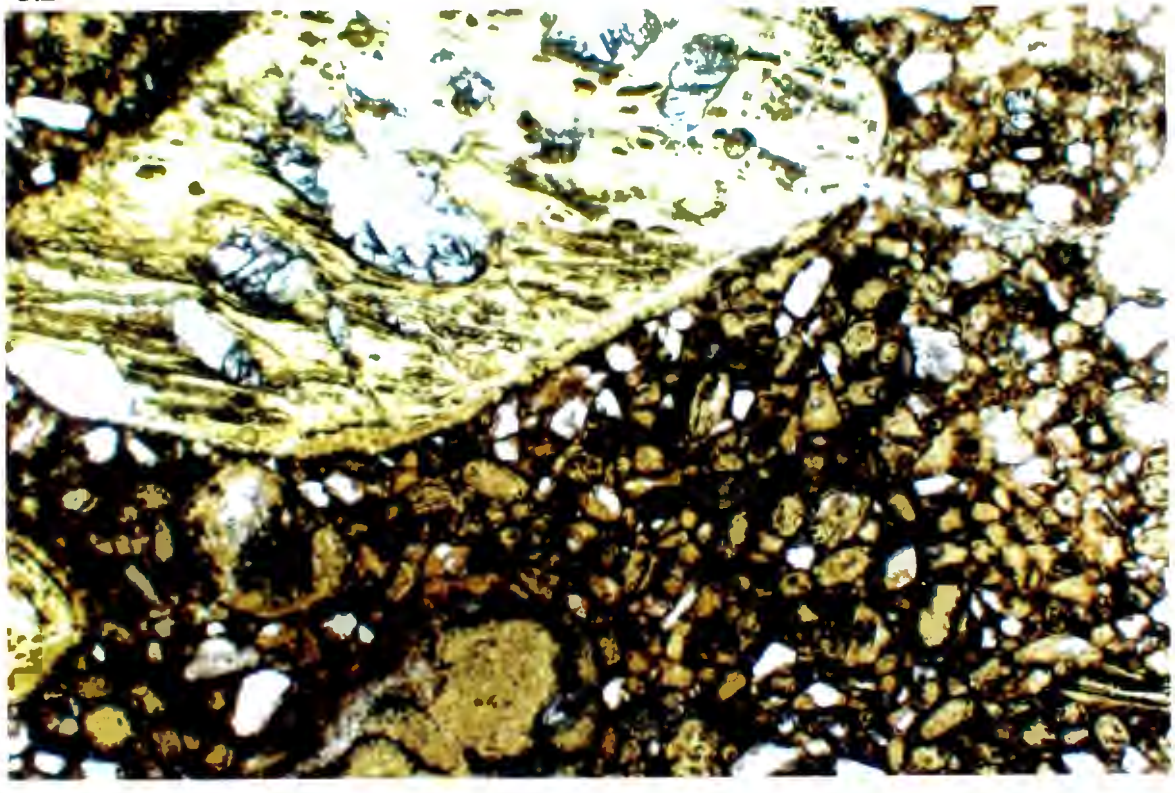

PLATE 3.1 Sample RRM 25, Western tuffisitic kimberlite.

Macrocrysts of olivine pseudomorphs and minor lithic fragments of quartz. Note the numerous small pieces of serpentinised olivine that are angular and appear to have been broken. Together with the small serpentinised olivine pieces are phenocrysts of olivine pseudomorphs. The opaques are medium to coarse grained.

Base of photomicrograph equals 8.3 mm.

PLATE 3.2 Sample RRM 25 , Western tuffisitic kimberlite.

A macrocryst of olivine pseudomorph showing secondary calcite alteration of the core. There are numerous small angular pieces of serpentinised olivine and a few phenocrysts of olivine pseudomorphs.

Base of photomicrograph equals 8.3 mm.

3.3

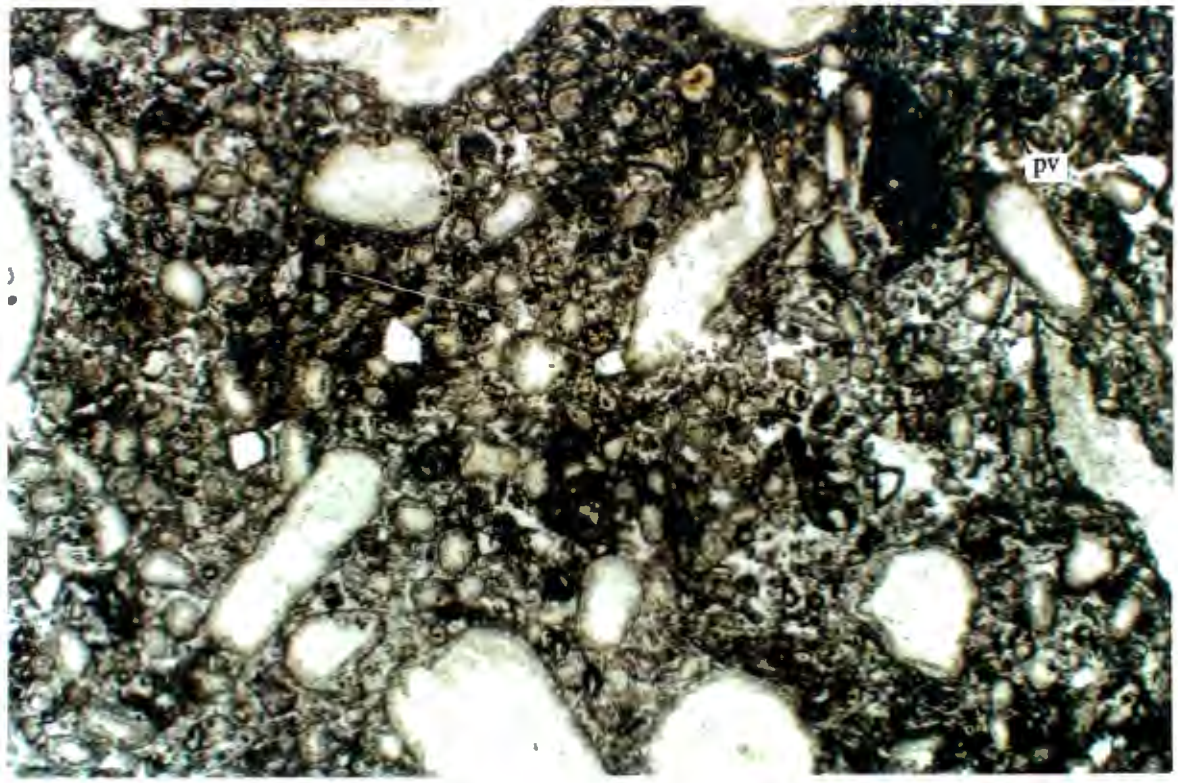

3.4

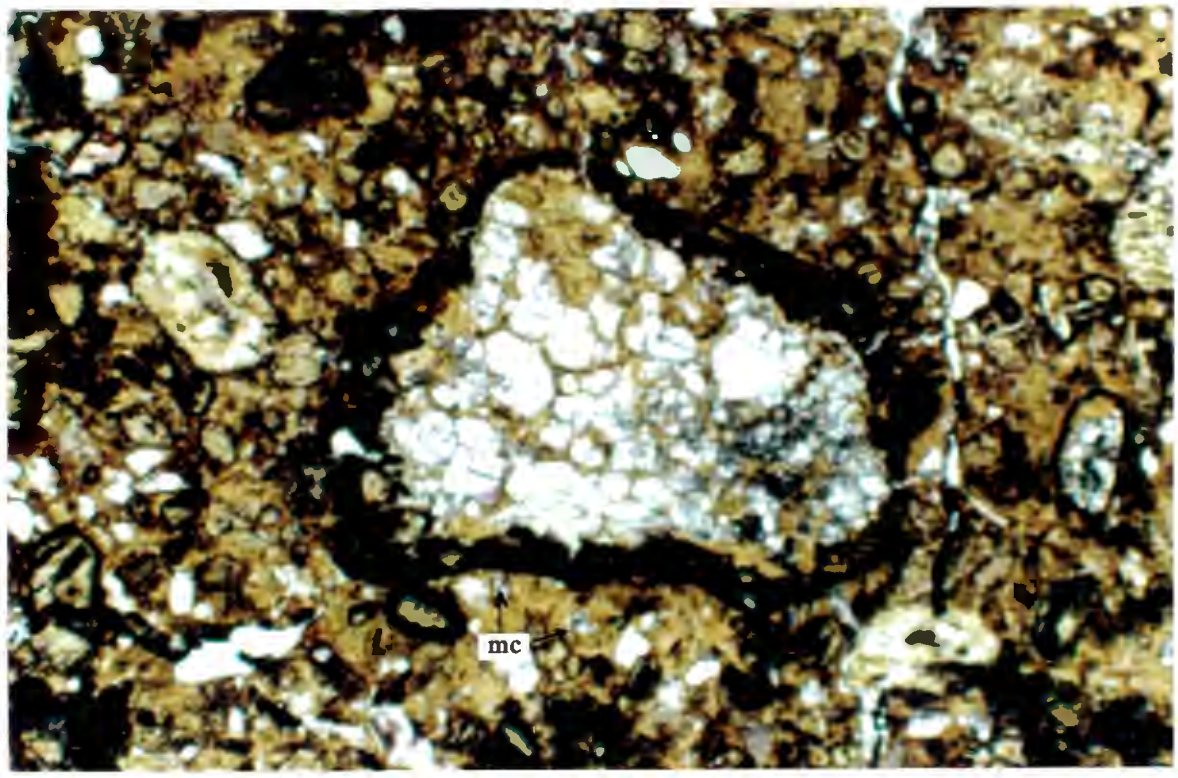

PLATE 3.3 Sample RRM 1 , Western tuffisitic kimberlite

Irregularly shaped macrocrysts of olivine pseudomorphs . Some have edges that appear to be corroded. Perovskite (pv) and fine grained opaques can be observed in the groundmass.

Base of photomicrograph equals 8.3 mm.

PLATE 3.4 Sample RRM 21 , Western tuffisitic kimberlite.

A large, less distinct pelletal lapillus with a highly altered pellet rim. The core shows alteration to secondary calcite. Some monticellite pseudomorphed by calcite (mc) can be observed in groundmass.

Base of photomicrograph equals 8.3 mm.

3.2.2.1 Macroscopic Description

The TKB is often identified by the characteristic abundance of country rock fragments, usually granitic and/or doleritic and autoliths. The fragments are generally more than 4mm in size although fragments less than 4mm also do exist. The TKB is dark green in colour and like its tuffisitic kimberlite variety, contains olivine pseudormophs which are generally less than 5mm.

3.2.2.2 Microscopic Description

In thin section, the TKB shows an abundance of lithic fragments of country rock and macrocrysts of olivine pseudomorphs which sometimes form cores of pelletal lapilli [Plates 3.5, 3.6 and 3.7]. The lithic fragments are mainly quartz and feldspar.

The macrocrysts of olivine pseudomorphs exhibit alteration to serpentine and are sometimes cored by secondary calcite [Plate 3.5]. The olivine pseudomorphs can also occur as angular fragments [Plate 3.6] which appear to have broken off from a larger macrocryst. There are a few irregular shaped pelletal lapilli which are skewed [plate 3.7]. The macrocrysts and pelletal lapilli comprise 30-40% of the kimberlite.

The quartz and feldspar grains together with other country rock fragments constitute about 30-60% of the kimberlite. These lithic fragments are often angular to sub-angular and can vary in size up to about 20mm.

Minor perovskite and spinels and rare phlogopite laths [Plate 3.8] are the groundmass minerals. The spinels are medium to coarse grained (up to 0.1mm) and constitute 1-2% of the kimberlite. The groundmass in the pellet rims shows extensive alteration to clays.

In summary the TKB is a perovskite-bearing serpentine kimberlite.

3.5

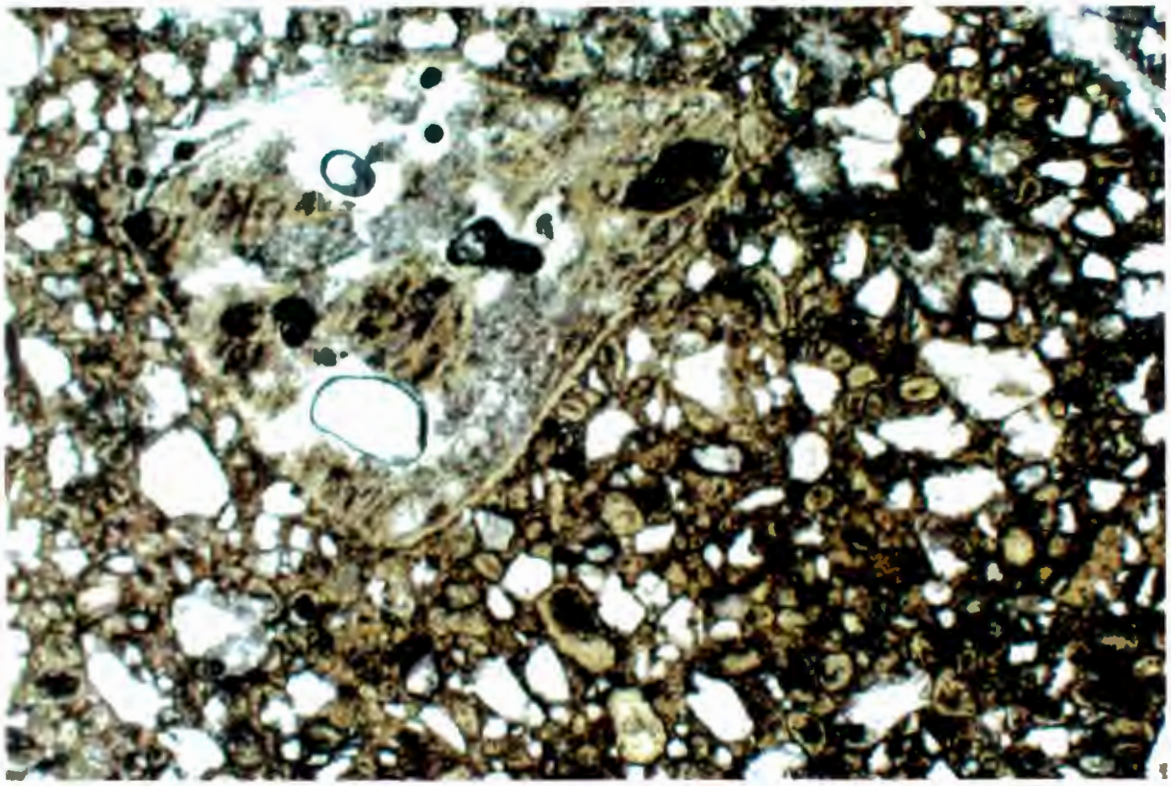

3.6

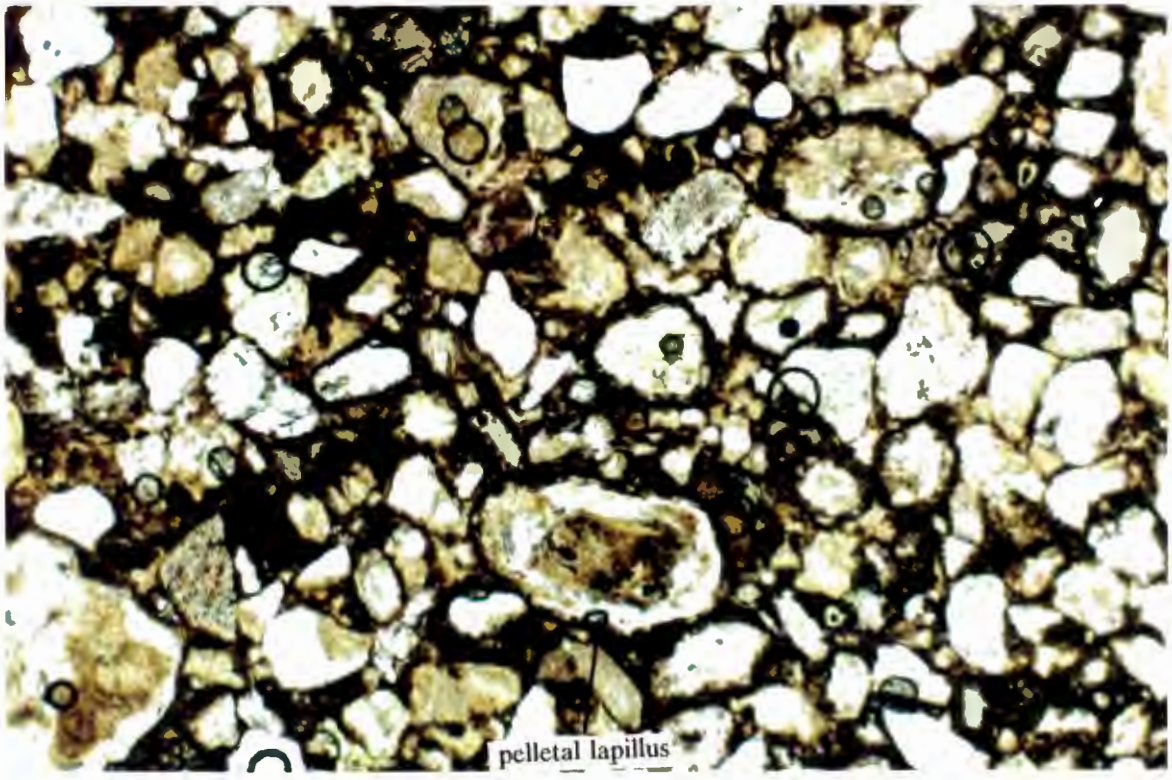

PLATE 3.5 Sample RRM 38 , Tuffisitic kimberlite breccia.

A large altered olivine macrocryst cored by secondary calcite. Numerous lithic fragments of quartz and other country rock fragments surround the macrocryst.

Base of photomicrograph equals 8.3 mm.

PLATE 3.6 Sample RRM 7 , Tuffisitic kimberlite breccia.

A less distinct pelletal lapillus surrounded by abundant lithic country rock fragments which are angular to subangular. Note that some of the olivine pseudomorphs are angular and appear to have been broken.

Base of photomicrograph equals 4.5 mm.

3.7

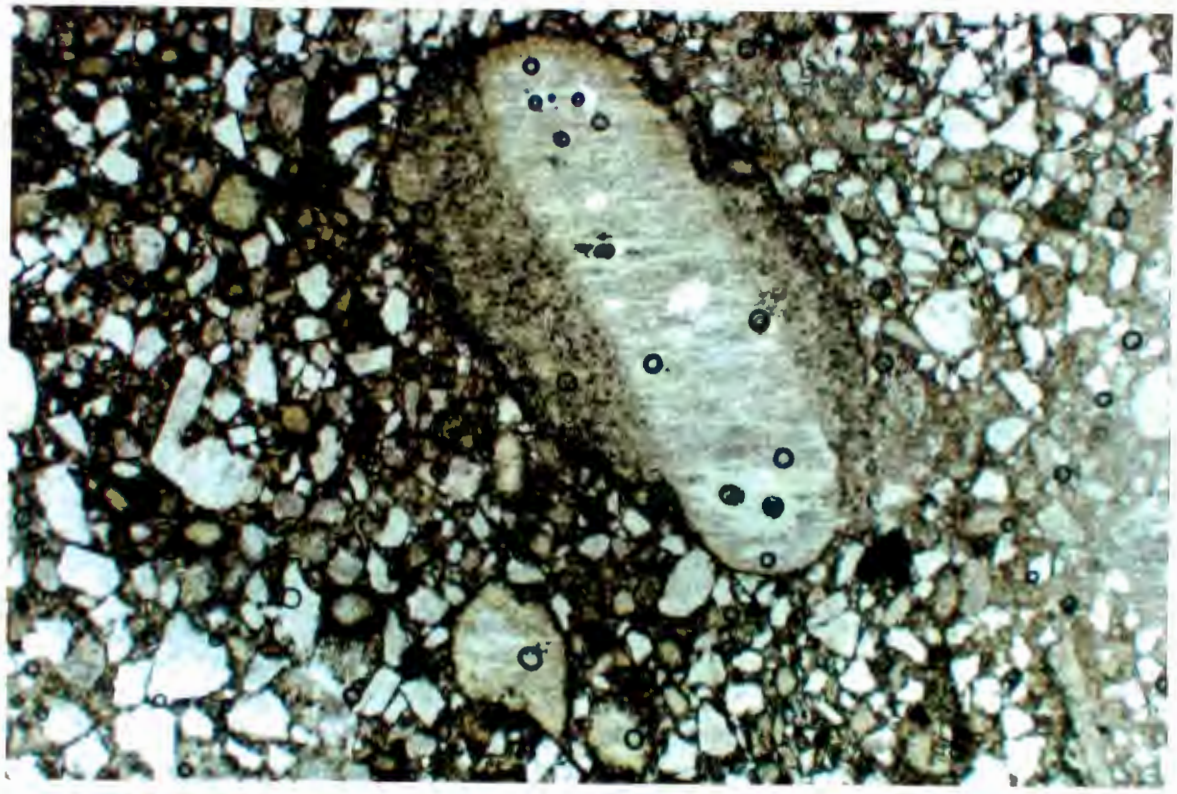

3.8

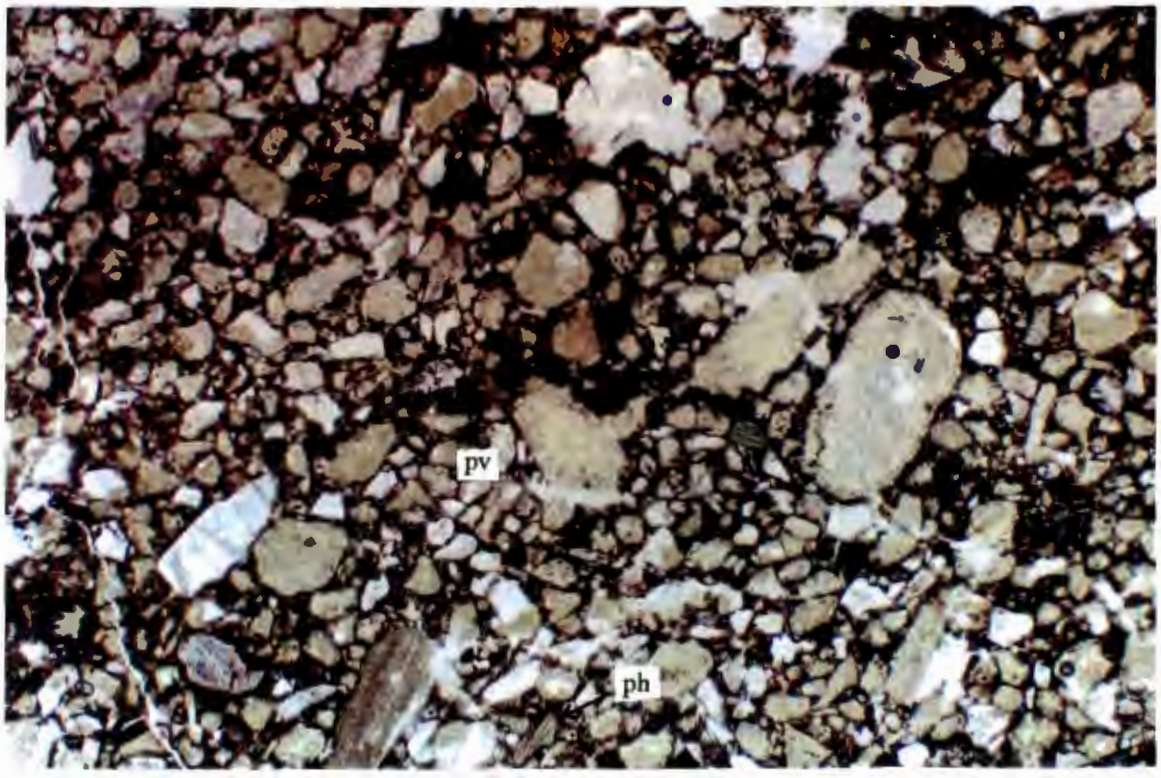

PLATE 3.7 Sample RRM 27 , Tuffisitic kimberlite breccia.

A skewed pelletal lapillus cored by an olivine pseudomorph macrocryst. Fine grained serpentine and clays constitute the pellet groundmass. Note the abundant angular to subangular lithic country rock fragments which are mainly quartz. Coarse grained opaques are observed in the groundmass.

Base of photomicrograph equals 8.3 mm.

PLATE 3.8 Sample RRM2 , Tuffisitic kimberlite breccia.

Minor perovskite (pv) and phlogopite (ph) with coarse grained opaques occuring together with numerous lithic fragments of country rock.

Base of photomicrograph equals 8.3 mm.

3.2.3 Eastern Tuffisitic Kimberlite (ETK)

3.2.3.1 Macroscopic Description

The ETK is conspicuously different from the WTK. It is distinguished by its blueish-green colour and by the complete absence of any granitic or paragneissic xenoliths. The country rock xenoliths incorporated into the ETK are mainly doleritic and amphibolitic. These xenoliths can vary in size up to about 50mm and constitute less than 15% by volume of the kimberlite. Unlike the WTK, the macrocrysts of olivine pseudomorphs in the ETK can be up to 50mm.

3.2.3.2 Microscopic Description

Olivine pseudomorphs in the ETK are usually spherical or sub-spherical globules or less regular segregations [Plates 3.9, 3.10, 3.11 and 3.12]. These globular or spherical bodies show some considerable degree of segregation. Diopside laths often form around the rims of the globules [Plates 3.10 and 3.11]. The process of segregation can be explained as the separation of magma, after crystallization of phenocrysts, into low-temperature immiscible K-rich silicate and CO2-rich carbonatitic fluids (Clemence 1982). The residual silicate phases must have remained essential liquid during emplacement and must have co-existed with the carbonatitic fluids at low temperatures. The carbonate fluids often form globules within the silicate fractions and hence the segregationary texture. The segregations are envisaged to have formed prior to fluidization as has been recorded elsewhere (eg. Clement 1982; Clement and Skinner 1985).

The country rock fragments form an insignificant proportion (<2%) of the kimberlite and are mainly doleritic and amphibolitic xenoliths. Fine grained serpentine, diopside, rare fine grained perovskite and spinels which constitute about 5% of the kimberlite make up the groundmass.

The ETK is a perovskite-bearing diopside kimberlite.

3.9

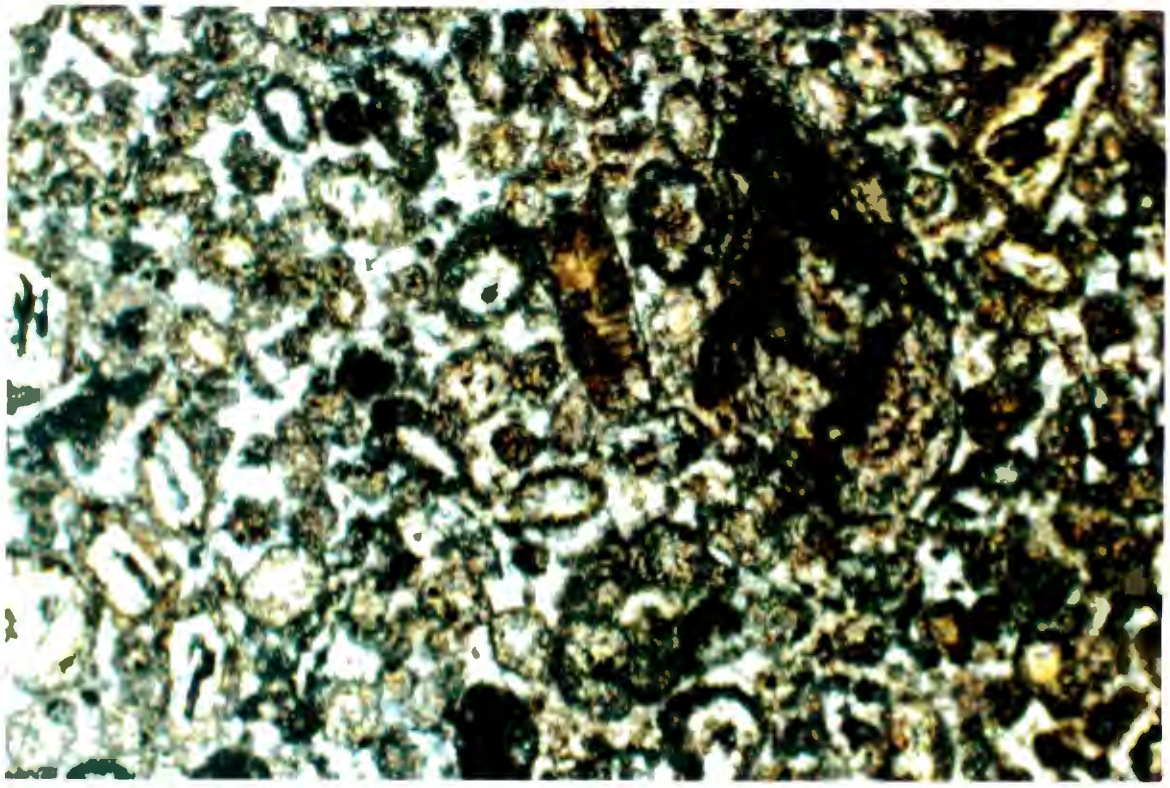

3.10

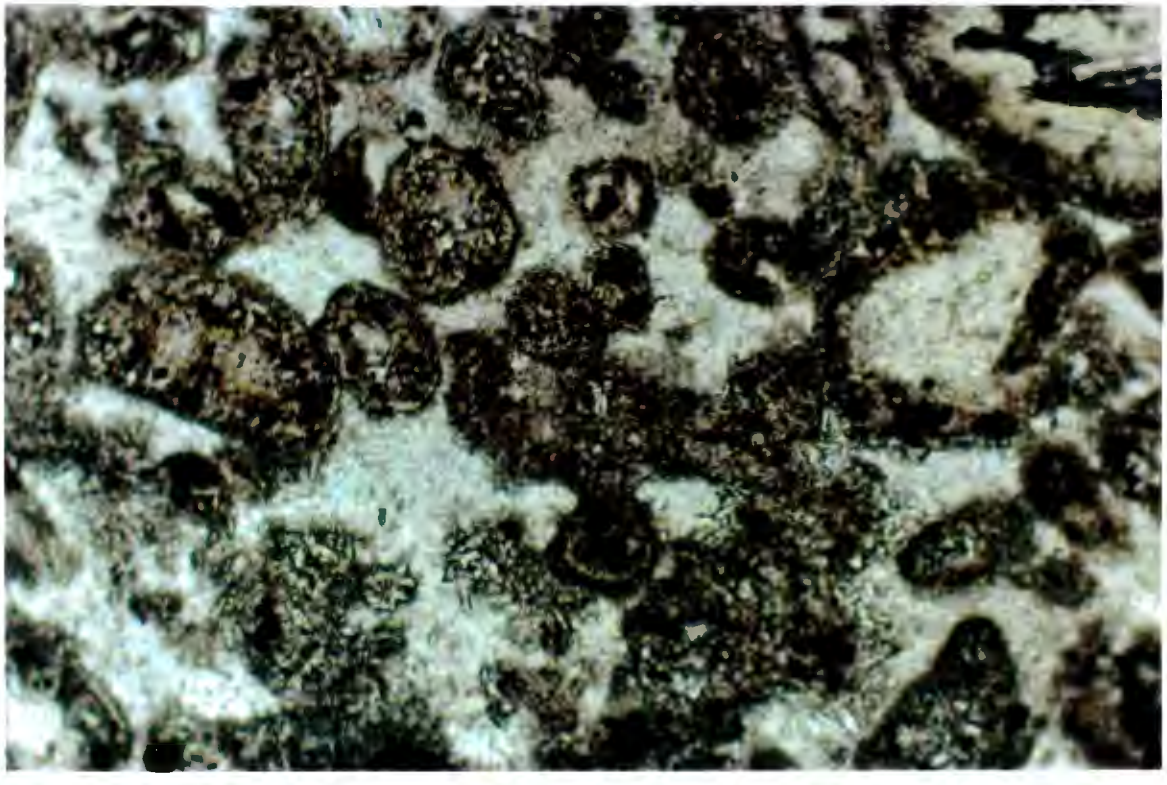

PLATE 3.9 Sample RRM 32 , Eastern tuffisitic kimberlite.

Spherical or less regular segregations set in a fine grained matrix of serpentine. Very fine grained diopside occupy the groundmass. (Crossed nicols).

Base of photomicrograph equals 4.5 mm.

PLATE 3.10 Sample RRM 32 , Eastern tuffisitic kimberlite.

Magnified section of plate 3.9 showing spherical or less regular segregationary texture with diopside laths (acicular) in the rims. This texture is formed prior to fluidization (Clement, 1982). Note the fine grained diopside and opaques in the groundmass.

Base of photomicrograph equals 1.8 mm.

3.11

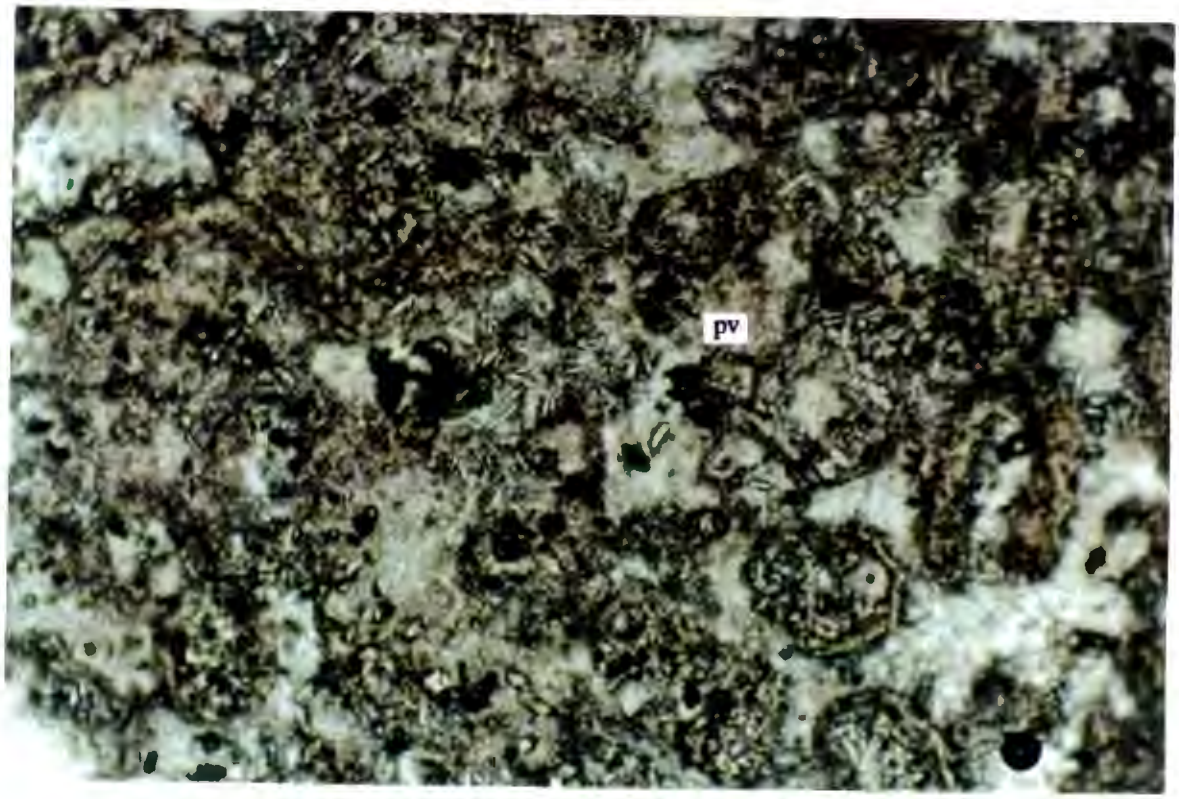

3.12

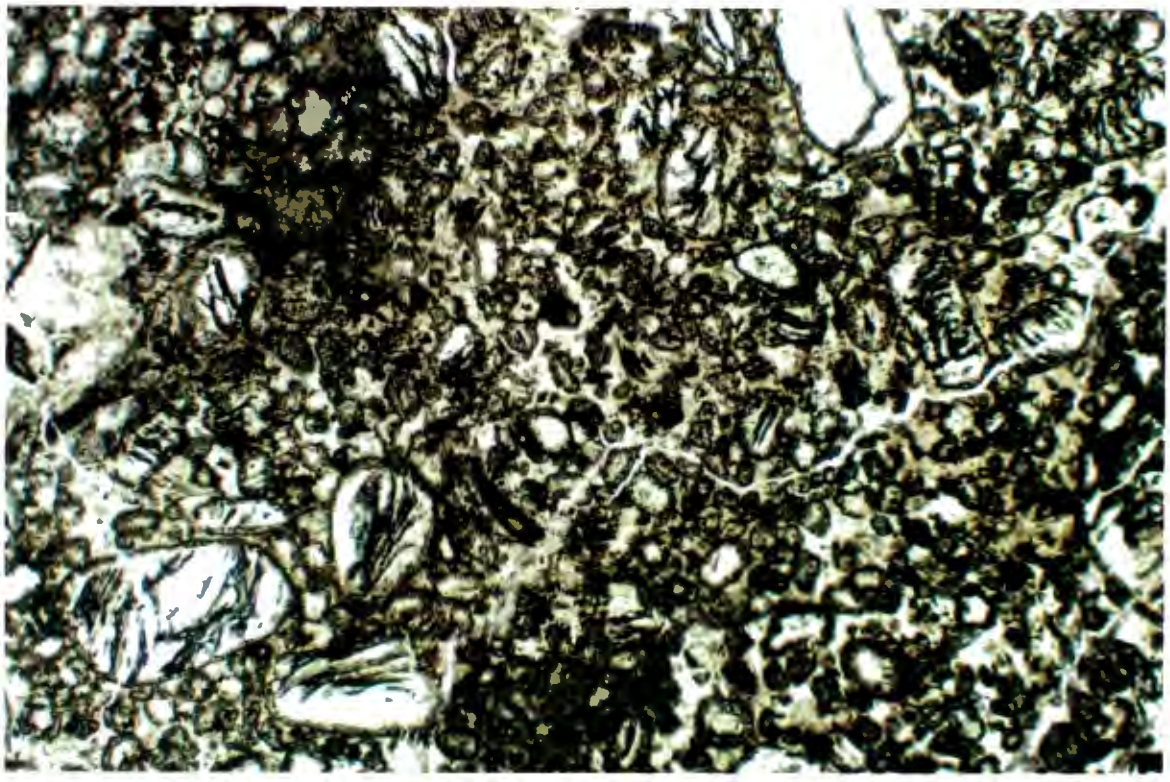

PLATE 3.11 Sample RRM 33 , Eastern tuffisitic kimberlite.

Another example of spherical or less regular segregationary texture in the eastern tuffisitic kimberlite. Note the abundance of acicular diopside laths. Fine grained perovskite (pv) and opaques can be observed in the groundmass.

Base of photomicrograph equals 1.8 mm.

PLATE 3.12 Sample RRM 31 , Eastern tuffisitic kimberlite.

Macrocrysts of olivine pseudomorphs occuring in association with small spherical or less regular segregations which are less distinct at lower magnification than in Plate 3.11 . Very few fine grained perovskite crystals can be observed in the groundmass.

Base of photomicrograph equals 8.3 mm.

3.2.4 Sandy/Crystal Tuff

3.2.4.1 Macroscopic Description

The sandy/crystal tuff has got a sandstone like appearance due to the abundance of quartz and feldspar in it. It is either reddish-brown (when iron oxide stained) or green in colour. Cross-bedding and graded bedding is evident in some of the blocks, suggesting a reworked crater-facies origin. In certain instances, pelletal lapilli cored by olivine pseudomorphs or country rock fragments are conspicuous. Clay minerals constitute the greater proportion of the groundmass.

3.2.4.2 Microscopic Description

Lithic country rock fragments are by far the major constituents comprising about 60-70% of the rock [Plates 3.13 and 3.14]. These xenoliths are mainly quartz, feldspar and granitic or paragnissic fragments. Some preferred orientation of the fragments is conspicuous in some sections [Plate 3.14]. This preferred orientation is most likely a result of sedimentary processes.

Pelletal lapilli cored by olivine pseudomorphs and the lithic fragments [Plate 3.13] often do occur. Olivine pseudomorphs form a lesser constituent (10 - 20%)of the kimberlite.

Rare perovskite grains and medium to coarse grained spinels (up to 0.1mm) and constituting 2-3% of the kimberlite together with fine grained clays make up the groundmass.

The groundmass around the pellets was found to be too altered to render a mineralogical classification.

3.13

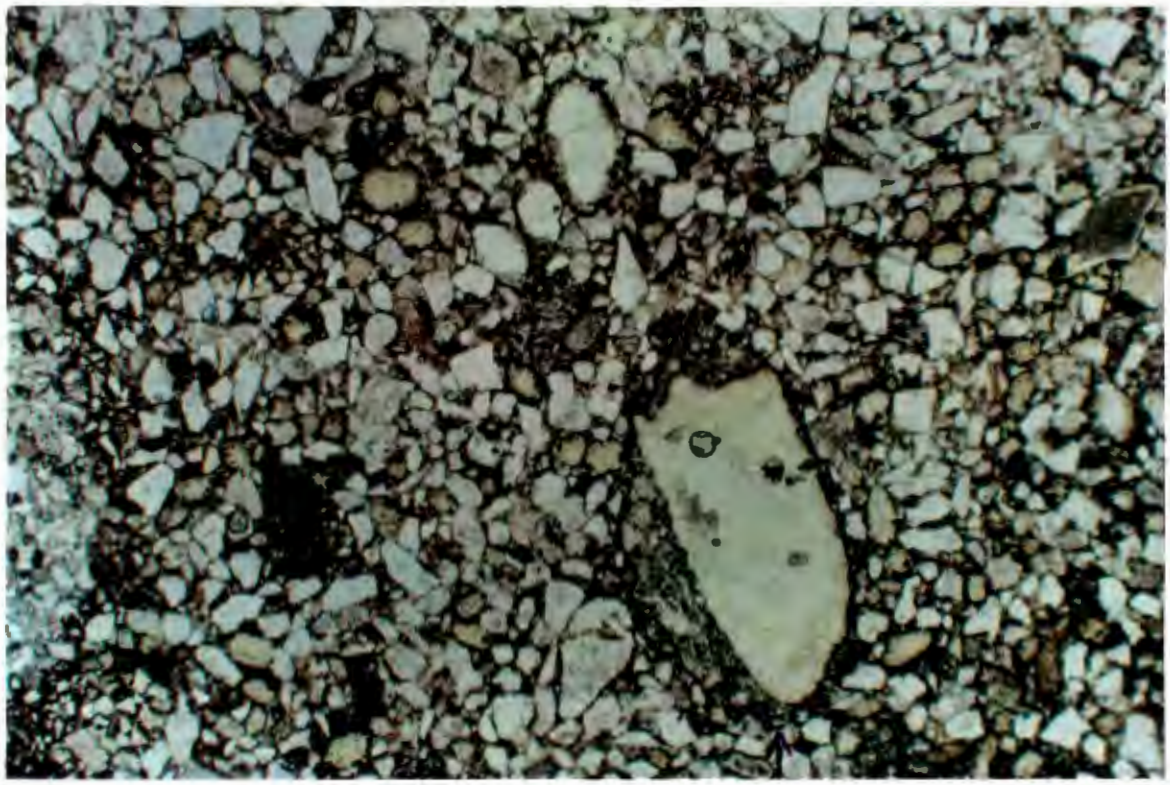

3.14

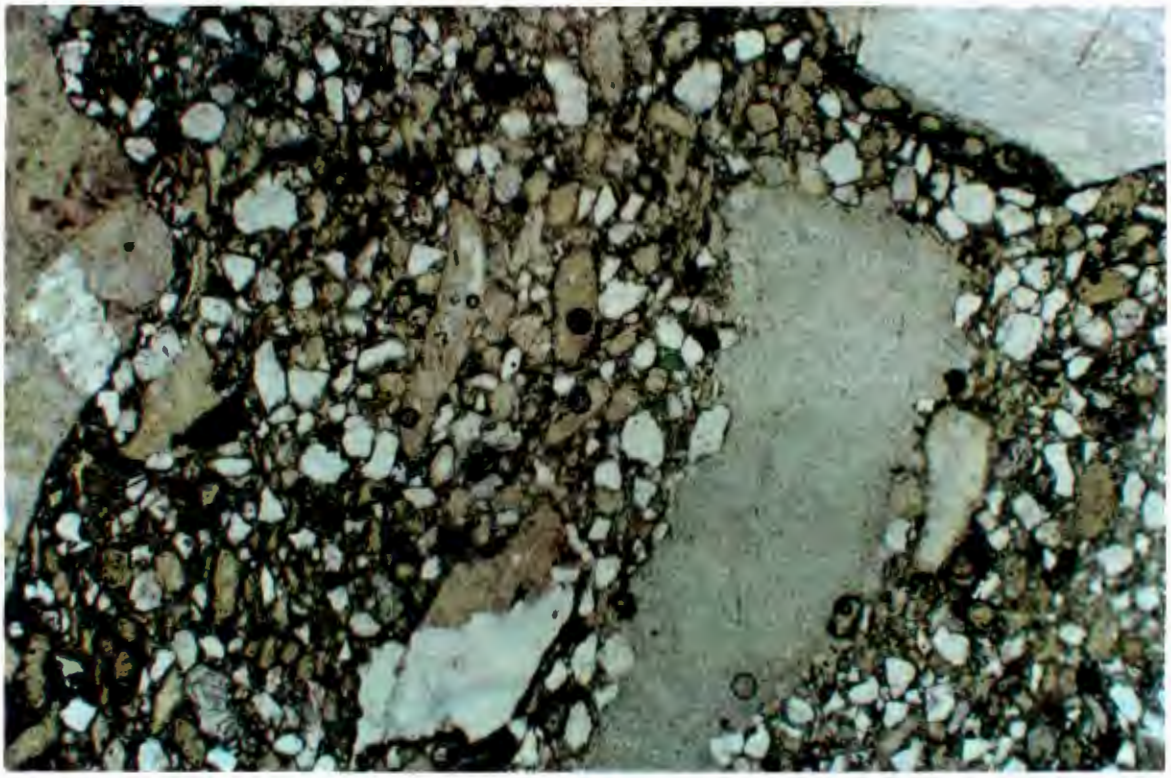

PLATE 3.13 Sample RRM 8 , Sandy tuff.

Pelletal lapilli development in sandy tuff. The pellets are cored by country rock fragments. Note the abundance of lithic country rock fragments which are mainly quartz.

Base of photomicrograph equals 8.3 mm.

PLATE 3.14 Sample RRM 28 , Sandy tuff.

Preferred orientation of lithic country rock fragments of quartz and feldspar in the sandy tuff. The preferred orientation is a result of sedimentary reworking of the sandy tuff.

Base of photomicrograph equals 8.3 mm.

3.2.5 Tuff-Bearing Breccia

3.2.5.1 Macroscopic Description

The tuff-bearing breccia is distinguished from the TKB by the presence of crystal and sandy tuff fragments. The tuff fragments can vary in size from less than 1cm to about a metre. The country rock fragments are the same as those already described in the TKB. Olivine pseudomorphs in a fine grained matrix of serpentine complete the mineral composition.

3.2.5.2 Microscopic Description

Plate 3.15 shows a contact feature of a sandy tuff fragment in a tuff-bearing breccia. The right hand side shows part of the sandy tuff fragment with abundant lithic country rock fragments and a lithic TBB kimberlite to the left.

The TBB kimberlite contains macrocrystic olivine pseudomorphs and lithic fragments of quartz and feldspar in an altered matrix of fine grained serpentine and clays, medium to coarse grained spinels and rare perovskite. The spinels are up to 0.1mm in size and constitute approximately 1% of the kimberlite.

The mineralogical classification of this kimberlite phase is difficult as the groundmass is too altered.

3.2.6 Hypabyssal Kimberlite

3.2.6.1 Macroscopic Description

The hypabyssal kimberlite is blue in colour and has a conspicuous macrocrystic texture due to the abundance of olivine pseudomorphs. In certain instances the hypabyssal kimberlite incorporates crustal xenoliths and these are often completely altered. The matrix consists of fine grained serpentine.

3.15

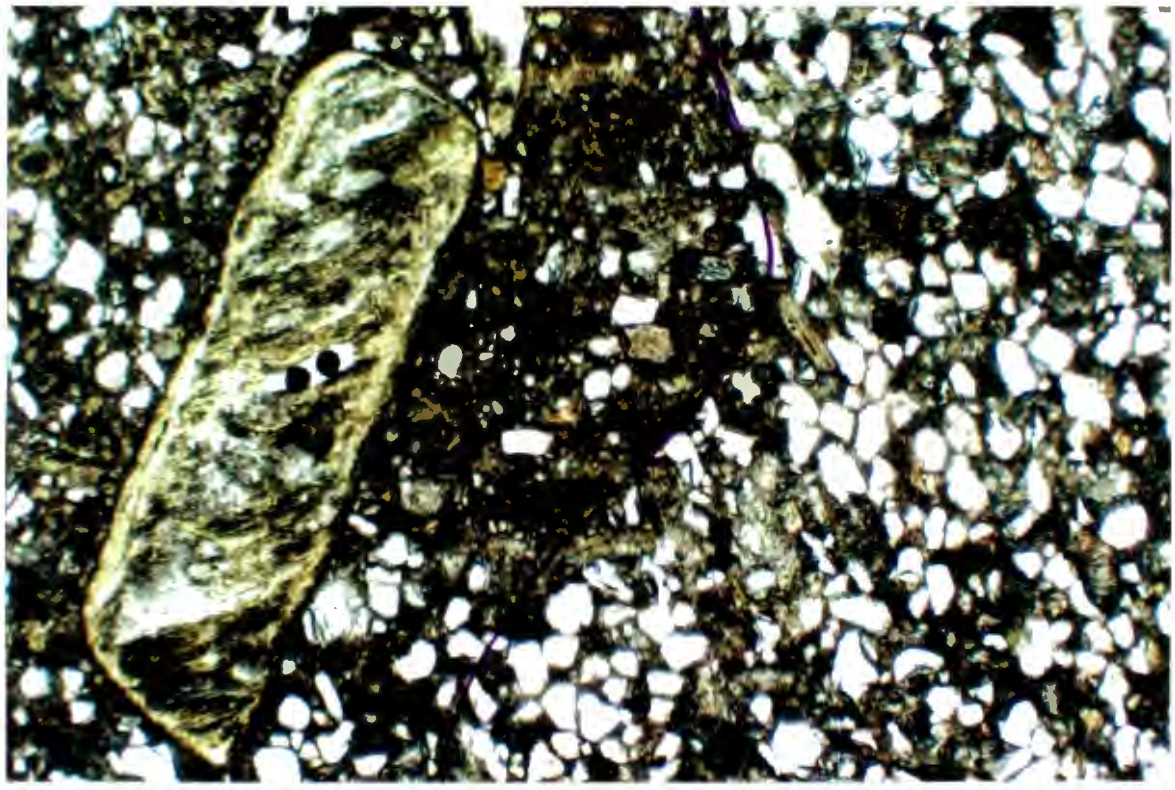

3.16

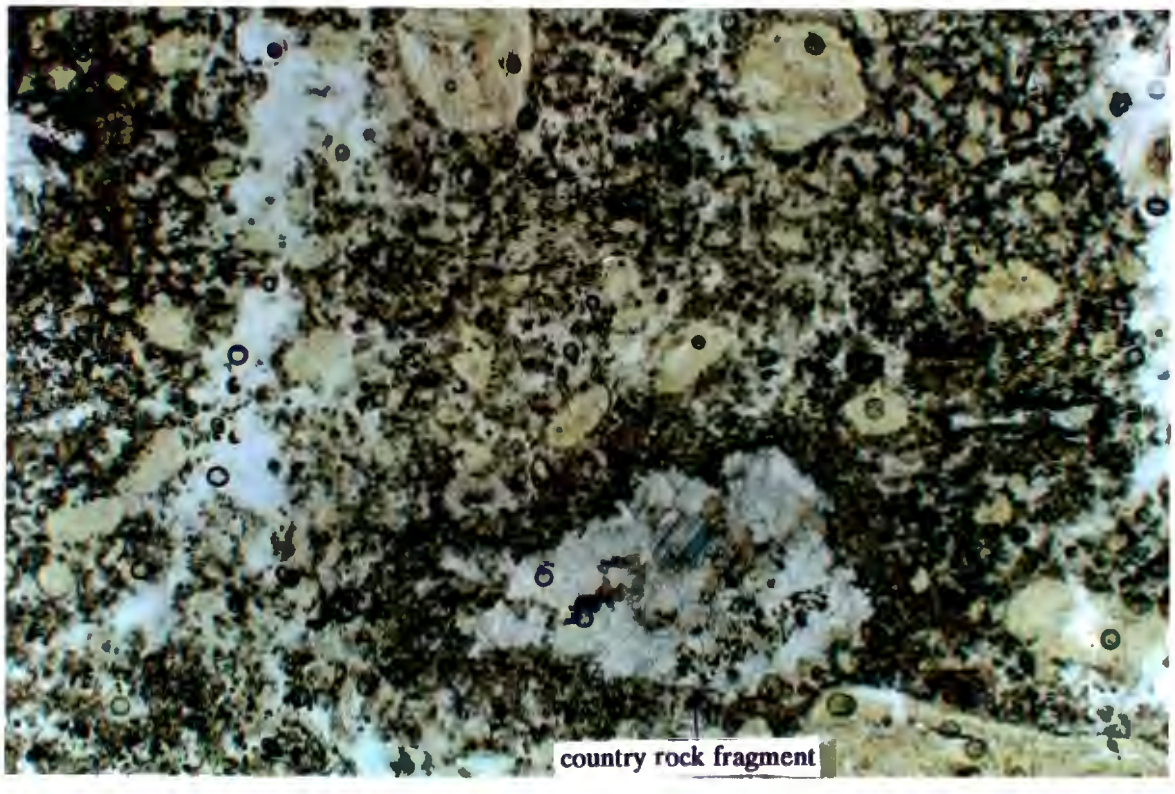

PLATE 3.15 Sample RRM 24 , Tuff-bearing breccia.

A contact feature of a sandy tuff fragment (right) in a tuff-bearing breccia(left). The sandy tuff fragment shows less distinct preferred orientation of grains. Fine grained serpentine and clay comprise the groundmass of the tuff-bearing breccia.

Base of photomicrograph equals 8.3 mm.

PLATE 3.16 Sample RRM 6 , Hypabyssal kimberlite.

A fragment of probably country rock material that has been altered to calcite. The edges of the fragment show evidence of corrosion due to reaction with the magma.

Base of photomicrograph equals 8.3 mm.

3.2.6.2 Microscopic Description

Plate 3.16 shows subrounded to rounded olivine pseudomorph macrocrysts with an abundance of opaques and a country rock fragment with corroded edges. There is evidence of a segregationary texture shown by the concentration of spinels on the rims of the olivine pseudomorphs [Plates 3.17 and 3.18].

Fine grained serpentine, coarse diopside [Plates 3.17 and 3.18] and abundant perovskite and spinels constitute the goundmass mineralogy. The spinels are coarse grained (up to 0.2mm) and constitute approximately 20 - 30% of the kimberlite.

The hypabyssal kimberlite is a perovskite-bearing opaque-mineral-rich diopside kimberlite.

3.17

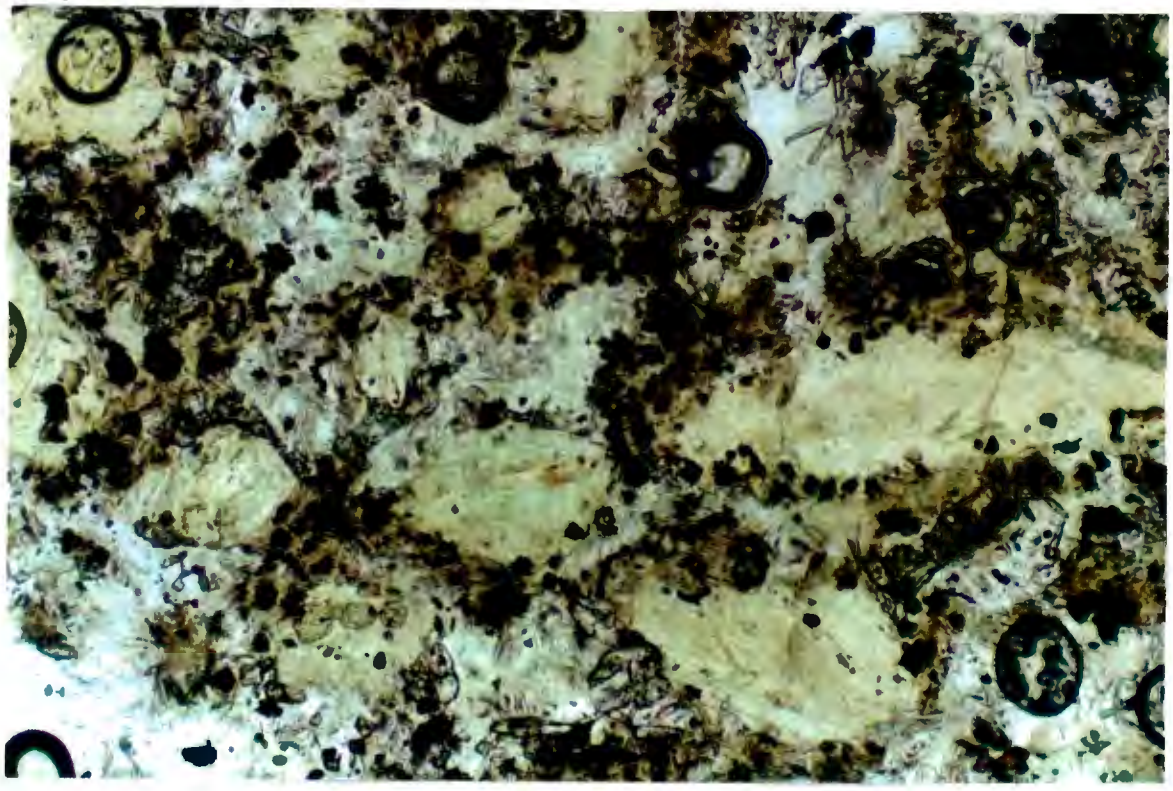

3.18

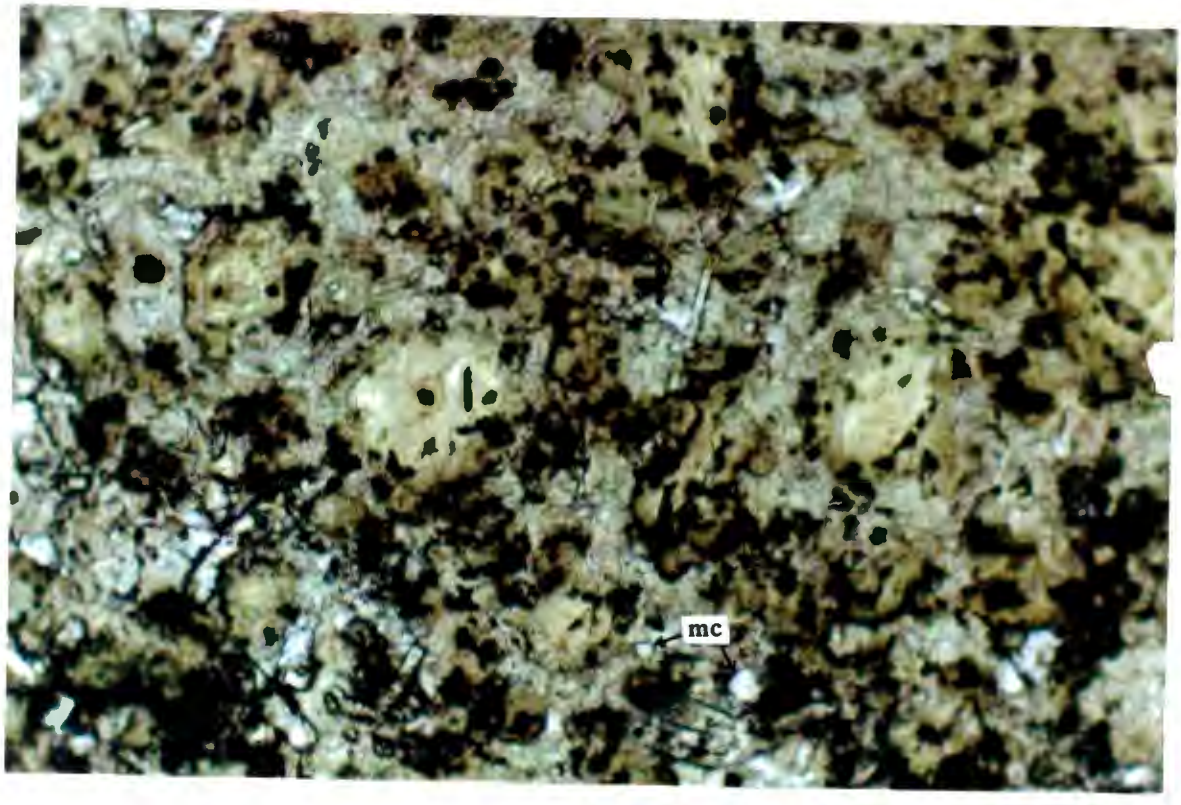

PLATE 3.17 Sample RRM 6 , Hypabyssal kimberlite.

Magnified section of plate 3.16 showing segregationary texture of opaques and perovskite and diopside surrounding the rims of olivine pseudomorphs.

Base of photomicrograph equals 1.8 mm.

PLATE 3.18 Sample RRM 35 , Hypabyssal kimberlite.

Segregationary texture as in plte 3.17. There is both fine and coarse grained diopside and monticellite (mc) can be observed in the groundmass.

Base of photomicrograph equals 1.8 mm.

4. RIVER RANCH DIAMONDS

4.1 INTRODUCTION

Diamonds from individual kimberlite sources show distinctive features with respect to such physical properties as size, colour, morphology and crystal clarity. Several studies (eg. Harris et al, 1975; Robinson, 1979; Robinson et al, 1989) showed that diamond characteristics for a particular source varied with the size of a diamond. Detailed studies of diamonds from a number of localities have also shown that within the individual localities multiple sub-populations of diamonds can exist. These sub-populations can be recognised on the basis of physical characteristics, inclusion paragenesis and stable isotope composition (Gurney, 1989). In this study, physical features of the diamonds are described from several size categories. The descriptions are based on Rombouts (1990) classification scheme. The Rombouts classification scheme is utilised in the TERRAC computer programme for the valuation of rough diamonds . In this scheme, diamonds are categorised in terms of their weight, form, colour and clarity (ie. intensity of inclusions and fractures). The classification scheme of Harris et al (1975) was also followed to describe the morphology of the diamonds, which TERRAC does not do.

Run-of-mine production was collected and analysed. Successive batches of diamonds were screened using Pierre sieves. The different screen sizes were each studied separately. In all, 10351 diamonds were individually inspected. Diamonds from every phase of the kimberlite were collected and results obtained and discussed in this study are therefore a true reflection of variations seen across the whole River Ranch diamond population. Unless otherwise stated, all the diamond distribution analyses throughout the study are expressed as a percentage of the number of stones and not as carats.

4.2 CLASSIFICATION SCHEME

4.2.1 Size Distribution

The Pierre sieve sizes used in this study are the marketing sizes used at River Ranch (ie. 5, 9, 11, 15, 18 and 21). In all, seven size categories were analysed (ie. -5, -9 + 5, -11 + 9, -15 + 11,

-18 + 15, -21 + 18 and +21). In the text, only the lower aperture size within a specific range is used (eg. the range -9 + 5 would just be quoted as +5). The Pierre sieve sizes used and the corresponding aperture sizes in millimetres are tabulated below.

Sieve Class	Diameter (in mm) of aperture (lower screen)	Average weight in carats (per stone)
+21	4.50	1.85
-21+18	4.18	0.57
-18+15	3.50	0.39
-15+11	2.65	0.20
-11+9	2.25	0.11
-9+5	1.50	0.05
-5	<1.50	0.02

The lowest (-5) and the highest (+21) ranges would include diamonds with a very wide range as these size ranges do not have lower and upper limits respectively. The breakdown in the number of stones analysed in each size fraction is as follows:-

+21 (n = 4491), +18 (n = 3129), +15 (n = 654), +11 (n = 577), +9 (n = 500),
+5 (n = 500), -5 (n = 500).

4.2.2 Colour

In the colour classification scheme the major colours were used. Within any particular major colour, the diamonds were further classified according to the intensity of the colour. An intensity range of 1 to 4 was used. The intensity is 1 if the colour is only visible as a faint hue, 2 if the hue is easily visible, 3 if the colour is strong and 4 if the colour is so strong as making the stone opaque. This intensity range cannot be used for white or colourless diamonds for obvious reasons. The major colours used are brown, white, grey and yellow. Rare or minor colours were classified as "Other".

4.2.3 Morphology

Five basic crystal forms were identified in the morphological classification namely octahedra, dodecahedra, macle, polycrystalline and fragments. In assigning a diamond to a particular crystal form, the following consideration was adopted after Harris et al (1975):

i. If the stone showed more than 50% of a specific shape it was placed in the relevant basic crystal form.
ii. If the crystal exhibited less than 50% shape (or form) it was designated a fragment.

For the diamond crystals in the octahedron - dodecahedron transition, the 50% rule was effectively applied. No subdivisions were made within this transition category. Figure 4.1 shows stages in the conversion of a diamond octahedron to a tetrahexahedroid. Macles were limited to the flattened octahedral twin on [111]. The polycrystalline form includes all crystal aggregates and any other diamonds with more than one crystal except macles.

4.2.4 Inclusions and Fractures

In this classification, the diamonds are grouped in terms of inclusion content and fracture intensity in them. An intensity range of 0 to 5 was used with 0 being a stone with no inclusion or fracture in it and 5 being a totally opaque crystal due to many inclusions and/or fractures. No account was taken of the type, colour or position of the inclusion or fracture within the diamond. The study was done on the four major colours found at River Ranch. No inclusion or fracture study was done on the rare colours.

4.3 RESULTS

A number of graphs were plotted in order to investigate the variation of the diamond physical properties with size range.

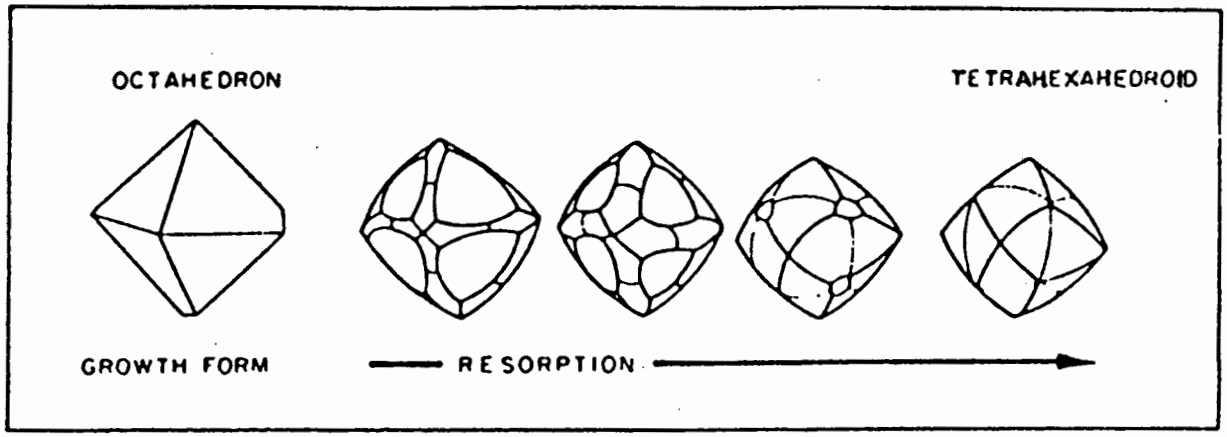

Figure 4.1 Stages in the conversion of a diamond octahedron to a tetrahexahedroid (After Robinson et al, 1989).

4.3.1 Size Distribution Analysis

Figure 4.2 is a distribution graph plotted from the computer programme, TERRAC, after all the diamonds are analysed using Rombouts classification. The distribution approaches a lognormal distribution. Rombouts (1990) established that diamond populations can be tested for lognormality by plotting size distributions on lognormal graph (Figure 4.2). Deviations from the lognormal model can be due to mixing of different stone populations within a deposit (eg. mixing eclogitic and peridotitic diamonds). The lognormal graph can provide information on how large a proportion of respective stones, carats and dollars are provided by different size fractions of the diamond population. Figure 4.2 shows that of the River Ranch diamond population, 50% of the value comes from the diamonds that are greater than 2 carats.

4.3.2 Colour

The total colour distribution is illustrated in Figure 4.3. About half the total population of the River Ranch diamonds are brown (50.9%). The white diamond population is the second largest with 26.1% followed by the grey colour with 21.2%. Yellow diamonds are very rare, constituting only 1.7% of the total population. There are some very rare diamond colours which have been classified under the "Other" category. These are very rare pink stones and even scarcer green diamonds, together constituting only 0.1% of the total population.

4.3.2.1 Colour vs Size Relationship

A colour-size relationship is illustrated in Figure 4.4. The percentages calculated for every colour are per individual size fraction and are not expressed as per total diamond population.

The brown diamond population increases from the -5 size range to the +21 size range. The -5 size range has the lowest percentage of 27.6% while the highest percentage of 56.0% is in the +18 size range.

The white diamonds decrease from the -5 size range to the +21 size range. The -5 size range has 43.3% while the +21 size range has22.8%.

Figure 4.2 The distribution of the number of stones, the amount of carats and the amount dollars for each size class as plotted on the lognormal graph (after Rombouts, 1990).

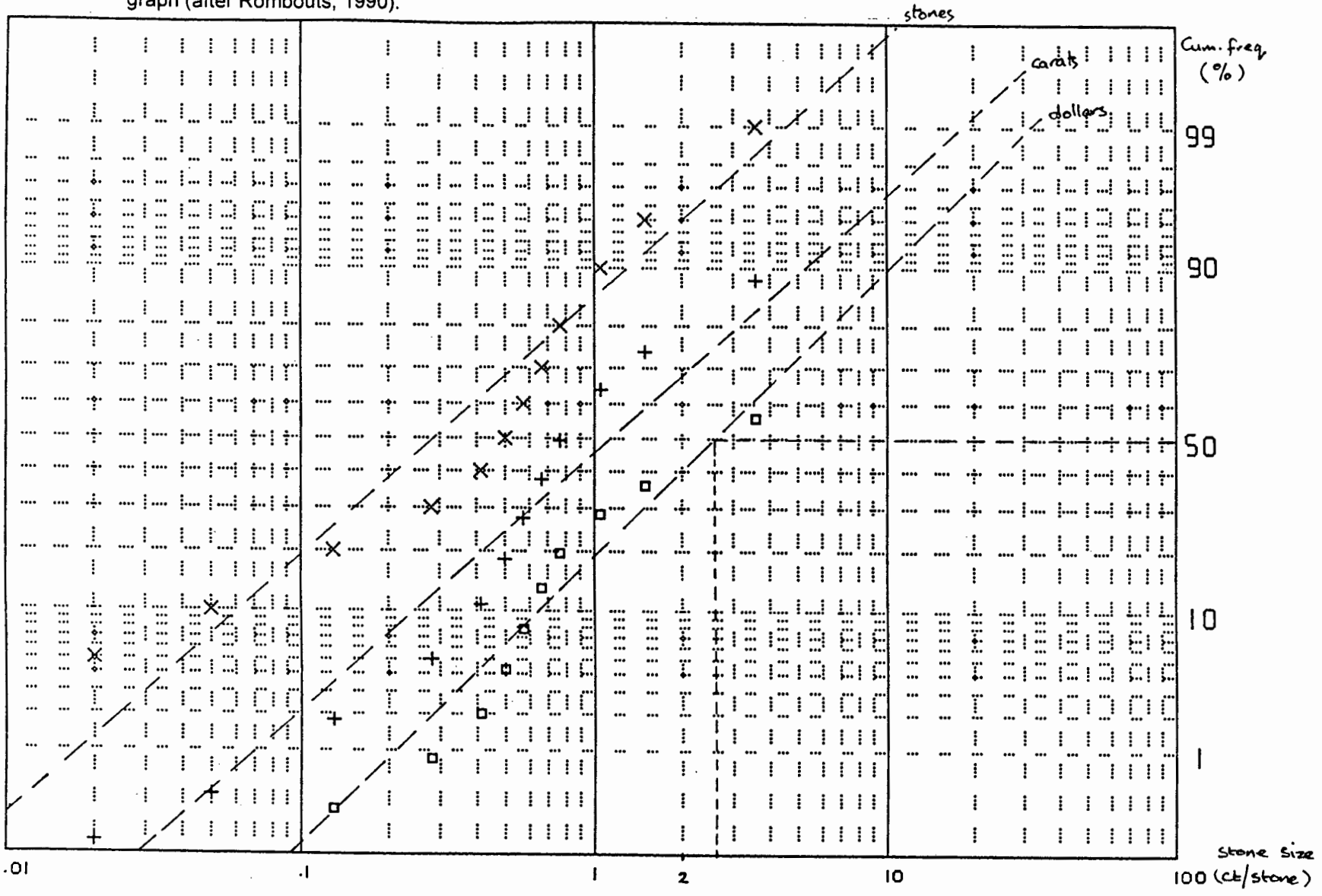

Lognormal graph: Cumulative frequency vs. size
x=stones, +=carats, o=dollars

Figure 4.3

RIVER RANCH DIAMONDS
total population colour distribution

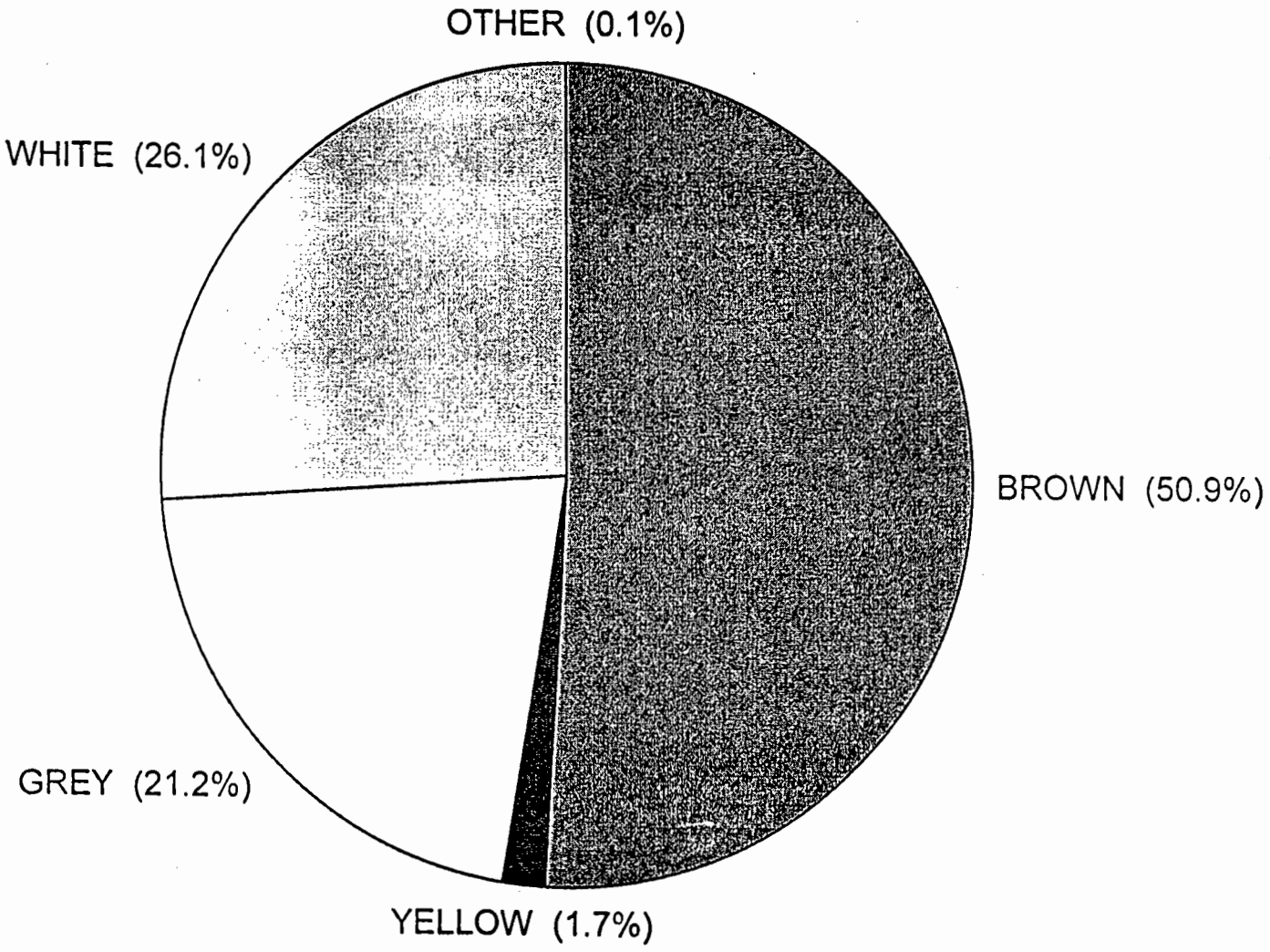

Figure 4.4

RIVER RANCH DIAMONDS
colour vs size relationship

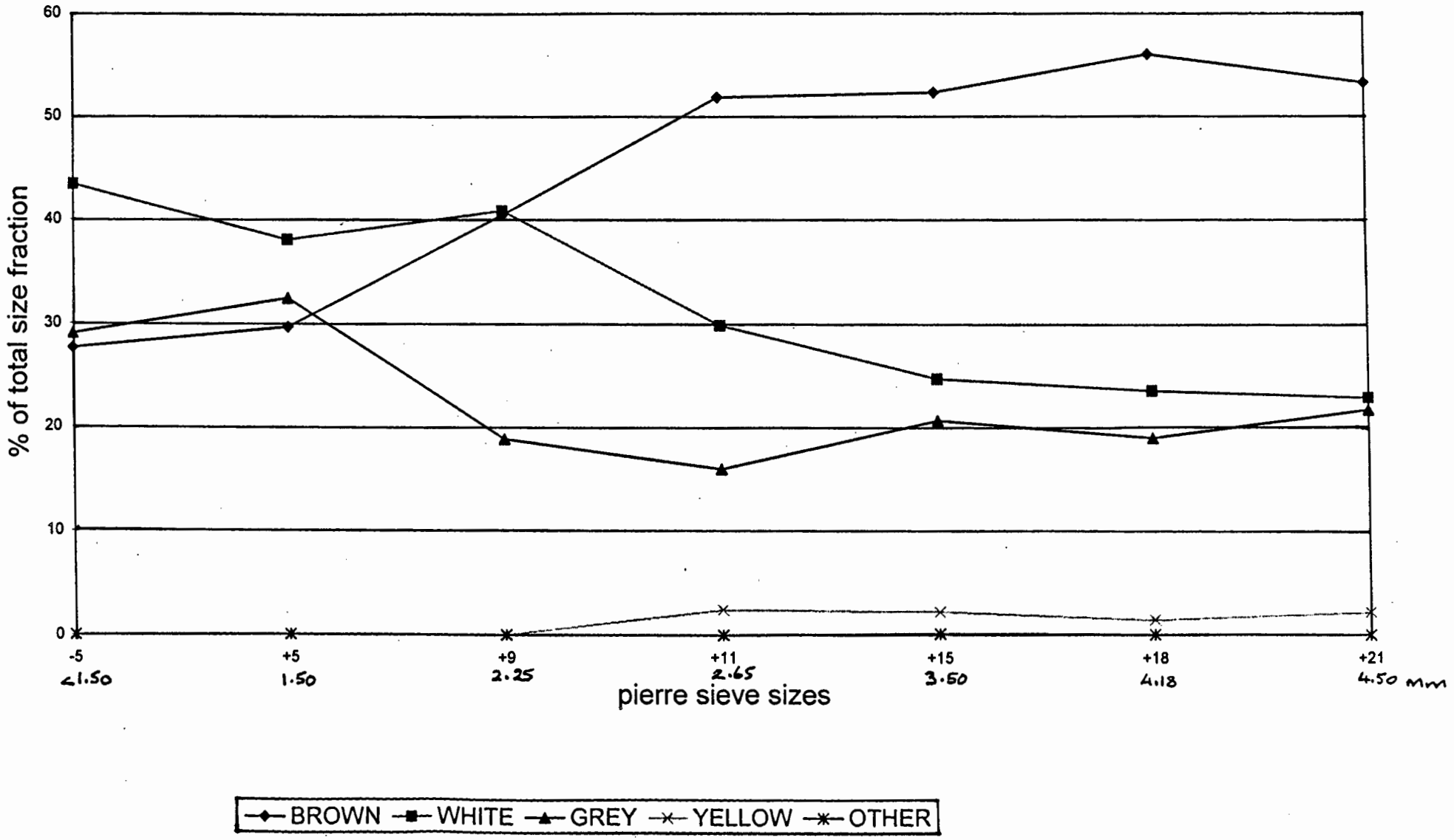

However the above trends may be deceiving because colours are more easily recognised in the larger stones than in the small sizes, which may lead to the detection of more browns in the larger diamonds.

Grey diamonds show a general decrease from the -5 size range to +21 . The highest percentage of 32.4% is in the +5 size range with the lowest percentage of 15.9% in the +11 size range.

There were no yellow diamonds in the -5, +5 and +9 size ranges. There is however a fairly constant distribution of the yellow diamonds in the other upper size ranges.

Diamonds with rare colours were found only in the +15 and +18 size ranges, but no particular significance is postulated to that. Probably other sizes of diamonds of rare colour would be found in a larger sample.

4.3.2.2 Colour Intensity vs Size Relationship

Analysis of the colour intensity - size relationship was done for the brown, grey and yellow coloured diamonds. An intensity scale of 1 to 4 was used with 4 being the deepest colour.

The brown diamonds are dominated by light coloured stones with an intensity of 1 which show an increase in percentage from -5 size range to +21 size range (Figure 4.5 and Appendix 4.2). There is a general decrease in the abundance of stones from light coloured stones (intensity 1) to the darkest colour (intensity 4). However there is an increase in the percentage of brown diamonds from the -5 size range to the +21 size range for all the intensity scales. This may be an artefact in that depth of colour appears more intense in a larger stone, as mentioned earlier.

The grey diamonds show a general decrease in population for every intensity scale from the -5 size range to the +21 size range (Figure 4.6 and Appendix 4.2). The light grey coloured diamonds (intensity 1) dominate over the rest of the colour intensities. There is a general decrease in population of stones from the light coloured grey diamonds (intensity 1) to the dark coloured diamonds (intensity 4).

Figure 4.5

RIVER RANCH DIAMONDS
brown colour intensity vs size

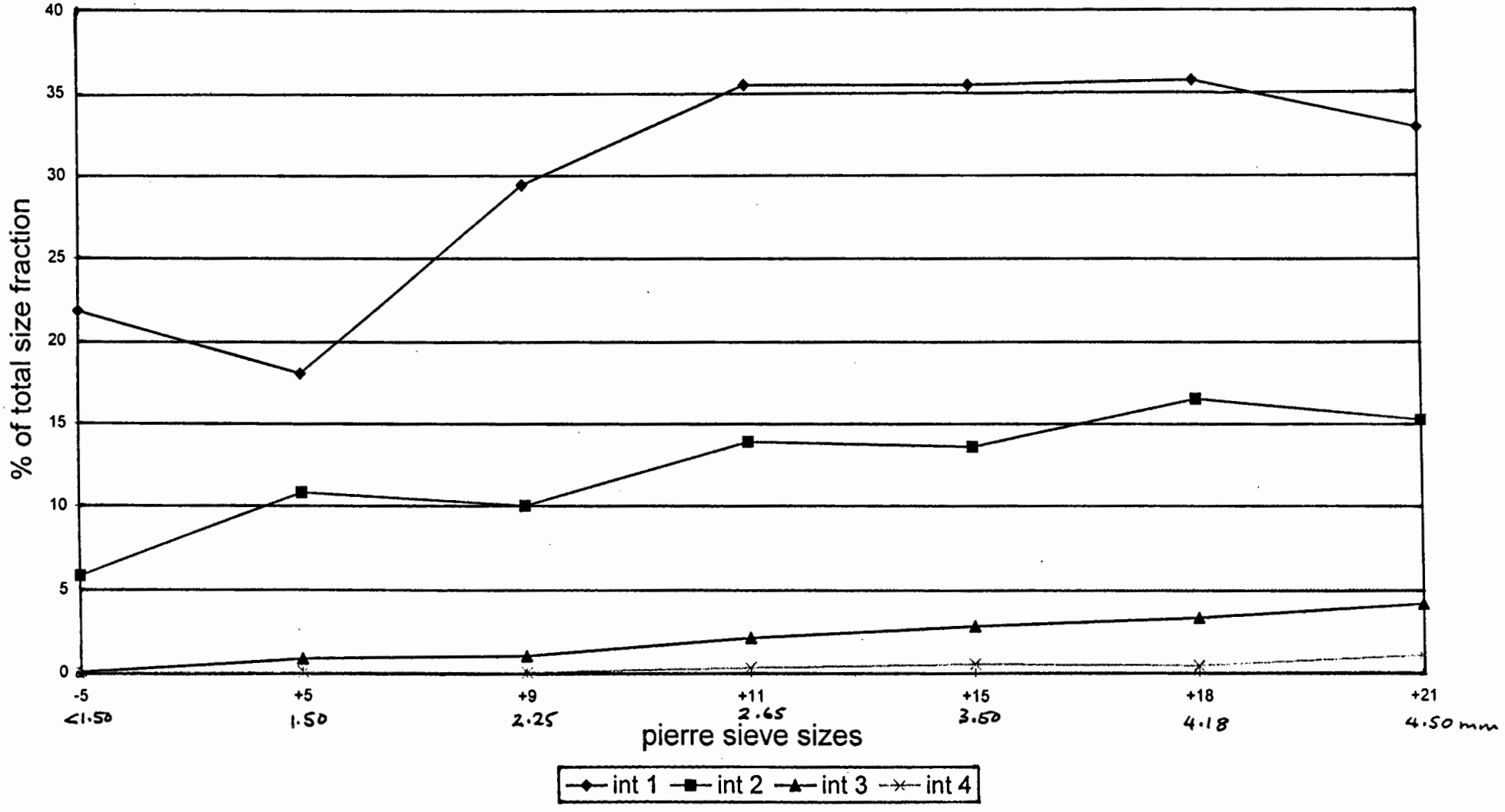

Figure 4.6

RIVER RANCH DIAMONDS
grey colour intensity vs size

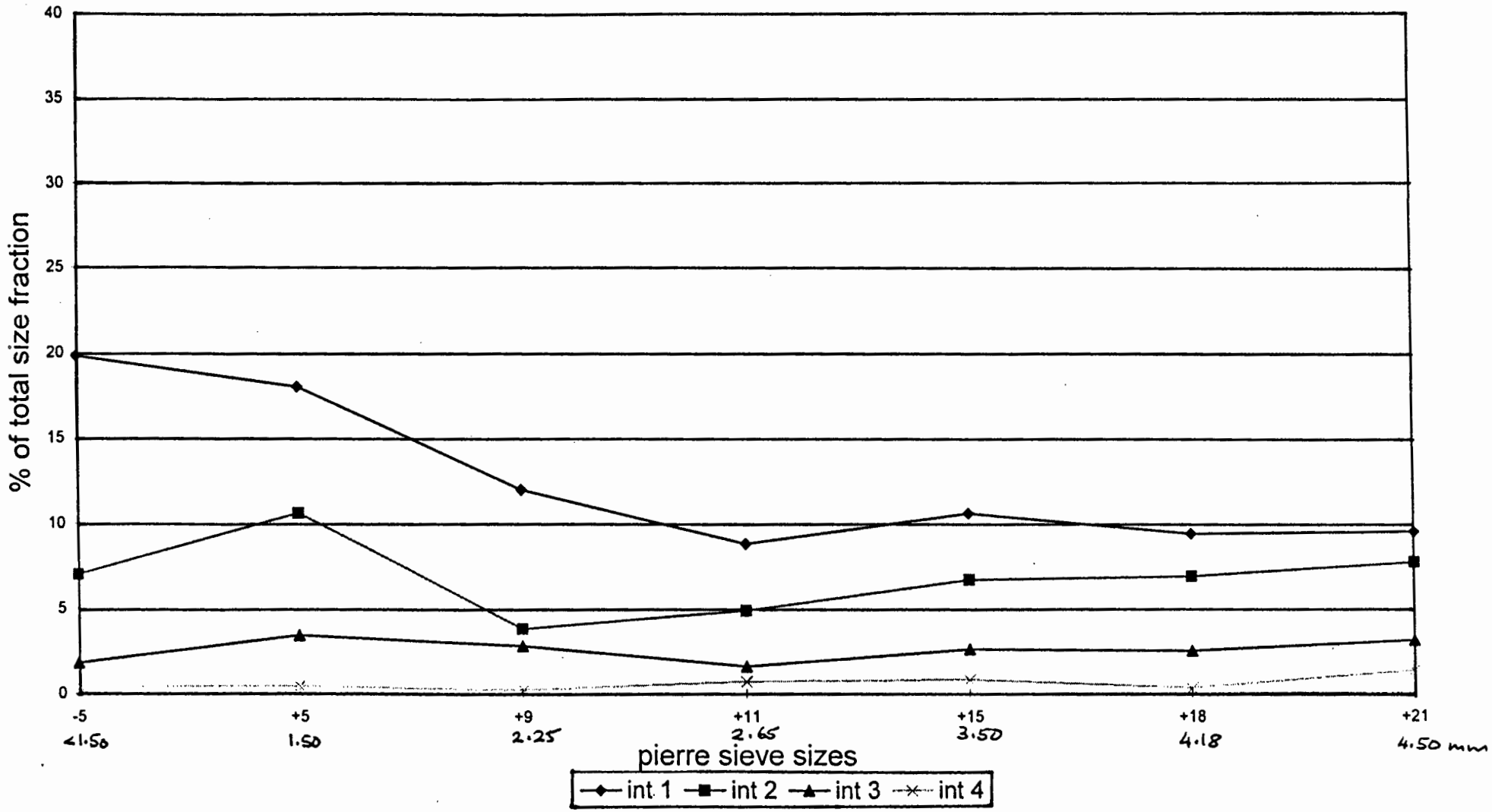

The yellow diamonds are too few to show any meaningful trend. For the size fractions in which the yellow diamonds were observed, there is a general constant percentage over the size ranges (Figure 4.7 and Appendix 4.2).

Overall the deep coloured diamonds (ie. diamonds with an intesity of 4) are very few and the predominant stones are the ones with a faint hue (ie. intesity of 1) for all the colours.

4.3.3 Morphology

The total population morphology distribution is illustrated in Figure 4.8. The fragments constitute the largest population with 47.8%. The dodecahedral shaped diamonds contribute the second largest population with 34.3%. Macles and polycrystalline diamonds constitute 6.2% and 6.0% respectively while the octahedral population constitute the least with 5.7%.

There is no evidence that any particular shape of diamond is preferentially broken relative to another for all the diamonds inspected. The true proportions of the various recognisable morphologies in the primary diamond suite at River Ranch is probably best represented therefore by ignoring the fragments. This approximates to multiplying the percentages of the other morphologies by two.

Rapidly formed diamonds such as aggregates of microcrystallites (framisite, stewartite), fibrous spheres (ballas), fibrous cubes and diamonds commonly coated with a fibrous overgrowth are extremely rare at River Ranch, since none were observed in this study. These observations are important in the assessment of the likelihood of a correlation existing between macro-diamond and micro-diamond populations as discussed later.

4.3.3.1 Morphology vs Size Relationship

The morphology - size relationship for the total population is illustrated in Figure 4.9. The percentages calculated for every crystal shape is per individual size fraction and is not expressed as a percentage of the total population. For ease of analysis, the relationship of each individual diamond morphology with size fraction is analysed.

Figure 4.7

RIVER RANCH DIAMONDS
yellow colour intensity vs size

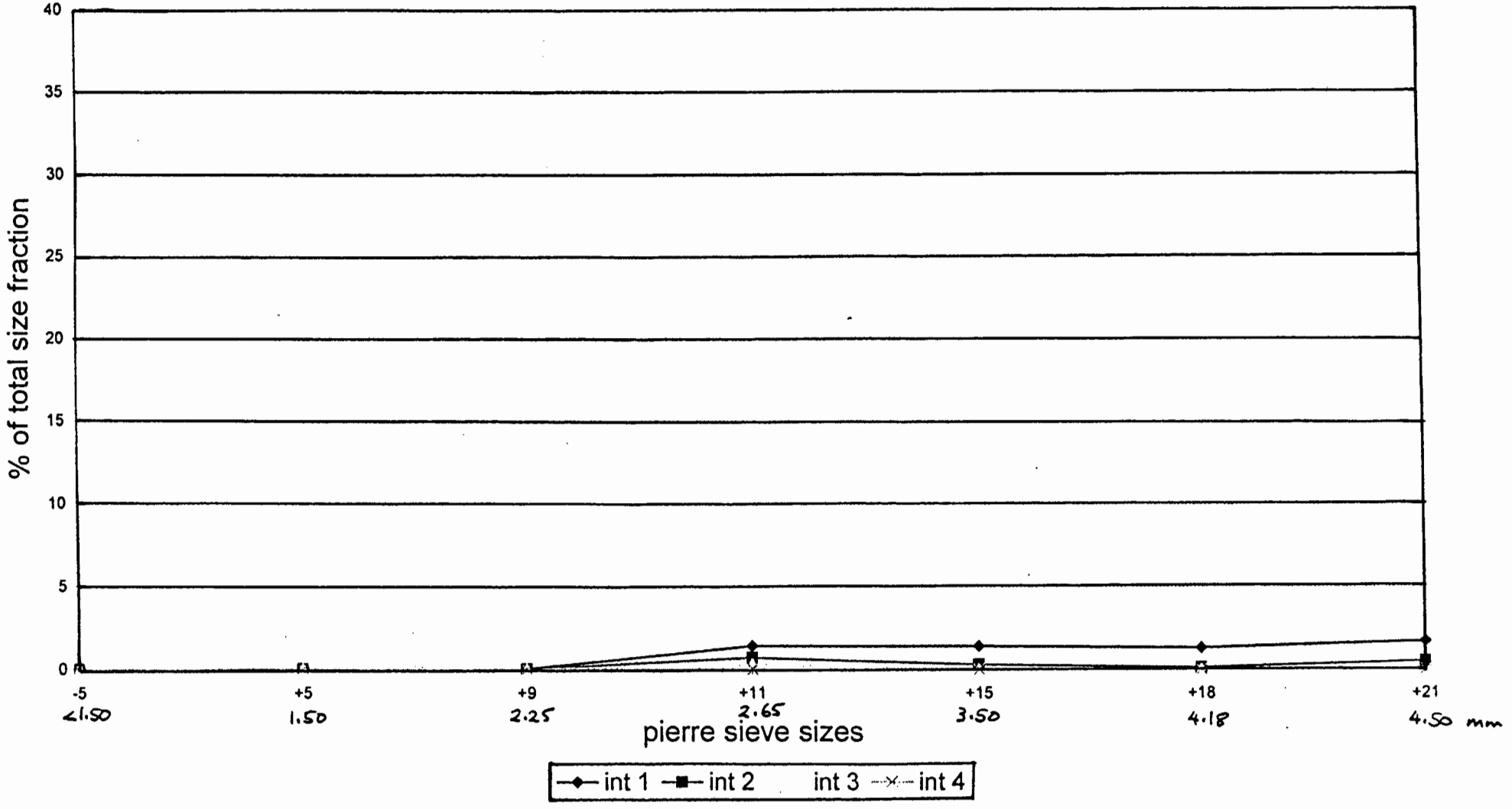

Figure 4.8

RIVER RANCH DIAMONDS
total population morphology distribution

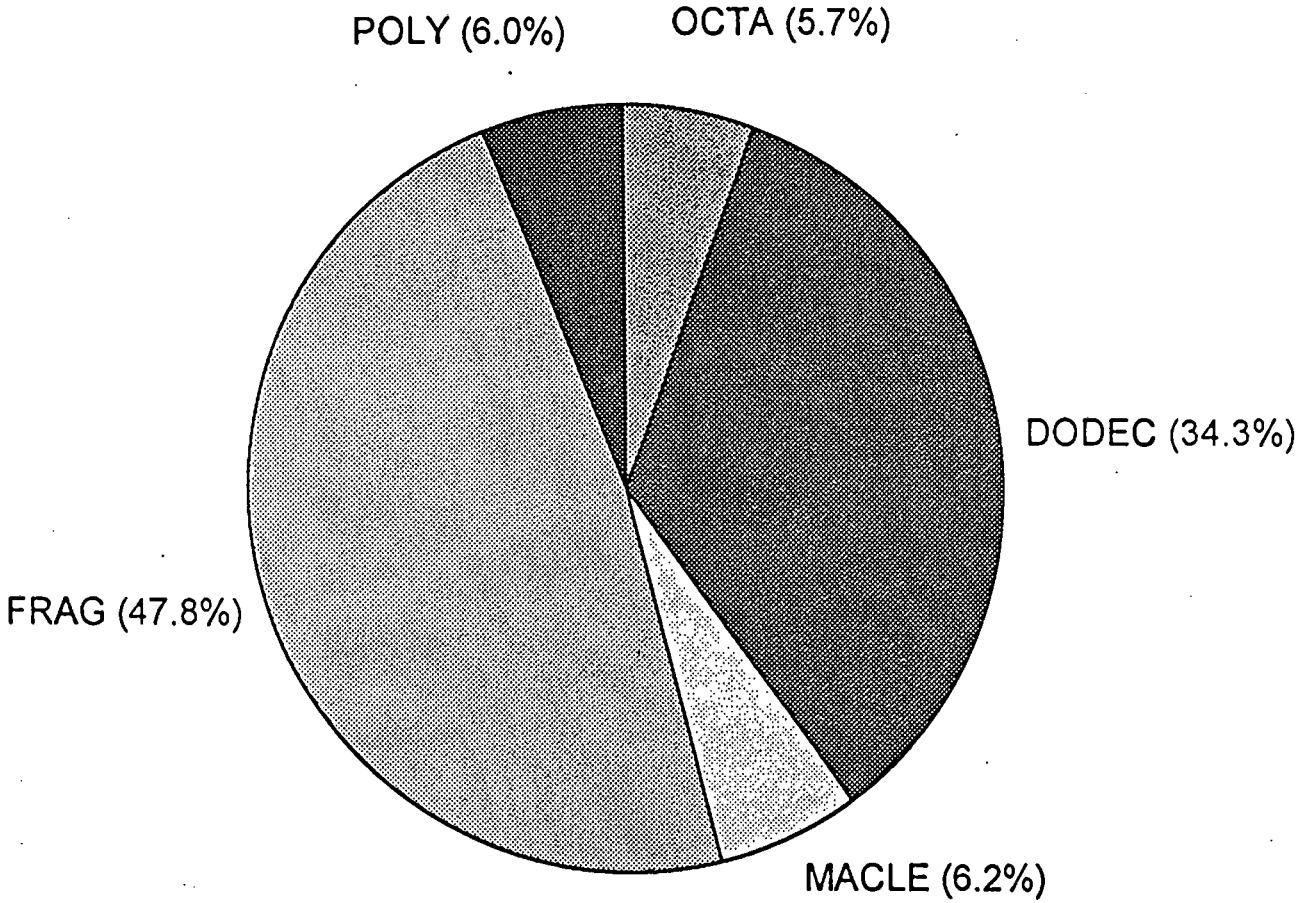

4.3.3.1.1 Octahedra

The octahedral diamonds show a constant proportion of about 10% between the -5 and +11 size range. There is an increase in the proportion to 15% around the +15 size range and then a marked drop in the larger size fractions (2.5% for +18 and 4.4% for +21).

4.3.3.1.2 Dodecahedra

There is a steady increase of dodecahedral diamonds from -5 to +18 size range. The highest proportion is in the +18 (44.0%) while the lowest is in the -5 (22.8%). There is however a drop in the dodecahedron proportion in the +21 size range (30.1%).

4.3.3.1.3 Macles

The macles also show a steady increase in proportion from the -5 to the +15 size range. The highest proportion of macles is in the +15 size range (8.4%) while the lowest is in the -5 (1.2%). There is a decrease in the +18 and +21 size ranges where percentages of 7.4% and 6.4% were obtained respectively.

4.3.3.1.4 Polycrystalline Diamonds

Polycrystalline diamonds develop from crystal aggregation. No detailed study of the individual crystal forms that make up the aggregates was done. Figure 4.9 shows that there is a general decrease in trend of polycrystalline diamonds from the -5 to the +21 size range. The highest proportion of 13.4% is in the +5 size range with the lowest proportion of 3.6% in the +18 size range. In general however these aggregates are not fine grained enough to be termed framisite or stewartite.

4.3.3.1.5 Fragments

Fragments are broken diamonds that have lost more than 50% of crystal size. They constitute the largest proportion of the population. Fragments decrease steadily in proportion from 55.2%

Figure 4.9

RIVER RANCH DIAMONDS
total population morphology vs size

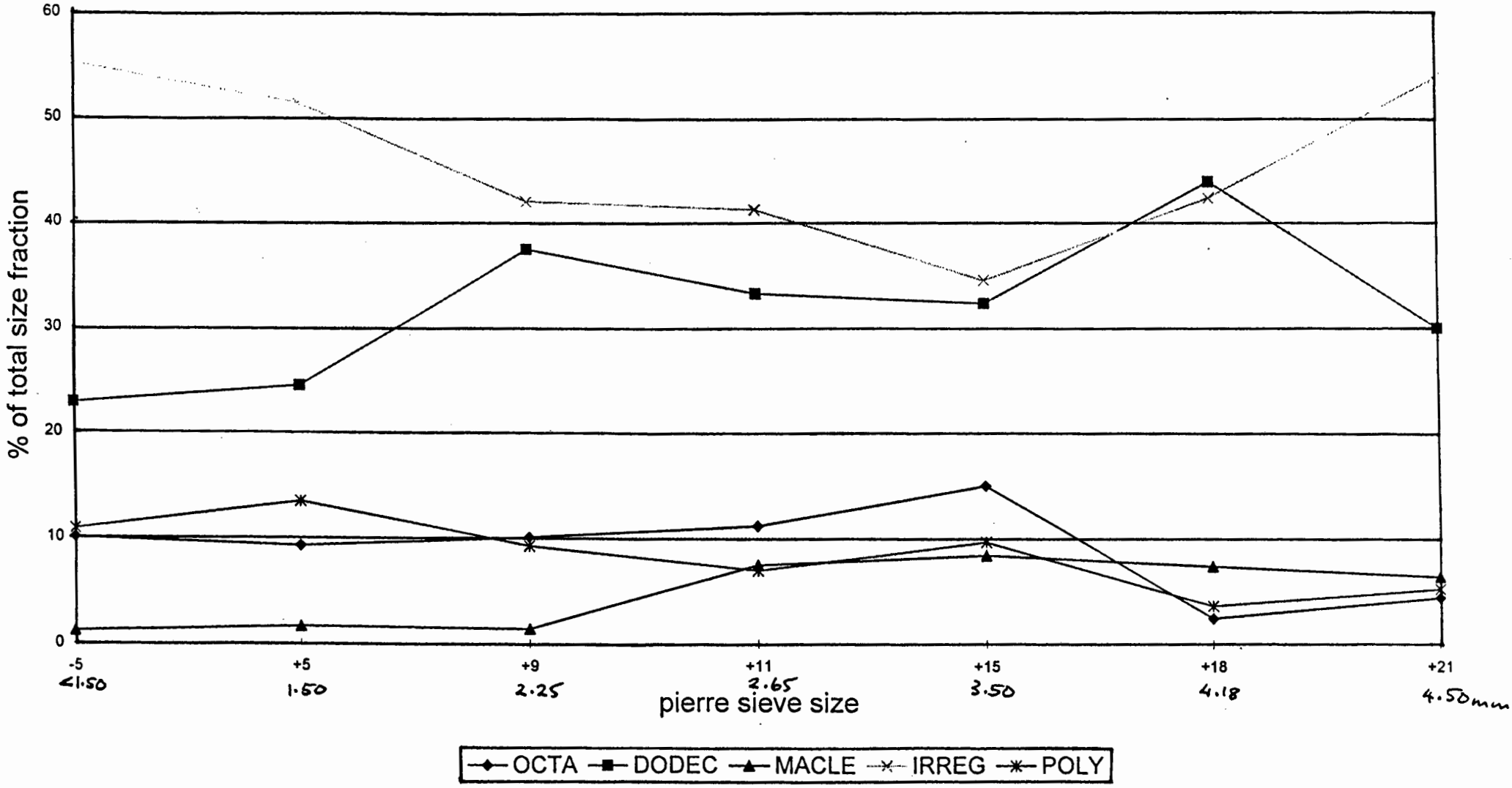

in the -5 fraction to 34.6% in the +15 size range. There is a reversal of the trend in the +18 and +21 size ranges where percentages of 42.4% and 53.8% were obtained respectively.

The large proportion of broken diamonds is most likely to have resulted from natural processes. This is not an unusual phenomenon as the occurence of abundant fragments has been reported from other diamondiferous kimberlites (eg. Robinson et al, 1989). It is highly unlikely that these diamonds could have broken during mining or metallurgical processes. The breakage surfaces observed are often resorbed as reported by Robinson et al (1989). It has been concluded that much diamond breakage is a consequence of stress resulting from differential expansion and contraction, between host and inclusion, during pressure release and cooling. Another reason is the response to stress by diamonds following plastic deformation in the mantle and depressurisation on emplacement. The trend also shows that a large proportion of the small diamonds are small pieces from the larger crystals.

4.3.3.1.6 Octahedron/Dodecahedron Ratio

Diamonds crystallise naturally as octahedra or cubes or combinations of both. The dodecahedral shape usually results from resorbtion. The resorbtion process of diamonds is not completely understood. Resorbtion through reaction with the kimberlite magma is one process through which diamonds lose mass and change shape. However it has also been observed at some localities that diamonds can get resorbed within the enclosing xenolith (Robinson, 1979).

The octahedron/dodecahedron ratio of the diamonds for each size fraction was calculated and is illustrated in Figure 4.10. The ratios show a decrease from 0.44 to 0.27 for the -5 to +9 size range. There is then a steady increase in the ratio to the +15 size range where the graph peaks at 0.46. The lowest ratio of 0.06 was obtained in the +18 size fraction. The +21 size range has a ratio of 0.15. This rapid decline in the ratio is unexpected and could reflect a different size distribution pattern for the two forms.

Robinson (1979) used the octahedron/dodecahedron ratio as a measure of resorbtion, a high ratio reflecting less resorbtion and vice versa. He also pointed out that given equal exposure to

Figure 4.10

RIVER RANCH DIAMONDS
octahedron / dodecahedron ratios vs size

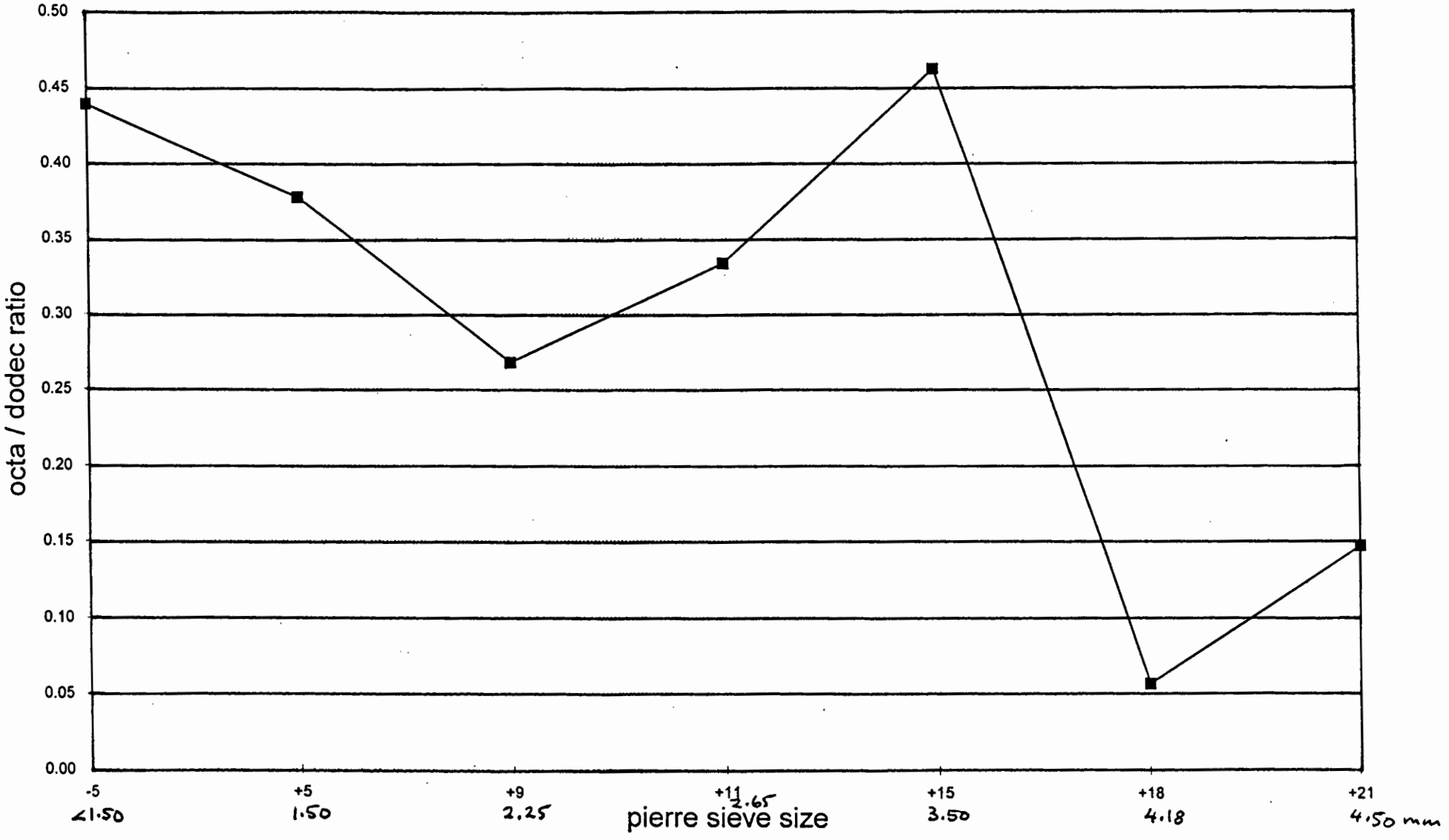

oxidising conditions, micro-diamonds should react out more rapidly than macro-diamonds due to their larger surface area per unit mass, resorbtion being essentially a surface process. On the other hand he also suggested that larger diamonds are more readily liberated from their mantle xenolith host into the kimberlite and may therefore spend longer periods exposed to oxidation conditions in the kimberlite magma. The observed pattern in Figure 4.10 does not fit with either of these contrasting proposals and provides some circumstantial evidence for mixing of multiple diamond populations.

4.3.3.1.7 Summary of River Ranch diamond characteristics

The proportion of diamond fragments is significantly higher than any other single morphology. The proportion of dodecahedral diamonds is much higher than the octahedrons with the octahedron/dodecahedron ratio showing no regular pattern. The high proportion of dodecahedra indicates a significant amount of resorbtion of the diamonds. Macles, polycrystalline and octahedral diamonds make up the balance of the overall population.

An important question is whether or not the dodecahedrons formed in the same event as the primary shapes but had a different subsequent history or did they form in a separate event? Another vital issue is how to deal with the fragments. If a correlation is to be established between macro- and micro-diamond content of the River Ranch kimberlite, how should the fragments be treated statistically? The observations in this study are helpful in revealing that small fibrous diamonds which can dominate micro-diamond populations are virtually absent. Such diamonds are virtually valueless and their presence in abundance complicates correlation studies of macro- and micro-diamonds. Diamonds with yellow colour are rare, whilst white and brown diamonds constitute a major part of the population. This is also a positive aspect. Yellow diamonds have had a thermal history that has been accompanied by nitrogen aggregation producing colour centres. This marks them separate to the white diamonds which either have not experienced the same thermal regime or have lower nitrogen or both. The virtual absence of yellow diamonds is another fact consistent with a simple origin for River Ranch diamonds. The presence of both white and brown diamonds can be compartible with the desirable simple picture since white diamonds can become brown with deformation, a

secondary process.

4.3.4 Inclusions and Fractures

Appendix 4.3 summarises the intensities in the inclusions and fractures for the different colours. Diamonds with an inclusion/fracture intensity of 3 and above are most abundant in the brown and grey colours. The white diamonds show a predominance of clear stones in the large size fraction with high inclusion intensities in the smaller size fraction.

Studies of River Ranch diamond inclusions by Kopylova et al (1995) have shown that more than 99% of the inclusions are harzburgitic garnets. This shows that the peridotitic paragenesis is the most predominant at River Ranch and suggests that the diamond population could therefore be treated as a single population. Work completed in this study is consistent with that interpretation.

4.4 COMMERCIAL ASPECTS

Compared to other diamond producing localities, the River Ranch population falls into the lower than average value category. These diamonds compete in a part of the market that has been in over-supply in the recent past. Argyle diamond mine which came into full production 10 years ago accounts for more than 30 million carats of this market's annual supply. In order to cope with this, a diamond industry was set up in India to cut low quality diamonds. This industry employs about 750 000 people. Although this industry has been successful in coping with high supply volumes, it has been difficult to maintain. In the last four years, in addition, the Russians have released large undefined quantities of these diamonds from the stockpile of their so called technical goods. During the same period the United States government has auctioned approximately 17 million carats of the same quality diamonds from their strategic stockpile. Recently, Argyle has broken off ties with the Central Selling Organisation who have in the past, successfully controlled supply on to the manufacturing market. The net-effect is that the average price of the River Ranch production has steadily declined since the mine came into operation. Direct figures about the average price of the River Ranch goods would be misleading because as mining progressed there has been a steady recovery of the smaller stones

with the upgrading of the recovery plant. Some reduction in the price is due to that. However the current price is not more than 60% of the price, four years ago. This has had an impact on the profit margin of the mine. It is therefore essential to put into place, good grade control hand in hand with effective and efficient mining.

The work that was done in this study was to characterise the diamonds so as to provide a base case study that could be used as a standard against which future production could be characterised. In addition it provides a carefully described set of macro-diamonds that can be compared to micro-diamonds in the same kimberlite with the view of using the latter for grade control in the mine.

In diamondiferous kimberlites, a statistical relationship can exist between the micro-diamond population and the macro-diamonds (Rombouts, 1995). If such a statistical relationship is determined to exist, then micro-diamond counts from small samples can be used to estimate the grade of the commercial size stones. For such a method to be applicable, a relatively stable diamond size distribution is necessary. If variations in stone size distribution occur in different kimberlite phases, then separate micro-diamond / macro-diamond stone number ratios would have to be established for each ore type (Deakin and Boxer, 1989). The diamond inclusion studies of Kopylova et al (1995) which demonstrate that most of the diamonds (>99%) are derived from disaggregated harzburgite is the most significant evidence that the River Ranch diamonds have a comparatively simple origin compared to other localities where eclogitic and occasionally websteritic diamonds are important as well as peridotitic varieties. In respect of the predominance of one paragenesis, River Ranch resembles Argyle. This Australian lamproite has diamonds predominantly sourced from eclogite and an excellent micro- / macro-diamond correlation has been established (eg. Deakin and Boxer, 1989). Whilst some of the observations noted in this study of River Ranch diamonds are equivocal, overall there are ample reasons to suggest that attempts to correlate micro- and macro-diamond contents of the various phases present in the diatreme could provide positive results.

APPENDIX 4.1

RIVER RANCH DIAMONDS

morphology and colour distributions for each size fraction (as a percentage of size total)

PIERRE SIEVE SIZE (+21)

DIAMOND COLOUR	OCTA	DODEC	MACLE	IRREG	POLY	TOTAL
BROWN	1.8	16.3	3.5	29.6	1.9	53.1
WHITE	2	8.6	2.6	9	0.7	22.9
GREY	0.5	4.6	0.2	13.8	2.6	21.7
YELLOW	0.2	0.5	0.1	1.4	0.02	2.22
OTHER	0	0	0	0.04	0	0.04
TOTAL	4.5	30	6.4	53.84	5.22	99.96

PIERRE SIEVE SIZE (+18)

DIAMOND COLOUR	OCTA	DODEC	MACLE	IRREG	POLY	TOTAL
BROWN	0.9	23.9	4.2	25.2	1.4	55.6
WHITE	1.3	12.2	2.8	6.1	1	23.4
GREY	0.2	7.3	0.3	9.9	1.3	19
YELLOW	0.03	0.5	0.06	0.9	0	1.49
OTHER	0	0.03	0	0.06	0	0.09
TOTAL	2.43	43.93	7.36	42.16	3.7	99.58

PIERRE SIEVE SIZE (+15)

DIAMOND COLOUR	OCTA	DODEC	MACLE	IRREG	POLY	TOTAL
BROWN	7.8	18.2	4.6	18	3.7	52.3
WHITE	4	9.8	2	8.1	0.8	24.7
GREY	2.6	3.7	1.1	8.1	5.2	20.7
YELLOW	0.6	0.8	0.8	0.2	0	2.4
OTHER	0	0	0	0.2	0	0.2
TOTAL	15	32.5	8.5	34.6	9.7	100.3

PIERRE SIEVE SIZE (+11)

DIAMOND COLOUR	OCTA	DODEC	MACLE	IRREG	POLY	TOTAL
BROWN	5.9	17	3.8	21.5	3.6	51.8
WHITE	3.5	11.4	2.3	12	0.7	29.9
GREY	1.6	3.8	0.9	7.1	2.6	16
YELLOW	0.2	1	0.5	0.7	0	2.4
OTHER	0	0	0	0	0	0
TOTAL	11.2	33.2	7.5	41.3	6.9	100.1

APPENDIX 4.1 continued

RIVER RANCH DIAMONDS

morphology and colour distributions for each size fraction (as a percentage of size total)

PIERRE SIEVE SIZE (+9)

DIAMOND COLOUR	OCTA	DODEC	MACLE	IRREG	POLY	TOTAL
BROWN	4	13.2	1.2	18.8	3.2	40.4
WHITE	5	18.8	0.2	14	2.8	40.8
GREY	1	5.4	0	9.2	3.2	18.8
YELLOW	0	0	0	0	0	0
OTHER	0	0	0	0	0	0
TOTAL	10	37.4	1.4	42	9.2	100

PIERRE SIEVE SIZE (+5)

DIAMOND COLOUR	OCTA	DODEC	MACLE	IRREG	POLY	TOTAL
BROWN	1.2	6.6	0.2	19.2	2.4	29.6
WHITE	7	13	1.4	13.6	3	38
GREY	1	4.8	0	18.6	8	32.4
YELLOW	0	0	0	0	0	0
OTHER	0	0	0	0	0	0
TOTAL	9.2	24.4	1.6	51.4	13.4	100

PIERRE SIEVE SIZE (-5)

DIAMOND COLOUR	OCTA	DODEC	MACLE	IRREG	POLY	TOTAL
BROWN	2.8	5.2	0.4	17.8	1.4	27.6
WHITE	6.2	12.8	0.6	21.4	2.4	43.4
GREY	1	4.8	0.2	16	7	29
YELLOW	0	0	0	0	0	0
OTHER	0	0	0	0	0	0
TOTAL	10	22.8	1.2	55.2	10.8	100

APPENDIX 4.2

RIVER RANCH DIAMONDS

colour intensity variations

COLOUR INTENSITY		NUMBER OF STONES						
		+21	+18	+15	11	+9	+5	-5
BROWN	1	1479	1120	232	205	147	90	109
	2	681	515	89	80	50	54	29
	3	185	104	18	12	5	4	0
	4	45	12	3	2	0	0	0
GREY	1	428	293	69	51	60	90	99
	2	346	215	44	28	19	53	35
	3	141	77	17	9	14	17	9
	4	59	9	5	4	1	2	2
YELLOW	1	76	42	9	8	0	0	0
	2	21	4	2	4	0	0	0
	3	2	0	0	2	0	0	0
	4	0	0	0	0	0	0	0

COLOUR INTENSITY		PERCENTAGE OF SIZE FRACTION						
		+21	+18	+15	11	+9	+5	-5
BROWN	1	32.9	35.8	35.5	35.5	29.4	18	21.8
	2	15.2	16.5	13.6	13.9	10	10.8	5.8
	3	4.1	3.3	2.8	2.1	1	0.8	0
	4	1.0	0.4	0.5	0.3	0	0	0
GREY	1	9.5	9.4	10.6	8.8	12	18	19.8
	2	7.7	6.9	6.7	4.9	3.8	10.6	7
	3	3.1	2.5	2.6	1.6	2.8	3.4	1.8
	4	1.3	0.3	0.8	0.7	0.2	0.4	0.4
YELLOW	1	1.7	1.3	1.4	1.4	0	0	0
	2	0.5	0.1	0.3	0.7	0	0	0
	3	0.0	0.0	0.0	0.3	0	0	0
	4	0.0	0.0	0.0	0.0	0	0	0

APPENDIX 4.3

RIVER RANCH DIAMONDS
inclusions and fracture intensity variations

COLOUR	INCL/FRACT INTENSITY	NUMBER OF STONES						
		+21	**+18**	**+15**	**+11**	**+9**	**+5**	**-5**
BROWN	0	66	95	29	17	10	9	6
	1	59	40	14	6	3	1	3
	2	272	261	45	42	9	15	12
	3	675	500	99	104	45	49	38
	4	692	505	79	64	79	52	44
	5	626	350	76	66	56	22	35
WHITE	0	189	216	30	32	39	45	35
	1	84	74	13	15	9	18	6
	2	250	174	30	39	19	38	27
	3	351	215	53	53	70	64	95
	4	136	49	27	27	56	25	48
	5	16	7	8	6	11	0	6
GREY	0	1	0	0	0	1	0	0
	1	1	0	1	0	0	0	0
	2	19	21	6	5	0	1	3
	3	221	142	16	22	9	21	14
	4	315	220	40	19	22	34	38
	5	417	211	72	46	62	106	90
YELLOW	0	25	12	4	2	0	0	0
	1	7	4	1	0	0	0	0
	2	15	5	2	3	0	0	0
	3	34	10	2	5	0	0	0
	4	13	12	1	4	0	0	0
	5	5	3	1	0	0	0	0

COLOUR	INCL/FRACT INTENSITY	PERCENTAGE OF SIZE FRACTION						
		+21	**+18**	**+15**	**+11**	**+9**	**+5**	**-5**
BROWN	0	1.5	3.0	4.4	2.9	2	1.8	1.2
	1	1.3	1.3	2.1	1.0	0.6	0.2	0.6
	2	6.1	8.3	6.9	7.3	1.8	3	2.4
	3	15.0	16.0	15.1	18.0	9	9.8	7.6
	4	15.4	16.1	12.1	11.1	15.8	10.4	8.8
	5	13.9	11.2	11.6	11.4	11.2	4.4	7
WHITE	0	4.2	6.9	4.6	5.5	7.8	9	7
	1	1.9	2.4	2.0	2.6	1.8	3.6	1.2
	2	5.6	5.6	4.6	6.8	3.8	7.6	5.4
	3	7.8	6.9	8.1	9.2	14	12.8	19
	4	3.0	1.6	4.1	4.7	11.2	5	9.6
	5	0.4	0.2	1.2	1.0	2.2	0	1.2
GREY	0	0.0	0.0	0.0	0.0	0.2	0	0
	1	0.0	0.0	0.2	0.0	0	0	0
	2	0.4	0.7	0.9	0.9	0	0.2	0.6
	3	4.9	4.5	2.4	3.8	1.8	4.2	2.8
	4	7.0	7.0	6.1	3.3	4.4	6.8	7.6
	5	9.3	6.7	11.0	8.0	12.4	21.2	18
YELLOW	0	0.6	0.4	0.6	0.3	0	0	0
	1	0.2	0.1	0.2	0.0	0	0	0
	2	0.3	0.2	0.3	0.5	0	0	0
	3	0.8	0.3	0.3	0.9	0	0	0
	4	0.3	0.4	0.2	0.7	0	0	0
	5	0.1	0.1	0.2	0.0	0	0	0

5. RIVER RANCH MANTLE MINERAL CHEMISTRY

5.1 INTRODUCTION

Mantle macrocryst minerals associated with kimberlites are considered to be largely derived from disaggregated peridotitic and eclogitic mantle xenoliths during the process of kimberlite emplacement (Wagner, 1914). Some of these mantle minerals have been used for more than a hundred years as "indicator" in exploration for diamonds. In the past two decades, significant advances have been made in refining the use of their compositions for assessing the diamond potential of kimberlites (eg. Gurney, 1984; Griffin et al, 1989; Griffin and Ryan, 1993; Gurney et al, 1993; Gurney and Zweistra, 1995).

Diamond bearing kimberlites often have peridotitic garnets and chromites that exhibit similar chemical compositions to the respective mineral inclusions in diamond. This relationship was first recognised by Gurney and Switzer (1973) in peridotitic garnets derived from the Finsch kimberlite. For the peridotitic diamond paragenesis, there are three sub-groupings namely garnet harzburgite, chromite harzburgite and garnet lherzolite with the harzburgites being calcium depleted relative to the lherzolites (Gurney et al 1993). With respect to diamonds garnet harzburgite is most important, followed by chromite harzburgite and garnet lherzolite being the least important.

The assessment of the diamond potential of any kimberlite deposit requires an accurate interpretation of the indicator mineral compositions. The interpretation of such data relies on the recognition of those mantle macrocryst minerals which are co-genetic with diamond and assigning a "score" to them depending on the desirability of their compositions (Gurney and Zweistra, 1995). Based on the assumption that the abundance of such `high scoring' mantle minerals in a kimberlite is indicative of a better diamond content, a semi-quantitative assessment of the diamond content of any kimberlite can thus be made. However this can not be viewed in isolation of other factors like resorption of the diamonds and the diamond sampling efficiency of the transporting magma (Gurney and Zweistra, 1995).

A megacryst suite which includes garnet and clinopyroxene exists at River Ranch. Megacrysts are not directly related to diamonds but can provide useful information about the thickness of the mantle root sampled by the kimberlite, provided pressure-temperature conditions of their crystallisation can be obtained. Their discrete nature and large size, which often far exceeds that of crystals in peridotite xenoliths suggests that megacrysts are derived from an incompletely consolidated magma body at the base of the lithosphere (eg. Harte 1983).

Mantle minerals for this study were collected from the run-of-mine production. Concentrate whose size, range in diameter from 0.425mm to 2mm was examined. The oversize concentrate (>2mm) was also examined for megacryst minerals. Minerals found in the concentrate include peridotitic garnets, chromites and clinopyroxene and Cr-poor garnet and clinopyroxene megacrysts. Although it is difficult to distinguish between peridotitic clinopyroxenes and clinopyroxene megacrysts in the concentrate, peridotitic clinopyroxenes tend to have a bright emerald green colour whereas the megacrysts have a dull lustre. Simple plots of Cr_2O_3 vs Mg# can also be used to distinguish peridotitic clinopyroxenes from the megacrystic clinopyroxenes. No kimberlitic ilmenites were observed.

5.2 SAMPLE PREPARATION AND ANALYTICAL TECHNIQUE

Mineral grains were hand picked using a binocular microscope and were mounted in araldite for analysis on the electron microprobe. Major element analyses were obtained on a Cameca Camebax Microbeam electron microprobe at the Department of Geological Sciences, University of Cape Town. The instrument conditions, standards and detection limits for the analyses are tabulated in Appendix 5.1. For most elements, a peak counting time of 10 seconds was used with the exception of Na in garnets and Ni and V in chromites for which a counting time of 30 seconds was used. Reduction of all data was performed on-line. The Bence-Albee method (Bence and Albee, 1968) was used for the correction of matrix effects.

5.3 PERIDOTITIC GARNETS

Harzburgitic garnets show high MgO and Cr_2O_3 contents but are low in CaO contents compared to the lherzolitic variety (eg Gurney, 1984). Simple plots of CaO vs Cr_2O_3 in garnets can be used to distinguish harzburgitic garnets from lherzolitic garnets as defined in the trend of Sobolev et al (1973) and Hatton (1978). More importantly, such plots can be used to demonstrate the presence or absence of diamonds with considerable confidence and to make semi-quantitative estimates of the peridotitic diamond potential of a diatreme (Gurney and Zweistra, 1995).

A suite of more than 100 garnet macrocrysts of different colours (red, mauve and lilac coloured) were selected for analysis. The majority of garnets in the River Ranch concentrate are red. No orange garnets were observed (these would possibly indicate an eclogitic source for diamonds). There are a number of brown garnet macrocrysts that were also picked from the concentrate. These have been analysed separately and are discussed in the next section.

The major element compositions of the peridotitic garnets analysed are tabulated in Appendix 5.2. They are characterised by Cr_2O_3 1.98 - 9.21 wt %, MgO 15.29 - 24.04 wt%, CaO 0.76 - 8.53 wt% and TiO_2 not detected (ND) - 1.10 wt%. However the majority of the garnets have $TiO_2 < 0.50$ wt% and only one grain yielded an exceptional high TiO_2 content of 1.10 wt%. The majority of the subcalcic garnets have their TiO_2 contents below detection (ie. < 0.04 wt%). None of the high titanium garnets have been found to be sub-calcic (Figure 5.3).

A plot of CaO vs Cr_2O_3 (Figure 5.1) shows that there is a cluster of garnets that fall on to the lherzolitic trend. There is one outlier with a very high CaO content (8.53 wt%). In the "diamond in" field, there are a suite of garnets with a range of both chromium and calcium defining no particular trend and extending to very low (<1%) calcium contents. These garnets are broadly similar to sub-calcic inclusions in diamonds world-wide and provide strong evidence of the presence of a diamondiferous harzburgite source rock for River Ranch. On the basis of the parameters reported by Gurney and Zweistra (1995), River Ranch should be well diamond mineralised.

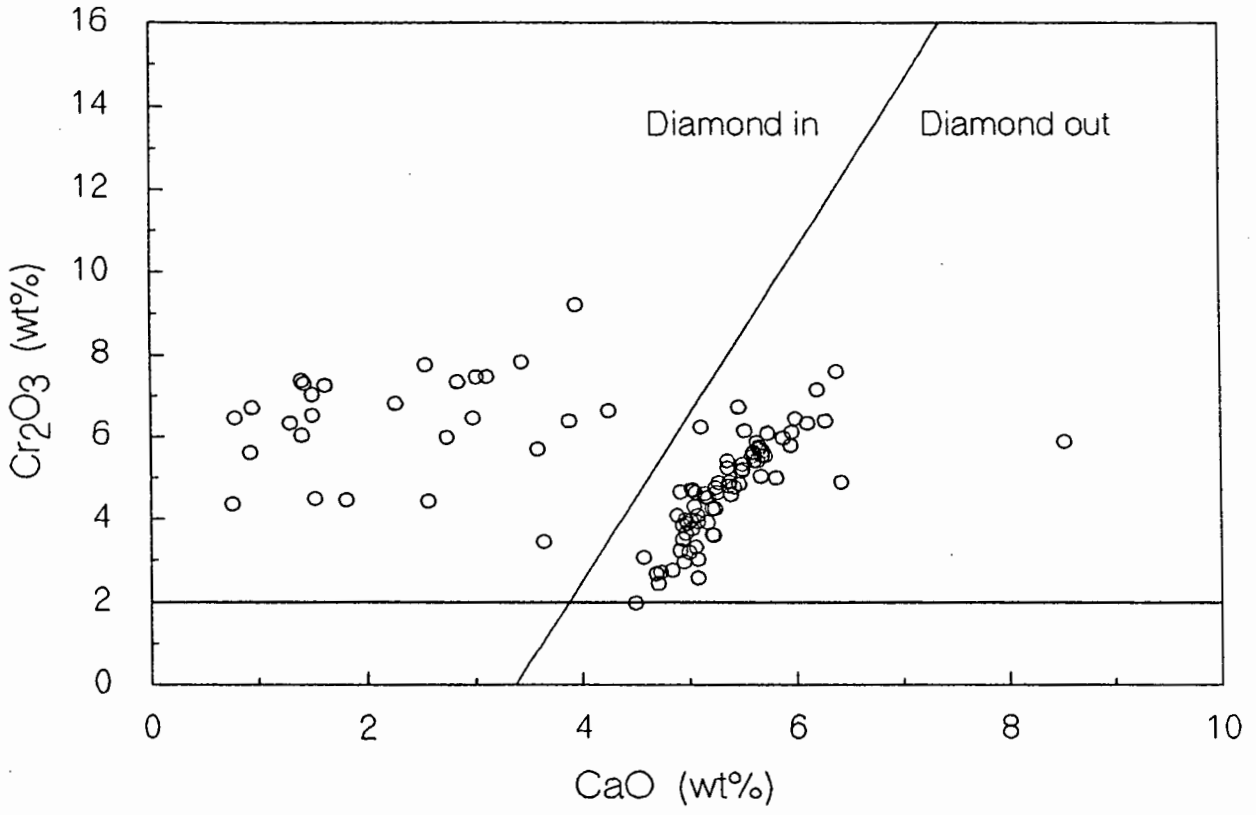

Figure 5.1 A plot of CaO vs Cr_2O_3 for concentrate peridotitic garnets from River Ranch. The diagonal line distinguishes the garnets that are co-genetic with diamond,'diamond in', from the non co-genetic ones,'diamond out' (Gurney et al, 1993).

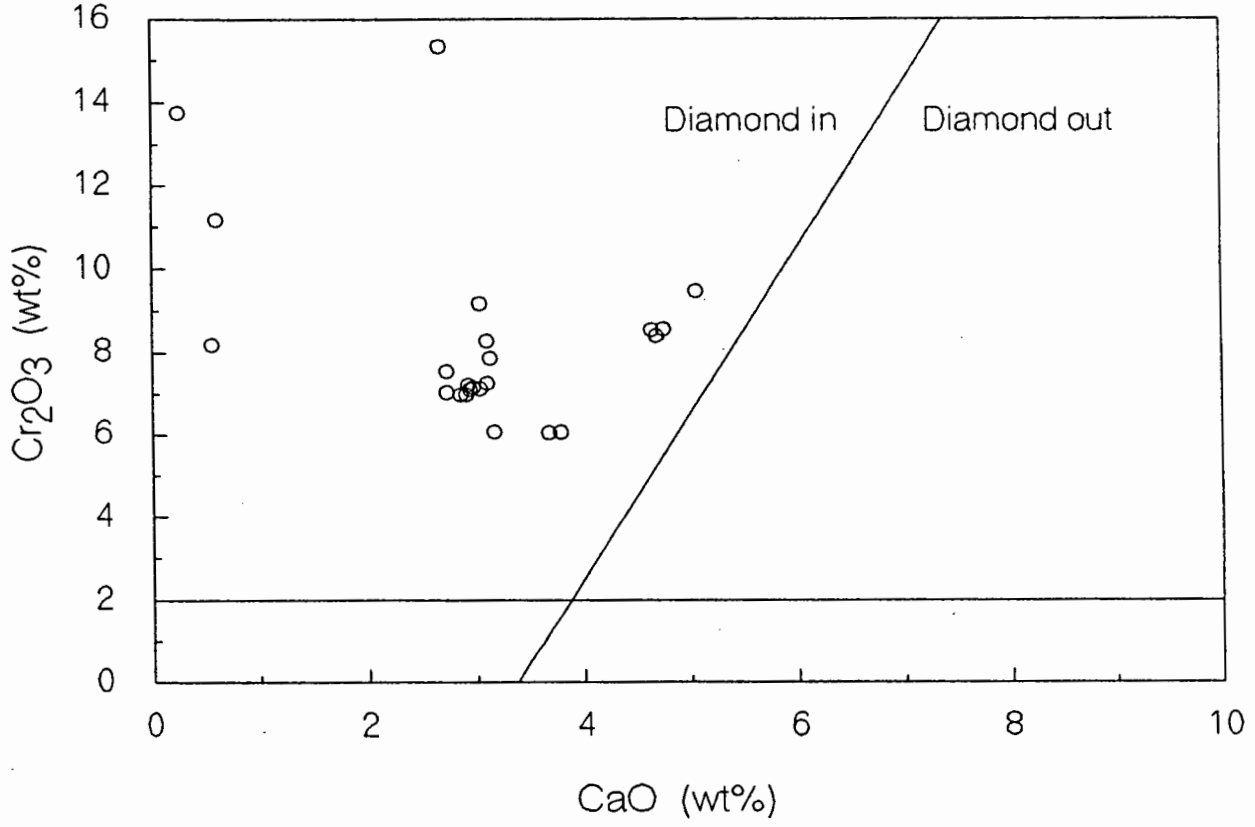

Figure 5.2 A plot of CaO vs Cr_2O_3 for peridotitic garnet diamond inclusions from River Ranch. Data from Kopylova et al (1995).

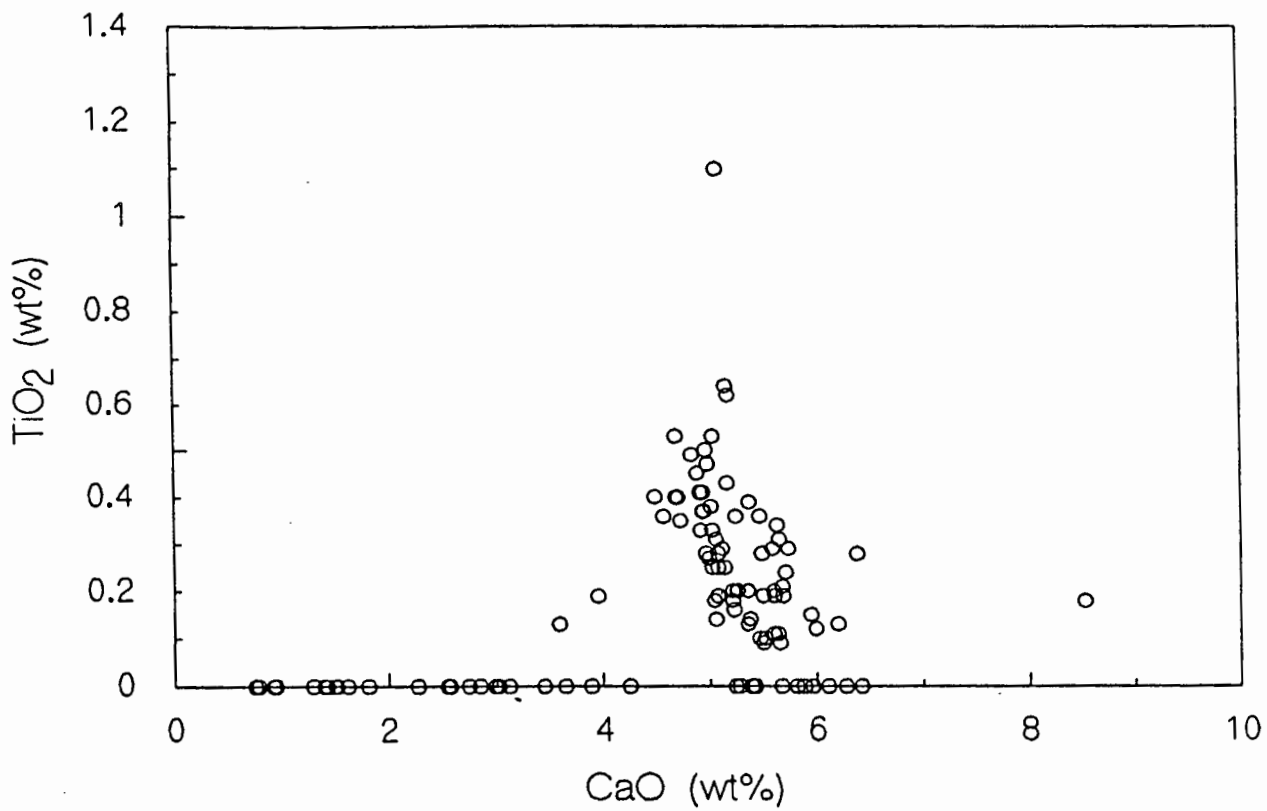

Figure 5.3 A plot of CaO vs TiO_2 for peridotitic garnets from the River Ranch concentrate.

Studies of peridotitic garnet inclusions from River Ranch (Kopylova et al, 1995) show that more than 99% of garnet diamond inclusions are harzburgitic (Figure 5.2) and these have generally higher Cr contents than the concentrate garnets (Cr_2O_3 6.04 - 16.55 wt%). Similar differences elsewhere have been attributed to post crystallisation protection of diamond inclusions from sub-solidus re-equilibration by the host diamond (eg. Gurney et al, 1979; Daniels, 1991). The compositional change of the mantle minerals in xenoliths compared to the diamond inclusions may have developed during long periods of residence in the mantle. This period can be as long as 3000 Ma, in the case of peridotitic garnet inclusions (Richardson et al, 1984; Richardson et al, 1993). The diamond inclusion study and the macrocrysts in the kimberlite both indicate that eclogite is not a major diamond source at River Ranch as only 0.3% of the inclusions are of an eclogitic paragenesis and the occurence of eclogitic macrocrysts is also very low.

5.4 LOW-Cr GARNET MACROCRYSTS

Within the River Ranch heavy mineral suite there is a significant population of brown garnet macrocrysts with low Cr_2O_3 contents. Major element analyses of these brown garnets (Appendix 5.3) showed that a lot of them are sub-crustal and not from the upper mantle. These sub-crustal garnets are of no interest to this study. However five selected garnets are mantle derived. These five garnets had detectable Na_2O contents (Na_2O>0.07 wt%) and are characterised by Cr_2O_3 1.76 - 2.51 wt%, MgO 20.49 - 21.09 wt%, CaO 4.43 - 4.60 wt%, Na_2O 0.07 - 0.09 wt% and TiO_2 0.39 - 0.56 wt%. Compared to the larger megacrysts (section 5.7.1, Appendix 5.6) the macrocrysts have lower TiO_2 contents (see also Figures 5.4 and 5.7).

5.5 CHROMITES

A proportion of the chromites from a diamondiferous kimberlite may have similar compositions to chromite inclusions in diamonds. Lawless (1974) and Sobolev (1974) both noted that chromites associated with diamonds have characteristic high MgO and high Cr_2O_3 (>60 wt%) contents. Gurney (1984) defined a chromite inclusion field indicative of the presence of diamonds by plotting MgO vs Cr_2O_3.

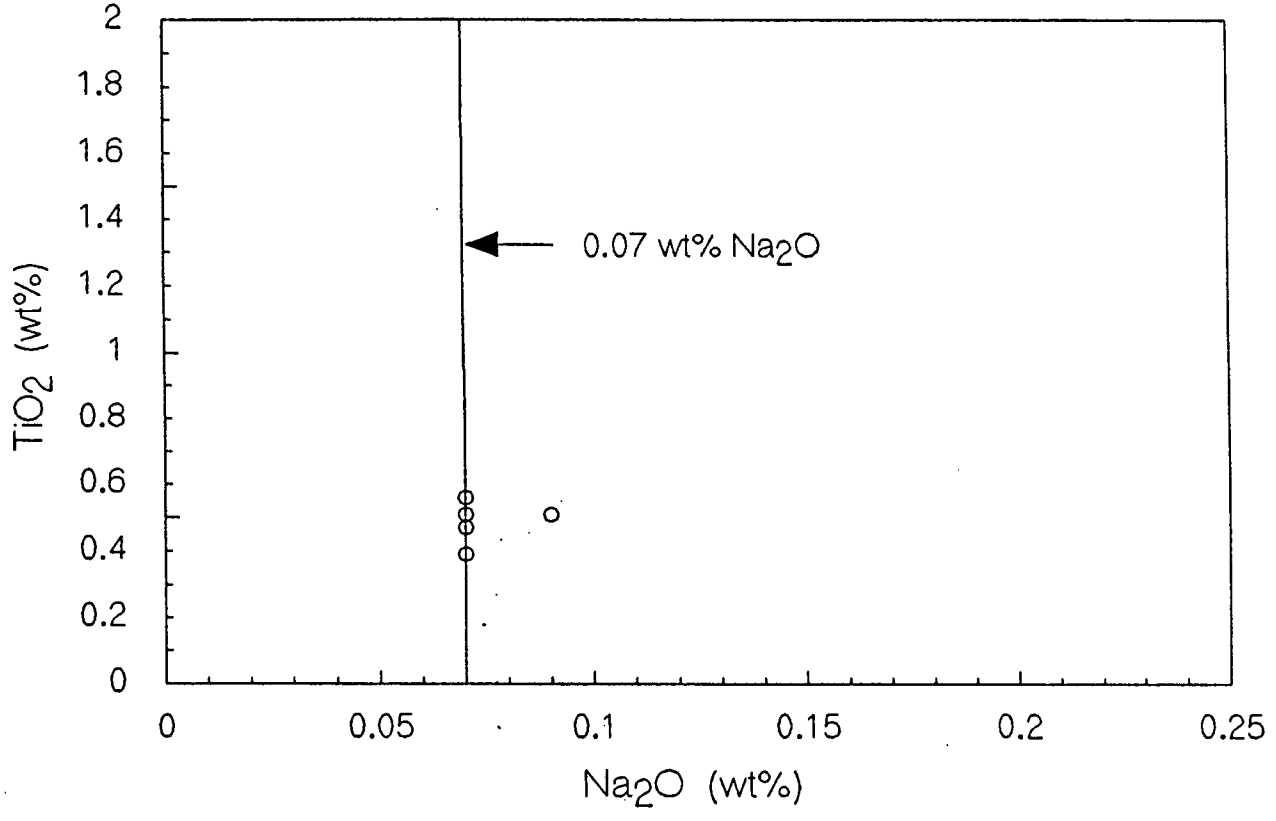

Figure 5.4 A plot of Na_2O vs TiO_2 for low-Cr garnet macrocrysts from the River Ranch concentrate. Garnets with Na2O levels > 0.07 wt% are derived from the diamond stability field.

The concentrate chromites from any one diatreme may be composed of sub-populations as described by Griffin and Ryan (1993). One population represents chromites of lherzolitic and harzburgitic xenoliths and are therefore xenocrystic in origin. Other populations do not correspond to any xenolithic composition but show chemical compositions similar to groundmass spinels in kimberlites. This later sub-population is interpreted to be of magmatic origin and represents phenocrysts that crystallized from the kimberlite magma (Griffin and Ryan, 1993). Simple plots of TiO_2 vs Cr_2O_3 can be used to distinguish phenocrystic chromites from the xenocrystic chromites. The phenocrystic chromites plot on the magmatic trend and have TiO_2 >0.6 wt%. The xenocrystic chromites have TiO_2<0.6 wt%.

Chromites in the River Ranch concentrate exhibit three shapes. The small grains are commonly euhedral (octahedral) while the larger grains are either subhedral or totally anhedral. However relationships between grain shape and type of chromite (ie. xenocryst or phenocryst) have not been established.

Appendix 5.4 shows the chemical analyses of the chromites. The compositions are characterised by TiO_2 contents that range from not detected to 3.79 wt%, Al_2O_3 5.95 - 23.24 wt%, Cr_2O_3 40.56 - 64.07 wt% and MgO 9.83 - 14.56 wt%. The molecular Cr/(Cr + Al) ratio (=Cr#) ranges from 0.539 - 0.876. Studies of concentrate chromite populations from southern Africa have indicated that the average Cr# may indicate the economic potential of the kimberlite (Daniels, 1994). Kimberlites with a concentrate chromite population whose average Cr# > 0.8 have been found to be economic. On the other hand no kimberlite with a Cr# < 0.8 has been found to be economic. The River Ranch concentrate chromite population has an average Cr# of 0.8 . The percentage of grains with Cr# less than 0.8 is about 23%.

A plot of MgO vs Cr_2O_3 (Figure 5.5) shows a cluster of chromites with high Cr_2O_3 content (>60 wt%) and most of these plot in the diamond inclusion field of Gurney (1984). A plot of TiO_2 vs Cr_2O_3, (Figure 5.6) shows that some of the chromites fall on a magmatic crystallization trend. A cluster of them are chromites with TiO_2 contents less than 0.6 wt% but others are of undefined origin.

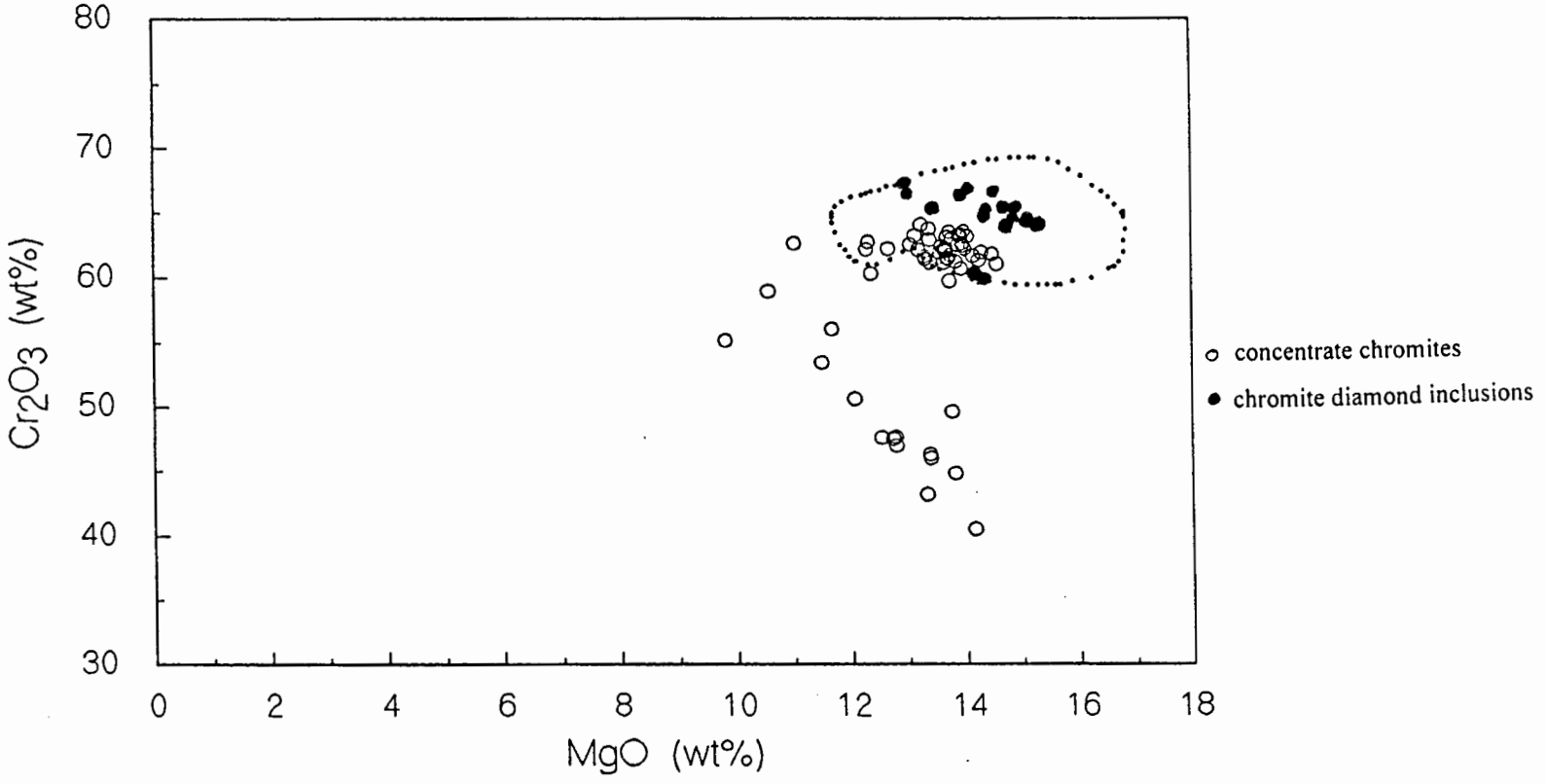

Figure 5.5 A plot of MgO vs Cr2O3 for concentrate chromites and chromite diamond inclusions from River Ranch. The compositional field is for diamond inclusions from worldwide as defined by Gurney (1984).

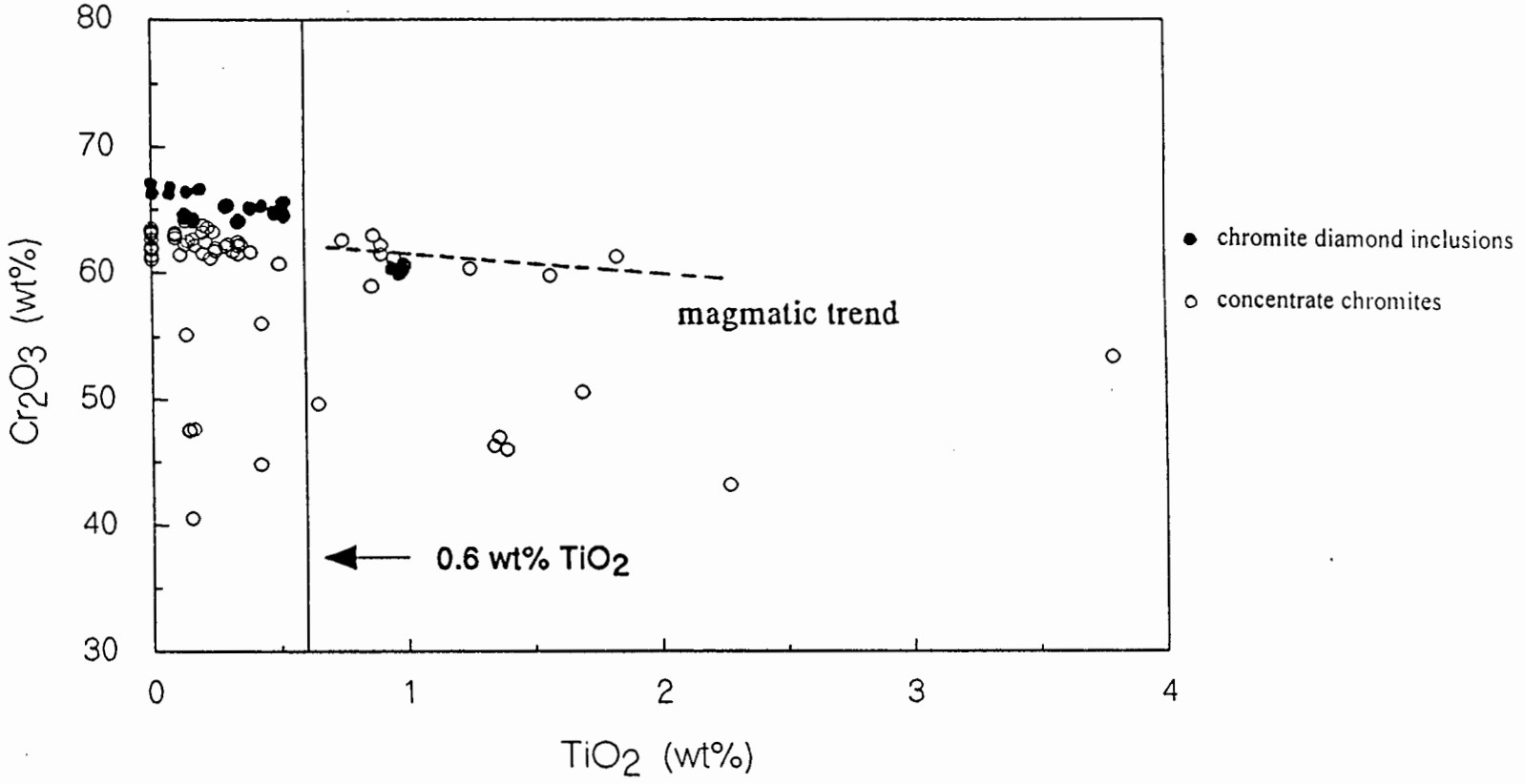

Figure 5.6 A plot of TiO2 vs Cr2O3 for concentrate chromites and chromite diamond inclusions from River Ranch. Chromite xenocrysts normally have TiO2 contents < 0.06 wt%.

Chromite diamond inclusion studies by Kopylova et al (1995) show that the Cr_2O_3 contents in these chromites range from 61 - 69 wt%. Most plot in the diamond inclusion field (Figure 5.5). However the diamond inclusions show higher Cr_2O_3 contents than the concentrate chromites. This can again be explained by post crystallization shielding from sub-solidus re-equilibration by the host diamond as is the case with the garnets. The diamond inclusion chromites define a trend on the TiO_2 vs Cr_2O_3 plot (Figure 5.6). This is unusual as these chromites are xenocrysts and not phenocrysts. There is also a sub-population with TiO_2 > 0.6 wt%. The unusual titanium enrichment in some River Ranch diamond inclusion chromites means that the general rules established for other kimberlites do not strictly apply to River Ranch. Chromites with up to 1% TiO_2 can justifiably be considered to be indicative of diamond potential at this locality.

5.6 CLINOPYROXENES

The concentrate clinopyroxenes have Al_2O_3 contents ranging from 0.95 - 3.31 wt%, Cr_2O_3 0.34 - 3.56 wt% and Na_2O 0.29 - 2.50 wt% (Appendix 5.5). The majority of the clinopyroxenes have K_2O contents below detection limit (ie. 0.01 wt%). Two grains had K_2O contents of 0.05 wt% each and one had 0.11 wt% K_2O. The Ca/(Ca+Mg) ratios of these pyroxenes range from 0.35 to 0.51.

5.7 MEGACRYSTS

Megacrysts, which are also termed discrete nodules, are by definition mantle derived large (>1cm) crystals. They commonly occur as monomineralic crystals but lamellar and granular ilmenite-silicate intergrowths do occur as well.

The megacryst suite studied in the River Ranch concentrate consists of garnets and clinopyroxenes. Large crystals (> 1cm) were picked from the oversize concentrate. Single chippings from crushed individual nodules were obtained for analysis. No co-existing phases were observed hence no crystallisation temperature estimates could be made.

5.7.1 Garnet Megacrysts

The Cr-poor garnet megacryst suite at River Ranch is characterised by the following major element compositions: TiO_2 0.49 - 1.02 wt%, Cr_2O_3 1.15 - 3.50 wt%, FeO 8.65 - 10.77 wt%, MgO 18.13 - 19.19 wt% and Na_2O not detected - 0.08 wt% (Appendix 5.6). The majority of the megacrysts have Na_2O contents $\leq$ 0.07 wt% (Figure 5.7) except for one analysis which had 0.08 wt% Na_2O. The Mg# [= Mg/(Mg + Fe)] for the garnet megacrysts ranges from 75 - 80.

5.7.2 Clinopyroxene Megacrysts

The clinopyroxenes have Cr_2O_3 contents ranging from 0.78 - 1.09 wt%; Al_2O_3 2.05 - 2.98 wt% and Na_2O 1.22 - 1.80 wt%. The Mg# ranges from 86 - 89 with Ca# [= Ca/(Ca + Mg)] ranging from 31 - 39. There is a positive correlation between the Ca# and the Mg# (Figure 5.8). This is contradictory to trends on other clinopyroxene megacrysts studied in southern Africa where the trends show a regular increase in Ca# with decreasing Mg# (eg Gurney et al, 1991). The River Ranch megacryst suite does not show a normal crystallization trend, since an increase in Ca# normally denotes falling temperature. In view of this unusual correlation (Figure 5.8), there is the possibility that clinopyroxene megacrysts at River Ranch did not equilibrate with orthopyroxene and therefore no attempt has been made to calculate a temperature of equilibration from Ca#. However the Ca# range (31-38) is within that found at Monastery Mine, the type locality for Cr-poor megacrysts in southern Africa.

5.8 MINERAL COMPOSITION AND DIAMOND POTENTIAL

The technique of assessing the diamond potential of any kimberlite diatreme can also be used to focus on individual intrusive phases in a single diatreme. Gurney and Zweistra (1995) emphasised the application of a scoring system in assessing the desirability of the composition of the mineral. In the case of River Ranch, the concentrate peridotitic garnets that have similar mineral compositions to diamond inclusions are the ones that can score high. These garnets can often be colour selected from the rest of the population. Studies of such garnets in mapped kimberlite phases at River Ranch might assist with mine development planning. Such a technique could be a useful tool in grade control as a cheap and easy alternative to the often

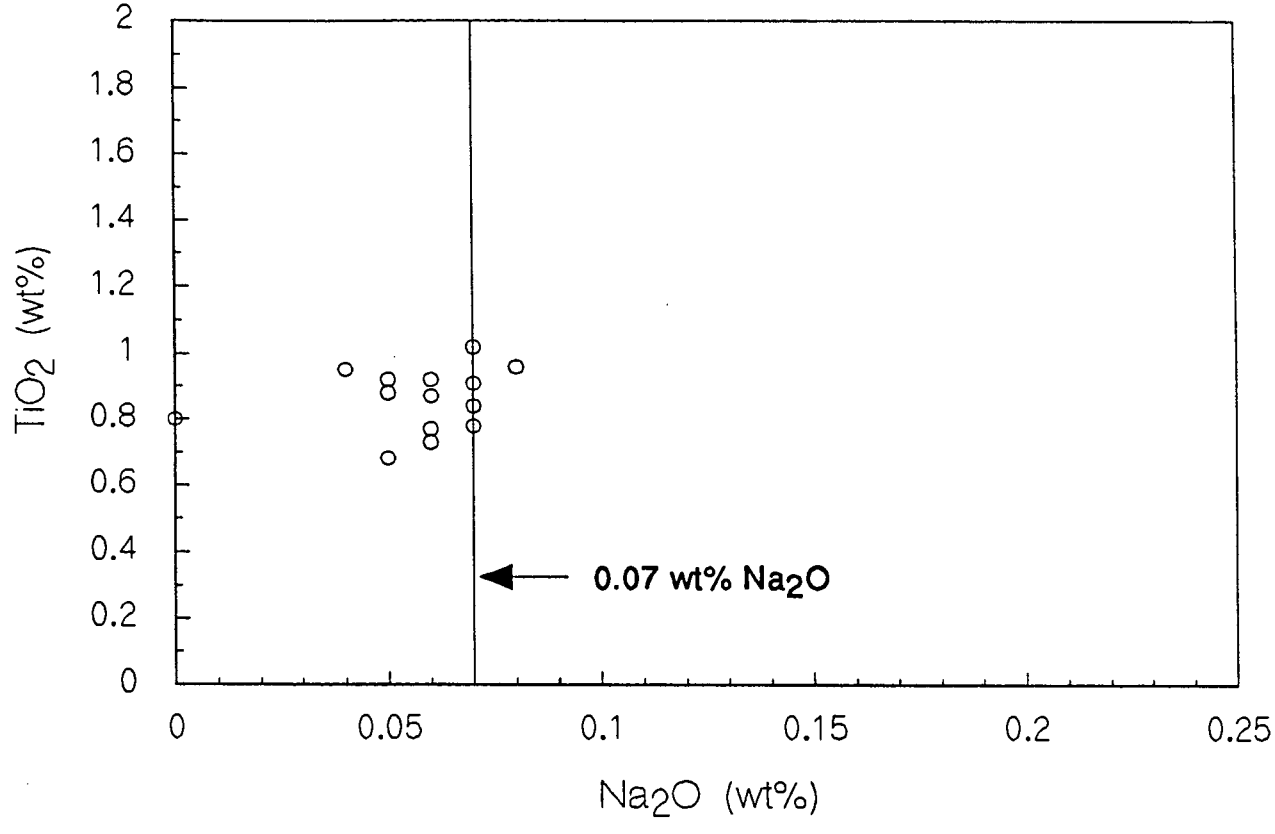

Figure 5.7 A plot of Na_2O vs TiO_2 for Cr-poor garnet megacrysts from the River Ranch concentrate.

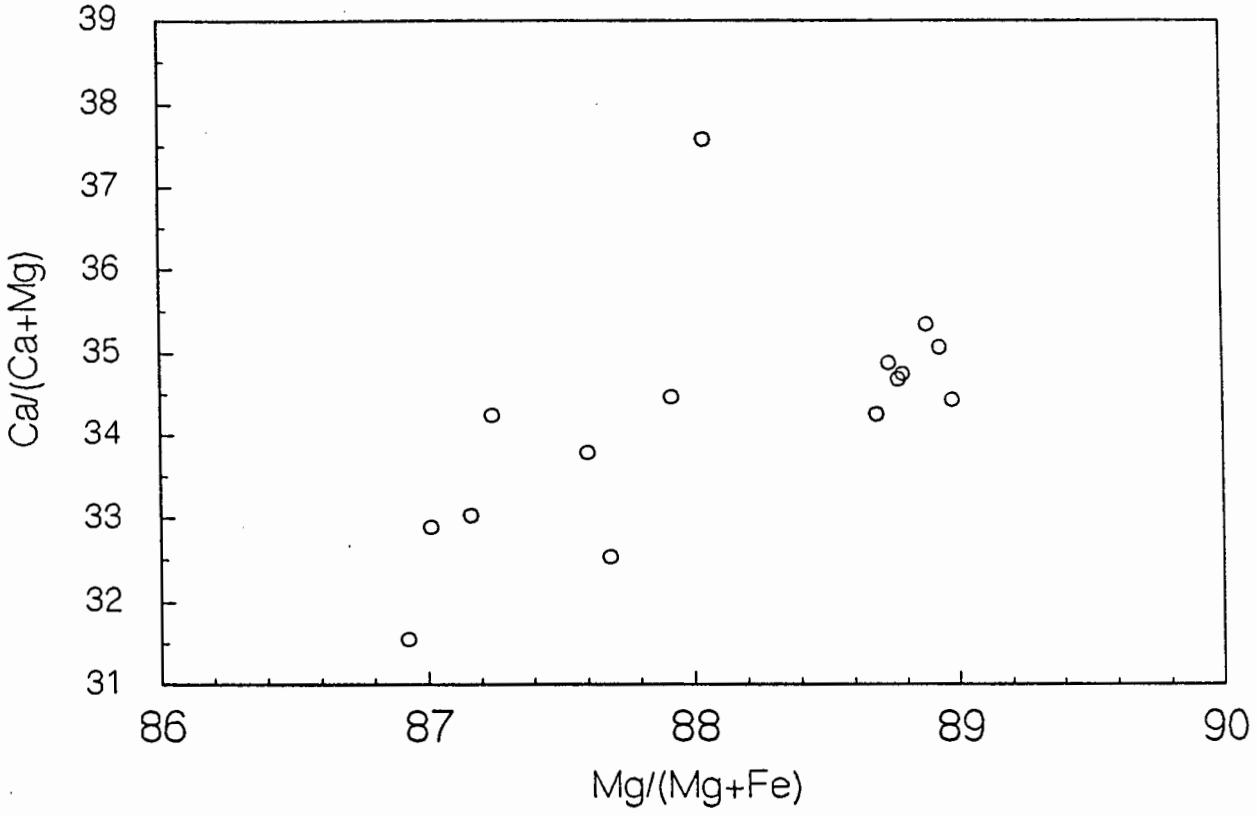

Figure 5.8 A plot of Mg# vs Ca# for clinopyroxene megacrysts from the River Ranch concentrate. Note the positive trend shown by the plot.

expensive bulk sampling exercise. The work that was done in this study was to characterise the mineral compositions from the whole River Ranch population, so as to use as a reference standard against which to compare individual kimberlite characteristics.

APPENDIX 5.1

THE ELECTRON MICROPROBE

1. INSTRUMENT CONDITIONS

Accelerating potential = 15kV
Beam current = 40nA
Beam diameter = 1um

2. STANDARDS

OXIDE	GARNET	SPINEL	PYROXENE
SiO2	K-P	K-P	Diop
TiO2	Rut	Rut	Rut
Al2O3	K-P	Chro	K-P
Cr2O3	Chro	Chro	Chro
FeO	K-P	Ilm	K-P
MnO	Rhod	Rhod	Rhod
MgO	K-P	Chro	Diop
CaO	K-P	K-P	Diop
Na2O	K-H		K-H
K2O			K-H

KEY

K-P = Kakanui Pyrope
K_H = Kakanui Hornblende
Diop = Synthetic Diopside
Rut = Synthetic Rutile
Chro = Chromite 52NL11
Rhod = Synthetic Rhodonite
Ilm = Sythetic Ilmenite

3. DETECTION LIMITS

OXIDE	GARNET	SPINEL	PYROXENE
SiO2	0.05	0.05	0.05
TiO2	0.04	0.04	0.04
Al2O3	0.04	0.05	0.03
Cr2O3	0.05	0.05	0.05
FeO	0.07	0.08	0.07
MnO	0.07	0.08	0.06
MgO	0.03	0.04	0.03
CaO	0.03	0.03	0.03
Na2O	0.01	NA	0.03
K2O	NA	NA	0.01

KEY

NA = not analysed

APPENDIX 5.2

RIVER RANCH CONCENTRATE

GARNETS

SAMP No.	MINID	OXY	SiO2	TiO2	Al2O3	Cr2O3	FeO	MnO	MgO	CaO	TOTAL	Si	Ti	Al	Cr	Fe2+	Mn	Mg	Ca	SUM
RRCM9/1	GAR	12	41.41	0.29	19.39	6.09	6.45	0.23	19.89	5.74	99.49	2.991	0.016	1.651	0.348	0.390	0.014	2.141	0.444	7.995
RRCM9/2	GAR	12	41.39	0.11	19.84	5.60	6.14	0.30	20.03	5.60	99.01	2.990	0.006	1.691	0.320	0.371	0.018	2.159	0.434	7.993
RRCM9/3	GAR	12	42.00	0.33	20.32	4.66	6.20	0.24	20.25	4.92	98.92	3.021	0.018	1.723	0.265	0.373	0.015	2.171	0.379	7.965
RRCM9/5	GAR	12	41.81	0.41	20.77	3.86	6.90	0.25	20.35	4.94	99.29	3.002	0.022	1.757	0.219	0.414	0.015	2.178	0.380	7.987
RRCM9/6	GAR	12	41.69	0.64	20.24	4.53	6.66	0.27	19.92	5.16	99.11	3.004	0.035	1.719	0.258	0.401	0.016	2.140	0.399	7.972
RRCM9/7	GAR	12	41.77	0.18	21.15	4.30	5.26	0.26	20.13	5.05	99.10	2.998	0.010	1.789	0.244	0.376	0.016	2.153	0.389	7.975
RRCM9/8	GAR	12	41.50	0.09	19.76	5.76	6.71	0.28	19.49	5.66	99.25	3.002	0.005	1.685	0.329	0.406	0.017	2.102	0.439	7.985
RRCM9/10	GAR	12	41.82	ND	21.02	4.26	6.42	0.24	19.54	5.24	98.54	3.002	0.000	1.790	0.243	0.388	0.015	2.104	0.406	7.968
RRCM9/11	GAR	12	42.02	0.40	22.39	1.98	7.38	0.23	19.94	4.50	98.84	3.011	0.022	1.891	0.112	0.442	0.014	2.129	0.346	7.967
RRCM9/12	GAR	12	41.44	0.14	20.42	4.89	6.35	0.28	19.99	5.38	99.89	2.994	0.008	1.739	0.279	0.384	0.017	2.153	0.416	7.990
RRCM9/13	GAR	12	41.85	0.53	19.66	4.68	6.75	0.25	20.02	5.04	98.78	3.027	0.029	1.676	0.268	0.409	0.015	2.158	0.390	7.972
RRCM9/14	GAR	12	42.21	ND	22.07	3.46	6.02	0.29	21.98	3.65	99.68	2.989	0.000	1.842	0.194	0.356	0.017	2.320	0.277	7.995
RRCM9/16	GAR	12	41.56	0.29	19.42	6.24	6.41	0.25	20.42	5.12	99.71	2.990	0.016	1.647	0.355	0.386	0.015	2.189	0.395	7.993
RRCM9/17	GAR	12	41.34	ND	19.10	6.33	6.32	0.26	19.20	6.11	98.66	3.014	0.000	1.641	0.365	0.386	0.016	2.087	0.477	7.986
RRCM9/18	GAR	12	41.25	0.24	19.56	5.54	6.89	0.32	19.38	5.71	98.89	2.999	0.013	1.676	0.319	0.419	0.019	2.100	0.445	7.990
RRCM9/20	GAR	12	41.67	ND	19.70	6.32	6.57	0.27	22.74	1.30	98.57	3.000	0.000	1.672	0.360	0.396	0.017	2.440	0.100	7.985
RRCM9/22	GAR	12	41.90	ND	21.70	4.38	6.19	0.22	23.39	0.76	98.54	2.983	0.000	1.822	0.247	0.369	0.013	2.484	0.058	7.979
RRCM9/23	GAR	12	41.96	ND	19.58	6.81	6.57	0.33	21.71	2.27	99.23	3.012	0.000	1.657	0.386	0.395	0.020	2.323	0.175	7.968
RRCM9/24	GAR	12	41.63	ND	19.38	7.03	6.40	0.27	22.43	1.50	98.64	3.001	0.000	1.646	0.401	0.386	0.017	2.410	0.116	7.977
RRCM10/1	GAR	12	41.69	ND	19.94	6.46	6.60	0.27	21.28	2.99	99.23	2.997	0.000	1.689	0.367	0.397	0.017	2.280	0.231	7.978
RRCM10/2	GAR	12	42.09	ND	19.25	7.25	5.55	0.17	23.35	1.62	99.28	3.005	0.000	1.620	0.409	0.331	0.010	2.485	0.124	7.984
RRCM10/3	GAR	12	42.03	ND	21.46	4.47	6.58	0.38	22.37	1.81	99.10	2.995	0.000	1.803	0.252	0.592	0.023	2.376	0.138	7.979
RRCM10/4	GAR	12	41.17	ND	19.06	7.75	6.05	0.32	22.18	2.55	99.08	2.971	0.000	1.620	0.442	0.365	0.019	2.385	0.197	7.999
RRCM10/5	GAR	12	41.60	ND	19.86	6.46	6.22	0.30	23.70	0.79	98.93	2.979	0.000	1.676	0.366	0.373	0.018	2.530	0.061	8.003
RRCM10/6	GAR	12	41.69	ND	19.45	7.30	6.13	0.32	22.84	1.43	99.16	2.989	0.000	1.644	0.414	0.368	0.019	2.441	0.110	7.985
RRCM10/7	GAR	12	41.25	0.20	19.72	5.63	5.89	0.23	20.08	5.60	98.60	2.993	0.011	1.685	0.323	0.357	0.014	2.171	0.435	7.990
RRCM10/8	GAR	12	41.94	ND	20.05	6.71	6.21	0.29	23.61	0.95	99.76	2.979	0.000	1.678	0.377	0.369	0.017	2.500	0.072	7.992
RRCM10/9	GAR	12	41.14	ND	20.43	5.05	6.71	0.31	19.93	5.67	99.24	2.974	0.000	1.740	0.289	0.405	0.019	2.147	0.439	8.013
RRCM10/10	GAR	12	41.02	ND	20.85	4.90	6.91	0.39	18.63	6.42	99.12	2.975	0.000	1.782	0.281	0.419	0.024	2.014	0.499	7.994
RRCM10/11	GAR	12	41.51	ND	20.13	5.98	6.56	0.39	21.68	2.74	98.99	2.987	0.000	1.708	0.340	0.395	0.024	2.325	0.211	7.990
RRCM10/12	GAR	12	41.42	ND	20.22	4.77	6.73	0.22	19.75	5.42	98.53	3.009	0.000	1.752	0.274	0.409	0.014	2.139	0.422	7.999
RRCM10/13	GAR	12	40.96	ND	18.81	7.47	6.90	0.29	20.86	3.12	98.41	2.988	0.000	1.617	0.431	0.421	0.018	2.268	0.244	7.987
RRCM10/14	GAR	12	42.22	ND	21.19	4.49	5.33	0.27	23.70	1.52	98.72	3.002	0.000	1.775	0.253	0.317	0.016	2.511	0.116	7.990
RRCM10/15	GAR	12	41.69	ND	19.23	7.36	6.44	0.43	23.46	1.40	99.01	3.000	0.000	1.631	0.419	0.388	0.026	2.408	0.108	7.980

APPENDIX 5.2 continued

SAMP No.	MINID	OXY	SiO2	TiO2	Al2O3	Cr2O3	FeO	MnO	MgO	CaO	TOTAL	Si	Ti	Al	Cr	Fe2+	Mn	Mg	Ca	SUM
RRCM10/16	GAR	12	41.58	ND	19.02	7.46	6.51	0.35	20.97	3.02	98.91	3.009	0.000	1.622	0.427	0.394	0.022	2.262	0.234	7.970
RRCM10/17	GAR	12	41.20	0.19	17.19	9.21	5.71	0.25	20.95	3.96	98.66	3.006	0.010	1.479	0.531	0.348	0.016	2.279	0.309	7.978
RRCM10/18	GAR	12	41.29	ND	2.22	5.00	6.25	0.31	15.59	5.81	98.74	2.997	0.000	1.730	0.287	0.396	0.019	2.119	0.520	8.000
RRCM10/19	GAR	12	40.74	ND	19.75	6.38	7.16	0.38	20.24	3.89	98.54	2.970	0.000	1.697	0.368	0.437	0.023	0.200	0.304	7.999
RRCM10/20	GAR	12	40.01	ND	19.63	6.52	5.66	0.23	23.35	1.50	98.90	3.004	0.000	1.654	0.369	0.339	0.014	2.489	0.115	7.984
RRCM10/21	GAR	12	42.27	ND	20.58	6.03	4.47	ND	24.04	1.40	98.79	0.008	0.000	1.725	0.339	0.266	0.000	2.550	0.107	7.995
RRCM10/23	GAR	12	41.40	0.14	20.51	4.65	6.37	0.30	20.32	5.06	98.75	2.991	0.008	1.747	0.265	0.385	0.018	2.189	0.392	7.995
RRCM10/25	GAR	12	41.17	ND	18.99	6.39	6.58	0.30	19.24	6.28	98.95	3.002	0.000	1.632	0.368	0.401	0.018	2.091	0.491	8.003
RRCM10/26	GAR	12	41.51	0.09	20.13	5.32	6.45	0.29	20.08	5.50	99.37	2.992	0.005	1.710	0.303	0.389	0.017	2.157	0.424	7.997
RRCM10/27	GAR	12	41.32	ND	20.92	4.88	6.30	0.32	19.82	5.28	99.14	2.996	0.000	1.775	0.278	0.379	0.020	2.127	0.407	7.982
RRCM12/1	GAR	12	42.17	0.25	21.97	3.04	6.61	0.24	20.07	5.08	99.43	3.007	0.013	1.847	0.172	0.395	0.015	2.134	0.388	7.971
RRCM12/4	GAR	12	41.19	0.29	19.46	5.52	6.64	0.24	19.87	5.59	98.80	2.993	0.016	1.637	0.317	0.403	0.015	2.152	0.435	7.998
RRCM12/6	GAR	12	41.45	0.18	20.94	4.25	5.93	0.29	20.52	5.22	98.81	2.984	0.010	1.777	0.242	0.359	0.018	2.203	0.403	7.996
RRCM12/7	GAR	12	41.45	0.25	20.17	4.72	6.44	0.28	20.25	5.03	98.57	3.000	0.014	1.721	0.270	0.390	0.017	2.186	0.390	7.988
RRCM12/10	GAR	12	41.67	0.20	20.40	4.65	6.41	2.60	20.01	5.26	98.62	3.011	0.011	1.738	0.265	0.371	0.018	2.155	0.407	7.976
RRCM12/11	GAR	12	41.54	0.19	19.79	5.41	6.71	0.30	19.43	5.61	99.01	3.009	0.011	1.689	0.310	0.406	0.018	2.101	0.435	7.979
RRCM12/12	GAR	12	41.87	0.19	19.58	5.66	6.50	0.23	19.67	5.69	99.39	3.019	0.010	1.664	0.323	0.392	0.014	2.114	0.440	7.976
RRCM12/13	GAR	12	41.66	0.47	20.99	3.88	6.57	0.23	20.20	4.99	98.99	2.996	0.025	1.779	0.220	0.395	0.014	2.165	0.384	7.978
RRCM12/14	GAR	12	41.25	0.21	19.70	5.54	6.95	0.30	19.21	5.68	98.84	3.000	0.011	1.688	0.319	0.423	0.018	2.082	0.442	7.983
RRCM12/18	GAR	12	41.33	0.12	19.00	6.44	5.99	0.28	19.44	5.99	19.59	3.011	0.006	1.632	0.379	0.365	0.017	2.111	0.467	7.980
RRCM12/19	GAR	12	41.58	0.10	20.51	4.85	6.74	0.27	19.85	5.47	99.37	2.994	0.006	1.740	0.276	0.406	0.017	2.131	0.422	7.992
RRCM12/23	GAR	12	41.22	0.13	18.79	7.14	6.06	0.28	19.54	6.20	99.36	2.991	0.007	1.606	0.410	0.367	0.017	2.113	0.482	7.993
RRCM12/24	GAR	12	41.07	ND	19.33	6.12	6.65	0.33	19.53	5.96	98.99	2.989	0.000	1.659	0.352	0.405	0.020	2.119	0.465	8.009
RRCM12/25	GAR	12	41.52	ND	19.06	7.33	6.40	0.28	21.03	2.85	98.47	3.012	0.000	1.630	0.420	0.388	0.017	2.274	0.222	7.963
RRCM12/26	GAR	12	41.60	0.43	20.57	3.93	6.48	0.24	20.31	5.17	98.73	3.002	0.023	1.749	0.224	0.391	0.014	2.184	0.400	7.987
RRCM12/27	GAR	12	41.05	0.18	19.62	5.88	6.06	0.25	19.98	8.53	98.55	2.985	0.010	1.681	0.338	0.368	0.015	2.165	0.431	7.993
RRCM12/28	GAR	12	41.24	0.39	20.02	4.81	6.58	0.30	19.87	5.37	98.58	2.994	0.021	1.713	0.276	0.400	0.019	2.150	0.418	7.991
RRCM12/29	GAR	12	41.49	ND	19.11	6.64	6.10	0.19	20.96	4.25	98.74	3.006	0.000	1.632	0.380	0.369	0.012	2.264	0.330	7.993
RRCM13/1	GAR	12	42.23	ND	20.62	5.61	6.49	0.32	22.86	0.93	99.06	3.010	0.000	1.732	0.316	0.387	0.019	2.429	0.071	7.964
RRCM13/2	GAR	12	42.15	0.36	21.47	3.08	6.67	0.29	20.46	4.57	99.05	3.017	0.019	1.811	0.175	0.399	0.018	2.182	0.350	7.971
RRCM13/3	GAR	12	41.35	0.31	19.47	5.70	6.45	0.26	19.67	5.65	98.86	3.001	0.017	1.665	0.327	0.392	0.016	2.128	0.439	7.985
RRCM13/4	GAR	12	41.44	0.62	20.18	4.53	6.69	0.28	20.04	5.18	98.96	2.994	0.034	1.718	0.259	0.404	0.017	2.158	0.401	7.985
RRCM13/5	GAR	12	41.37	0.36	18.80	6.72	5.87	0.30	20.12	5.47	99.01	2.999	0.020	1.606	0.385	0.356	0.018	2.175	0.425	7.984
RRCM13/6	GAR	12	41.94	0.19	19.63	5.21	6.52	0.28	19.84	5.50	99.11	3.028	0.011	1.670	0.298	0.394	0.017	2.135	0.425	7.978
RRCM13/7	GAR	12	41.61	ND	19.40	5.96	6.22	0.27	19.38	5.88	98.72	3.024	0.000	1.662	0.342	0.378	0.017	2.100	0.458	7.981
RRCM13/8	GAR	12	41.42	ND	18.68	7.83	6.57	0.29	20.39	3.45	98.63	3.013	0.000	1.601	0.450	0.400	0.018	2.210	0.269	7.961
RRCM13/9	GAR	12	41.60	0.10	19.25	6.14	6.58	0.29	19.27	5.52	99.05	3.019	0.005	1.646	0.352	0.399	18.000	2.084	0.452	7.975

APPENDIX 5.2 continued

SAMP No.	MINID	OXY	SiO2	TiO2	Al2O3	Cr2O3	FeO	MnO	MgO	CaO	TOTAL	Si	Ti	Al	Cr	Fe2+	Mn	Mg	Ca	SUM
RRCM13/10	GAR	12	41.96	0.38	20.79	3.98	6.51	0.23	20.06	5.02	98.93	3.017	0.020	1.762	0.226	0.392	0.014	2.150	0.387	7.968
RRCM13/11	GAR	12	41.77	0.19	20.85	4.10	6.34	0.31	20.13	5.08	98.78	3.009	0.010	1.771	0.233	0.382	0.019	2.161	0.392	7.977
RRCM13/12	GAR	12	41.98	0.41	21.19	3.25	6.80	0.29	20.45	4.91	99.36	0.007	0.022	1.789	0.184	0.407	0.017	2.181	0.377	7.984
RRCM13/13	GAR	12	41.80	0.40	22.02	2.45	7.24	0.28	20.49	4.71	99.39	2.987	0.021	1.855	0.139	0.433	0.017	2.183	0.361	7.996
RRCM13/14	GAR	12	41.71	0.11	20.06	5.42	6.18	0.29	19.94	5.64	99.35	3.003	0.006	1.702	0.309	0.372	0.018	2.140	0.435	7.985
RRCM13/15	GAR	12	41.80	0.37	21.25	3.51	6.58	0.26	20.66	4.94	99.67	2.991	0.020	1.792	0.198	0.394	0.016	2.205	0.379	7.993
RRCM13/16	GAR	12	41.96	0.40	21.75	2.69	6.95	0.27	20.62	4.69	99.33	2.998	0.022	1.831	0.152	0.415	0.017	2.196	0.359	7.990
RRCM13/17	GAR	12	41.52	0.33	20.92	3.77	6.65	0.26	20.39	5.03	98.87	2.992	0.018	1.776	0.215	0.400	0.016	2.190	0.388	7.995
RRCM13/18	GAR	12	41.27	0.20	19.98	5.41	6.64	0.28	20.04	5.36	99.18	2.983	0.011	1.702	0.309	0.401	0.017	2.160	0.415	7.998
RRCM13/19	GAR	12	41.69	0.31	21.37	3.34	7.23	0.24	20.23	5.06	99.47	2.988	0.017	1.806	0.189	0.434	0.014	2.161	0.388	7.997
RRCM13/20	GAR	12	42.01	ND	21.04	4.44	6.04	0.26	22.18	2.57	99.17	2.992	0.000	1.766	0.250	0.360	0.016	2.421	0.196	8.001
RRCM13/21	GAR	12	42.13	0.37	21.66	2.97	6.75	0.28	20.63	4.95	99.72	3.333	0.020	1.817	0.167	0.402	0.017	2.189	0.376	7.988
RRCM13/22	GAR	12	41.99	0.27	21.75	3.20	7.35	0.36	20.37	5.00	100.29	2.985	0.014	1.823	0.180	0.437	0.022	2.158	0.381	8.000
RRCM13/23	GAR	12	40.86	0.28	17.97	7.59	6.64	0.33	19.07	6.38	99.12	2.989	0.015	1.550	0.439	0.406	0.021	2.079	0.500	7.999
RRCM13/24	GAR	12	41.90	0.50	21.16	3.66	6.73	0.31	20.93	4.97	99.86	2.987	0.027	1.777	0.189	0.401	0.019	2.224	0.379	8.003
RRCM13/25	GAR	12	41.02	0.15	19.72	5.79	7.08	0.27	19.74	5.95	99.72	2.966	0.008	1.681	0.331	0.428	0.016	2.128	0.461	8.019
RRCM13/26	GAR	12	41.88	0.49	21.75	2.77	6.87	0.25	20.89	4.84	99.74	2.982	0.026	1.825	0.156	0.409	0.015	2.217	0.369	7.999
RRCM13/27	GAR	12	41.62	0.13	20.00	5.70	6.08	0.29	21.94	3.59	99.35	2.983	0.007	1.689	0.323	0.334	0.180	2.344	0.276	8.004
RRCM13/28	GAR	12	41.73	0.28	20.69	3.99	6.46	0.27	20.45	4.97	98.94	3.002	0.021	1.755	0.227	0.388	0.016	2.093	0.383	7.985
RRCM13/29	GAR	12	41.75	0.53	21.68	2.68	6.61	0.32	21.19	4.69	99.45	2.978	0.029	1.823	0.151	0.395	0.019	2.253	0.359	8.007
RRCM13/30	GAR	12	41.77	0.28	20.02	5.16	6.76	0.25	20.33	5.49	100.06	2.992	0.015	1.690	0.292	0.405	0.015	2.170	0.422	8.001
RRCM13/31	GAR	12	41.55	0.25	20.49	4.61	6.82	0.32	20.44	5.14	99.62	2.984	0.014	1.734	0.261	0.409	0.020	2.188	0.395	8.005
RRCM13/32	GAR	12	41.61	0.34	19.27	5.86	6.71	0.25	19.96	5.63	99.63	3.002	0.019	1.638	0.334	0.405	0.015	2.146	0.435	7.994
RRCM13/33	GAR	12	41.73	ND	20.82	4.60	6.89	0.32	20.22	5.39	99.97	2.989	0.000	1.758	0.260	0.413	0.019	2.159	0.413	8.011
RRCM13/34	GAR	12	41.68	0.28	21.31	3.94	5.89	0.26	21.11	5.08	99.55	2.974	0.015	1.792	0.222	0.352	0.016	2.244	0.388	8.003
RRCM13/35	GAR	12	41.91	0.20	21.46	3.63	6.85	0.29	20.69	5.22	100.25	2.980	0.011	1.799	0.204	0.408	0.017	2.192	0.398	8.009
RRCM13/36	GAR	12	42.07	0.35	21.95	2.72	6.81	0.30	20.88	4.73	99.81	2.990	0.019	1.839	0.153	0.405	0.018	2.212	0.361	7.997
RRCM13/37	GAR	12	41.41	0.13	20.29	5.24	6.44	0.30	20.29	5.36	99.43	2.980	0.007	1.721	0.298	0.388	0.018	2.176	0.413	8.001
RRCM13/38	GAR	12	41.68	0.45	20.79	4.09	6.52	0.33	20.48	4.89	99.23	2.992	0.042	1.759	0.232	0.392	0.020	2.192	0.376	7.987
RRCM13/39	GAR	12	41.36	1.10	20.62	2.59	10.00	0.29	19.02	5.08	100.06	2.984	0.060	1.754	0.148	0.604	0.014	2.045	0.392	8.005
RRCM13/40	GAR	12	41.71	0.16	21.52	3.61	6.34	0.23	20.70	5.23	99.50	2.980	0.009	1.812	0.204	0.379	0.014	2.205	0.400	8.003
RRCM13/41	GAR	12	41.38	0.36	20.31	4.76	6.20	0.24	20.62	5.25	99.12	2.980	0.019	1.724	0.271	0.374	0.015	2.214	0.406	8.003

APPENDIX 5.3

RIVER RANCH CONCENTRATE

LOW-Cr GARNET MACROCRYSTS

SAMP No.	MINID	OXY	SiO2	TiO2	Al2O3	Cr2O3	FeO	MnO	MgO	CaO	Na2O	TOTAL	Si	Ti	Al	Cr	Fe2+	Mn	Mg	Ca	Na	SUM
RRCM11/2	GAR	12	38.74	ND	22.52	ND	29.77	1.98	6.79	1.80	0.04	101.64	2.932	0.000	2.043	0.000	1.913	0.129	0.778	0.148	0.003	8.002
RRCM11/3	GAR	12	42.43	0.39	22.69	1.90	7.29	0.26	20.63	4.46	0.07	100.15	3.001	0.021	1.890	0.106	0.431	0.016	2.173	0.337	0.009	7.984
RRCM11/4	GAR	12	42.62	0.47	22.96	1.97	7.56	0.24	20.96	4.51	0.07	101.36	2.982	0.025	1.893	0.109	0.442	0.014	2.186	0.338	0.009	7.998
RRCM11/5	GAR	12	42.92	0.51	22.52	2.02	6.86	0.27	21.09	4.48	0.07	100.74	3.010	0.027	1.862	0.112	0.403	0.016	2.205	0.337	0.010	7.982
RRCM11/6	GAR	12	42.61	0.56	22.83	1.76	7.88	0.31	20.85	4.43	0.07	101.33	2.985	0.029	1.887	0.097	0.461	0.018	2.177	0.333	0.010	7.997
RRCM11/7	GAR	12	42.44	0.51	22.02	2.51	7.69	0.23	20.49	4.60	0.09	100.58	3.000	0.027	1.835	0.140	0.455	0.014	2.159	0.348	0.012	7.990
RRCM11/8	GAR	12	41.99	0.76	21.95	1.74	10.54	0.26	19.16	4.74	ND	101.14	2.988	0.041	1.841	0.098	0.627	0.016	2.032	0.361	0.000	8.004
RRCM11/9	GAR	12	41.50	0.08	23.38	1.26	13.20	0.47	15.85	5.84	ND	101.58	2.978	0.004	1.977	0.072	0.792	0.029	1.695	0.449	0.000	7.996
RRCM11/10	GAR	12	42.63	0.37	22.51	2.31	7.00	0.29	20.72	4.73	ND	100.56	3.002	0.020	1.868	0.129	0.412	0.017	2.175	0.357	0.000	7.980
RRCM11/11	GAR	12	41.85	0.99	21.22	1.76	10.22	0.31	18.71	5.18	ND	100.24	3.007	0.053	1.796	0.100	0.614	0.019	2.004	0.398	0.000	7.991
RRCM11/12	GAR	12	42.30	0.49	22.64	2.13	7.32	0.23	21.25	4.62	ND	101.28	2.982	0.026	1.868	0.118	0.428	0.014	2.217	0.347	0.000	8.000
RRCM11/13	GAR	12	42.74	0.57	23.93	0.76	7.40	0.33	20.83	4.09	ND	100.65	2.991	0.030	1.974	0.042	0.436	0.020	2.173	0.306	0.000	7.969
RRCM11/14	GAR	12	39.63	ND	23.07	0.23	19.53	0.59	12.01	4.27	ND	99.33	2.981	0.000	2.045	0.014	1.228	0.038	1.346	0.344	0.000	7.996
RRCM11/15	GAR	12	42.31	0.54	22.96	1.51	8.19	0.29	20.52	4.53	ND	100.85	2.980	0.029	1.906	0.084	0.483	0.017	2.154	0.342	0.000	7.995
RRCM11/16	GAR	12	43.01	0.40	23.61	1.04	6.98	0.15	21.86	4.30	ND	101.35	2.988	0.021	1.933	0.057	0.406	0.009	2.264	0.320	0.000	7.998
RRCM11/17	GAR	12	39.09	ND	22.76	ND	22.78	0.25	10.39	2.87	ND	98.14	3.004	0.000	2.062	0.000	1.464	0.016	1.190	0.236	0.000	7.972
RRCM11/18	GAR	12	42.57	0.53	22.11	2.17	7.49	0.25	20.59	4.54	ND	100.25	3.011	0.028	1.844	0.121	0.443	0.015	2.171	0.344	0.000	7.977
RRCM11/19	GAR	12	42.75	0.52	22.48	2.03	7.76	0.29	20.63	4.56	ND	101.05	3.003	0.028	1.861	0.113	0.456	0.017	2.163	0.343	0.000	7.984
RRCM11/20	GAR	12	42.41	0.51	22.30	2.45	7.83	0.30	20.38	4.78	ND	100.96	2.991	0.027	1.853	0.136	0.462	0.018	2.142	0.361	0.000	7.990
RRCM11/21	GAR	12	42.40	0.36	23.46	1.05	7.42	0.27	20.53	4.54	ND	100.03	2.994	0.019	1.952	0.059	0.438	0.016	2.160	0.343	0.000	7.981
RRCM11/23	GAR	12	43.20	0.34	23.54	1.47	6.37	0.38	21.56	4.62	ND	101.48	2.996	0.018	1.925	0.081	0.369	0.022	2.229	0.343	0.000	7.983
RRCM11/25	GAR	12	41.82	0.72	21.41	2.61	8.96	0.28	19.31	5.15	ND	100.26	2.992	0.039	1.806	0.148	0.536	0.017	2.059	0.395	0.000	7.992

APPENDIX 5.4

RIVER RANCH CONCENTRATE

CHROMITES

SAMP No.	MINID	OXY	SiO2	TiO2	Al2O3	Cr2O3	FeO	MnO	MgO	CaO	NiO	V2O5	TOTAL	Si	Ti	Al	Cr	Fe2+	Mn	Mg	Ca	Ni	V	SUM
RRCM2/2	CHR	4	ND	0.09	8.66	63.18	13.92	0.23	13.93	ND	ND	0.20	100.21	0.000	0.002	0.332	1.623	0.378	0.006	0.674	0.000	0.000	0.004	3.019
RRCM2/3	CHR	4	ND	0.30	8.62	62.27	15.08	0.18	13.67	ND	0.12	0.36	100.60	0.000	0.007	0.330	1.596	0.409	0.005	0.661	0.000	0.003	0.008	3.019
RRCM2/4	CHR	4	ND	0.09	8.14	62.97	14.32	0.24	13.77	ND	ND	0.18	99.72	0.000	0.002	0.314	1.632	0.396	0.007	0.673	0.000	0.000	0.004	3.025
RRCM2/6	CHR	4	ND	0.11	9.66	61.43	14.60	0.26	13.69	ND	ND	0.36	100.11	0.000	0.003	0.369	1.576	0.396	0.007	0.662	0.000	0.000	0.008	3.021
RRCM2/7	CHR	4	ND	0.20	7.47	63.75	15.12	0.30	13.38	ND	ND	0.19	100.41	0.000	0.005	0.289	1.653	0.415	0.008	0.654	0.000	0.000	0.004	3.028
RRCM2/8	CHR	4	ND	0.23	9.62	61.15	14.87	0.22	13.63	ND	ND	0.39	100.11	0.000	0.006	0.368	1.570	0.404	0.006	0.660	0.000	0.000	0.008	3.022
RRCM2/9	CHR	4	ND	0.13	12.15	55.17	22.39	0.28	9.83	ND	ND	0.42	100.37	0.000	0.003	0.473	1.441	0.618	0.008	0.484	0.000	0.000	0.009	3.036
RRCM2/11	CHR	4	ND	0.34	9.04	61.50	14.68	0.21	13.71	ND	ND	0.32	99.80	0.000	0.008	0.348	1.586	0.401	0.006	0.667	0.000	0.000	0.007	3.023
RRCM2/12	CHR	4	ND	0.43	10.42	56.04	20.39	0.24	11.68	ND	0.12	0.25	99.57	0.000	0.011	0.407	1.469	0.565	0.007	0.577	0.000	0.003	0.005	3.044
RRCM2/13	CHR	4	ND	0.87	6.94	62.94	15.28	0.22	13.39	ND	ND	0.33	99.97	0.000	0.021	0.269	1.639	0.421	0.006	0.658	0.000	0.000	0.007	3.021
RRCM3/2	CHR	4	ND	0.14	9.30	62.51	14.57	0.19	13.88	ND	ND	0.32	100.91	0.000	0.003	0.353	1.593	0.393	0.005	0.667	0.000	0.000	0.007	3.021
RRCM3/3	CHR	4	ND	ND	8.77	63.31	14.01	0.23	13.89	ND	ND	0.28	100.49	0.000	0.000	0.335	1.623	0.380	0.006	0.671	0.000	0.000	0.006	3.021
RRCM3/4	CHR	4	ND	ND	8.74	63.33	14.12	0.24	13.91	ND	0.13	0.28	100.75	0.000	0.000	0.333	1.618	0.382	0.006	0.670	0.000	0.003	0.006	3.018
RRCM3/5	CHR	4	ND	1.83	7.19	61.25	15.79	0.19	13.83	ND	0.13	0.31	100.52	0.000	0.045	0.276	1.579	0.430	0.005	0.672	0.000	0.003	0.007	3.017
RRCM3/6	CHR	4	ND	0.13	8.74	62.23	14.99	0.25	14.00	ND	0.11	0.25	100.70	0.000	0.003	0.334	1.593	0.406	0.007	0.676	0.000	0.003	0.005	3.027
RRCM3/7	CHR	4	ND	0.13	8.05	64.07	14.09	0.27	13.24	ND	ND	0.29	100.14	0.000	0.003	0.310	1.656	0.385	0.007	0.645	0.000	0.000	0.006	3.012
RRCM3/8	CHR	4	ND	0.42	20.17	44.82	21.02	0.23	13.79	ND	0.22	0.18	100.85	0.000	0.010	0.742	1.106	0.549	0.006	0.641	0.000	0.005	0.004	3.063
RRCM3/11	CHR	4	ND	0.34	8.50	62.48	15.35	0.26	13.95	ND	ND	0.39	101.27	0.000	0.008	0.324	1.595	0.414	0.007	0.671	0.000	0.000	0.008	3.027
RRCM3/12	CHR	4	ND	0.95	7.87	61.18	17.43	0.18	13.40	ND	ND	0.36	101.37	0.000	0.023	0.302	1.573	0.474	0.005	0.650	0.000	0.000	0.008	3.035
RRCM3/14	CHR	4	ND	ND	7.88	63.05	14.00	0.21	13.68	ND	ND	0.21	98.73	0.000	0.000	0.308	1.654	0.388	0.006	0.662	0.000	0.000	0.005	3.023
RRCM3/16	CHR	4	ND	0.50	9.24	60.72	15.92	0.21	13.93	ND	0.11	0.35	100.98	0.000	0.012	0.351	1.549	0.430	0.006	0.670	0.000	0.003	0.008	3.029
RRCM3/17	CHR	4	ND	0.20	9.30	61.52	16.47	0.17	13.54	ND	ND	0.30	101.50	0.000	0.005	0.354	1.569	0.444	0.005	0.651	0.000	0.000	0.006	3.034
RRCM3/18	CHR	4	ND	0.25	9.20	61.96	15.03	0.16	13.57	ND	ND	0.44	100.61	0.000	0.006	0.351	1.586	0.407	0.004	0.655	0.000	0.000	0.009	3.018
RRCM3/19	CHR	4	ND	ND	9.36	62.65	14.59	0.20	13.96	ND	ND	0.39	101.15	0.000	0.000	0.355	1.593	0.393	0.005	0.669	0.000	0.000	0.008	3.023
RRCM3/20	CHR	4	ND	1.34	15.86	46.27	23.11	0.26	13.36	ND	0.17	0.20	100.57	0.000	0.032	0.599	1.173	0.620	0.007	0.638	0.000	0.004	0.004	3.077
RRCM3/21	CHR	4	ND	ND	10.02	61.34	14.37	0.22	14.25	ND	ND	0.33	100.53	0.000	0.000	0.381	1.563	0.387	0.006	0.685	0.000	0.000	0.007	3.029
RRCM3/22	CHR	4	ND	0.14	17.12	47.58	22.52	0.28	12.54	ND	0.13	0.22	100.53	0.000	0.003	0.645	1.203	0.602	0.008	0.598	0.000	0.003	0.005	3.067
RRCM3/23	CHR	4	ND	ND	10.28	61.07	14.15	0.23	14.56	ND	ND	0.24	100.53	0.000	0.000	0.390	1.553	0.381	0.006	0.698	0.000	0.000	0.005	3.033
RRCM3/24	CHR	4	ND	0.20	8.67	63.22	14.25	0.27	14.05	ND	ND	0.31	100.97	0.000	0.005	0.330	1.613	0.385	0.007	0.676	0.000	0.000	0.007	3.023
RRCM3/27	CHR	4	ND	0.22	8.46	63.60	14.06	0.28	13.98	ND	0.13	0.28	101.01	0.000	0.005	0.321	1.621	0.379	0.008	0.671	0.000	0.003	0.006	3.014
RRCM3/28	CHR	4	ND	ND	10.25	61.82	13.98	0.23	14.48	ND	ND	0.28	101.04	0.000	0.000	0.386	1.564	0.374	0.006	0.691	0.000	0.000	0.006	3.027
RRCM3/29	CHR	4	ND	0.14	16.89	47.50	22.50	0.23	12.74	ND	0.15	0.19	100.34	0.000	0.003	0.638	1.204	0.603	0.006	0.609	0.000	0.004	0.004	3.071
RRCM3/30	CHR	4	ND	ND	9.95	61.96	14.19	0.24	14.29	ND	ND	0.32	100.95	0.000	0.000	0.376	1.572	0.381	0.006	0.684	0.000	0.000	0.007	3.026
RRCM3/31	CHR	4	ND	1.39	15.73	46.01	22.98	0.26	13.38	ND	0.20	0.15	100.10	0.000	0.034	0.597	1.172	0.619	0.007	0.643	0.000	0.005	0.003	3.080

APPENDIX 5.4 continued

SAMP No.	MINID	OXY	SiO2	TiO2	Al2O3	Cr2O3	FeO	MnO	MgO	CaO	NiO	V2O5	TOTAL	Si	Ti	Al	Cr	Fe2+	Mn	Mg	Ca	Ni	V	SUM
RRCM1/2	CHR	4	ND	ND	9.73	62.04	14.26	0.22	13.68	ND	ND	0.33	100.26	0.000	0.000	0.371	1.589	0.386	0.006	0.660	0.000	0.000	0.007	3.019
RRCM1/3	CHR	4	ND	0.21	8.37	62.40	14.41	0.18	13.59	ND	ND	0.30	99.46	0.000	0.005	0.324	1.620	0.396	0.005	0.665	0.000	0.000	0.007	3.022
RRCM1/4	CHR	4	ND	0.86	6.02	58.99	22.42	0.32	10.57	ND	ND	0.23	99.41	0.000	0.022	0.243	1.596	0.642	0.009	0.539	0.000	0.000	0.005	3.056
RRCM1/5	CHR	4	ND	2.27	15.56	43.23	23.68	0.24	13.31	ND	0.19	0.26	98.74	0.000	0.056	0.599	1.116	0.647	0.007	0.648	0.000	0.005	0.001	3.084
RRCM1/7	CHR	4	ND	0.25	8.25	61.72	14.20	0.19	13.73	ND	ND	0.28	98.62	0.000	0.006	0.321	1.614	0.393	0.005	0.677	0.000	0.000	0.006	3.022
RRCM1/8	CHR	4	ND	1.57	7.90	59.76	15.53	0.20	13.72	ND	ND	0.33	99.01	0.000	0.039	0.308	1.561	0.429	0.006	0.676	0.000	0.000	0.007	3.026
RRCM1/9	CHR	4	ND	0.17	8.83	62.20	14.16	0.24	13.63	ND	ND	0.30	99.53	0.000	0.004	0.340	1.608	0.387	0.007	0.664	0.000	0.000	0.007	3.017
RRCM1/10	CHR	4	ND	ND	7.55	63.53	14.89	0.16	13.72	ND	0.11	0.17	100.13	0.000	0.000	0.292	1.648	0.408	0.005	0.671	0.000	0.003	0.004	3.031
RRCM1/11	CHR	4	ND	0.16	5.95	62.66	19.63	0.27	11.03	ND	ND	0.23	99.93	0.000	0.004	0.237	1.676	0.555	0.008	0.556	0.000	0.000	0.005	3.041
RRCM1/12	CHR	4	ND	1.36	14.26	46.98	23.06	0.25	12.79	ND	0.18	0.22	99.10	0.000	0.034	0.551	1.219	0.633	0.007	0.625	0.000	0.005	0.005	3.079
RRCM1/13	CHR	4	ND	0.90	8.21	61.44	14.94	0.22	13.31	ND	ND	0.27	99.29	0.000	0.022	0.319	1.601	0.412	0.006	0.654	0.000	0.000	0.006	3.020
RRCM1/14	CHR	4	ND	1.69	10.90	50.62	23.37	0.27	12.07	ND	0.18	0.34	99.44	0.000	0.042	0.427	1.331	0.650	0.008	0.598	0.000	0.005	0.007	3.068
RRCM1/15	CHR	4	ND	0.34	7.54	62.16	15.88	ND	13.20	ND	ND	0.24	99.36	0.000	0.008	0.296	1.635	0.442	0.000	0.655	0.000	0.000	0.005	3.041
RRCM1/16	CHR	4	ND	0.15	23.24	40.56	20.34	0.21	14.14	ND	0.19	0.19	99.02	0.000	0.003	0.856	1.002	0.531	0.005	0.658	0.000	0.005	0.004	3.064
RRCM1/17	CHR	4	ND	0.90	6.59	62.20	17.62	0.27	12.29	ND	0.11	0.27	100.25	0.000	0.022	0.258	1.332	0.489	0.008	0.608	0.000	0.003	0.006	3.026
RRCM1/18	CHR	4	ND	0.32	9.34	61.66	14.16	0.21	14.15	ND	ND	0.26	100.40	0.000	0.008	0.367	1.573	0.382	0.003	0.680	0.000	0.000	0.006	3.022
RRCM1/19	CHR	4	ND	3.79	6.22	53.45	23.83	0.30	11.50	ND	0.18	0.32	99.59	0.000	0.096	0.249	1.432	0.676	0.009	0.581	0.000	0.005	0.007	3.055
RRCM1/20	CHR	4	ND	0.16	15.84	47.61	22.43	0.28	12.77	ND	0.15	0.14	99.38	0.000	0.004	0.607	1.225	0.610	0.008	0.619	0.000	0.004	0.003	3.080
RRCM1/21	CHR	4	ND	0.65	16.14	49.65	18.81	0.22	13.75	ND	0.14	0.25	99.61	0.000	0.016	0.608	1.254	0.503	0.006	0.655	0.000	0.004	0.005	3.051
RRCM1/22	CHR	4	ND	0.75	7.00	62.54	15.83	ND	13.05	ND	ND	0.22	99.39	0.000	0.019	0.275	1.648	0.441	0.000	0.648	0.000	0.000	0.005	3.036
RRCM1/23	CHR	4	ND	0.29	8.13	62.07	15.66	0.23	13.64	ND	ND	0.24	100.26	0.000	0.007	0.314	1.606	0.428	0.006	0.665	0.000	0.000	0.005	3.031
RRCM1/24	CHR	4	ND	0.24	7.92	63.27	14.58	0.17	13.13	ND	ND	0.20	99.51	0.000	0.006	0.307	1.647	0.401	0.005	0.644	0.000	0.000	0.004	3.014
RRCM1/25	CHR	4	ND	0.39	8.60	61.62	15.68	0.21	13.30	ND	ND	0.29	100.09	0.000	0.010	0.332	1.594	0.429	0.006	0.649	0.000	0.000	0.006	3.026
RRCM1/26	CHR	4	ND	0.09	7.29	62.76	16.49	ND	12.33	ND	ND	0.17	99.16	0.000	0.002	0.289	1.666	0.463	0.000	0.618	0.000	0.000	0.004	3.042
RRCM1/27	CHR	4	ND	ND	8.46	63.18	13.92	0.26	13.69	ND	ND	0.34	99.85	0.000	0.000	0.326	1.632	0.380	0.007	0.667	0.000	0.000	0.007	3.019
RRCM1/29	CHR	4	ND	1.25	7.51	60.31	17.76	0.21	12.37	ND	0.11	0.27	99.79	0.000	0.031	0.293	1.580	0.492	0.006	0.611	0.000	0.003	0.006	3.022
RRCM1/30	CHR	4	ND	0.35	7.97	62.23	15.36	0.24	12.67	ND	ND	0.27	99.09	0.000	0.009	0.312	1.633	0.426	0.007	0.627	0.000	0.000	0.006	3.020

APPENDIX 5.5

RIVER RANCH CONCENTRATE

CLINOPYROXENES

SAMP No.	MINID	OXY	SiO2	TiO2	Al2O3	Cr2O3	FeO	MnO	MgO	CaO	Na2O	K2O	TOTAL	Si	Ti	Al	Cr	Fe2+	Mn	Mg	Ca	Na	K	SUM
RRCM5/2	CPX	6	54.44	ND	1.70	0.83	2.01	0.11	16.95	23.02	0.89	ND	99.95	1.975	0.000	0.073	0.024	0.061	0.003	0.917	0.895	0.063	0.000	4.011
RRCM5/3	CPX	6	54.45	0.17	1.55	1.73	2.49	ND	17.89	19.85	1.49	ND	99.62	1.978	0.005	0.066	0.050	0.076	0.000	0.969	0.773	0.105	0.000	4.022
RRCM5/4	CPX	6	54.30	ND	1.66	2.80	1.85	ND	16.47	20.69	2.01	ND	99.78	1.977	0.000	0.071	0.081	0.056	0.000	0.894	0.807	0.142	0.000	4.028
RRCM5/5	CPX	6	54.56	ND	2.01	1.21	1.58	ND	16.96	21.95	1.30	ND	99.57	1.982	0.000	0.086	0.035	0.048	0.000	0.918	0.854	0.092	0.000	4.015
RRCM5/6	CPX	6	54.30	ND	2.42	2.42	1.71	ND	15.96	20.42	2.05	ND	99.28	1.981	0.000	0.104	0.070	0.052	0.000	0.868	0.798	0.145	0.000	4.018
RRCM5/7	CPX	6	53.91	ND	2.36	1.84	2.26	ND	16.26	20.82	1.92	ND	99.37	1.971	0.000	0.102	0.053	0.069	0.000	0.886	0.816	0.136	0.000	4.033
RRCM5/8	CPX	6	54.09	0.33	3.10	1.48	2.70	ND	15.97	19.98	2.29	ND	99.94	1.963	0.009	0.133	0.042	0.082	0.000	0.864	0.777	0.161	0.000	4.031
RRCM5/9	CPX	6	54.13	ND	2.36	1.61	1.81	ND	16.33	21.90	1.62	ND	99.76	1.969	0.000	0.101	0.046	0.055	0.000	0.886	0.853	0.114	0.000	4.024
RRCM5/10	CPX	6	53.61	0.11	2.07	0.81	2.98	ND	16.65	21.85	1.04	ND	99.12	1.967	0.003	0.090	0.023	0.091	0.000	0.910	0.859	0.074	0.000	4.017
RRCM5/11	CPX	6	53.51	0.13	2.20	0.98	1.31	ND	17.15	23.27	0.29	ND	99.47	1.952	0.004	0.095	0.028	0.040	0.000	0.932	0.909	0.065	0.000	4.025
RRCM5/13	CPX	6	54.06	0.13	2.80	2.60	1.72	ND	15.48	19.82	2.50	ND	99.11	1.974	0.004	0.121	0.075	0.053	0.000	0.843	0.775	0.177	0.000	4.022
RRCM5/14	CPX	6	54.38	0.20	1.71	1.97	2.44	ND	17.15	19.92	1.66	ND	99.43	1.981	0.005	0.074	0.057	0.074	0.000	0.931	0.778	0.117	0.000	4.017
RRCM5/15	CPX	6	53.70	ND	1.99	1.11	1.47	ND	16.98	23.02	0.98	ND	99.25	1.964	0.000	0.086	0.032	0.045	0.000	0.926	0.902	0.070	0.000	4.025
RRCM5/16	CPX	6	53.99	0.36	1.78	1.28	2.56	ND	17.58	20.32	1.49	ND	99.36	1.971	0.010	0.077	0.037	0.078	0.000	0.956	0.795	0.106	0.000	4.030
RRCM5/17	CPX	6	54.02	ND	2.76	2.26	1.46	ND	15.97	20.78	2.11	ND	99.36	1.967	0.000	0.118	0.065	0.044	0.000	0.867	0.811	0.149	0.000	4.021
RRCM5/18	CPX	6	53.55	0.32	3.31	2.08	2.04	ND	15.40	20.33	2.33	ND	99.36	1.954	0.009	0.142	0.060	0.062	0.000	0.837	0.795	0.165	0.000	4.024
RRCM5/19	CPX	6	54.05	0.19	1.75	2.02	2.32	ND	17.40	20.15	1.66	ND	99.54	1.971	0.005	0.075	0.058	0.071	0.000	0.946	0.788	0.118	0.000	4.032
RRCM5/20	CPX	6	54.49	0.10	1.68	0.95	3.13	ND	20.10	17.73	0.97	ND	99.15	1.975	0.003	0.072	0.027	0.095	0.000	1.086	0.689	0.068	0.000	4.015
RRCM5/21	CPX	6	53.73	0.14	1.96	1.02	1.84	ND	16.78	22.94	1.04	ND	99.45	1.961	0.004	0.084	0.029	0.056	0.000	0.913	0.897	0.074	0.000	4.018
RRCM5/22	CPX	6	53.94	0.14	1.52	0.77	2.55	ND	16.78	23.03	0.82	ND	99.55	1.973	0.004	0.065	0.022	0.078	0.000	0.915	0.902	0.058	0.000	4.017
RRCM5/23	CPX	6	54.06	ND	1.93	1.11	1.53	ND	17.01	22.66	1.09	ND	99.42	1.972	0.000	0.083	0.032	0.048	0.000	0.924	0.886	0.077	0.000	4.022
RRCM5/24	CPX	6	54.78	0.12	2.30	0.99	2.78	ND	19.53	17.39	1.32	0.11	99.32	1.976	0.003	0.078	0.028	0.084	0.000	1.050	0.672	0.092	0.005	4.008
RRCM5/25	CPX	6	53.82	0.13	1.84	0.99	2.44	ND	16.69	22.66	1.05	ND	99.62	1.967	0.004	0.079	0.029	0.074	0.000	0.909	0.887	0.074	0.000	4.023
RRCM5/26	CPX	6	54.10	0.21	1.95	1.11	3.01	ND	19.63	17.61	1.34	ND	98.87	1.971	0.003	0.084	0.032	0.092	0.000	1.066	0.688	0.094	0.000	4.030
RRCM5/27	CPX	6	53.53	ND	2.01	1.17	1.51	ND	16.77	22.96	1.06	ND	99.01	1.964	0.000	0.087	0.034	0.046	0.000	0.917	0.902	0.075	0.000	4.025
RRCM5/28	CPX	6	54.13	ND	1.72	1.08	1.54	ND	16.85	22.97	1.00	ND	99.29	1.979	0.000	0.074	0.031	0.047	0.000	0.918	0.900	0.071	0.000	4.020
RRCM5/29	CPX	6	54.40	0.14	2.01	1.49	2.92	0.14	19.05	17.52	1.50	ND	99.17	1.972	0.004	0.086	0.043	0.088	0.004	1.030	0.681	0.105	0.000	4.013
RRCM5/30	CPX	6	54.30	0.30	2.28	1.09	3.56	0.13	19.04	16.59	1.62	ND	98.91	1.973	0.008	0.098	0.031	0.108	0.004	1.031	0.646	0.114	0.000	4.013
RRCM5/31	CPX	6	53.79	ND	2.03	1.26	1.51	ND	16.75	22.84	1.07	ND	99.25	1.965	0.000	0.088	0.036	0.046	0.000	0.912	0.894	0.076	0.000	4.017
RRCM5/32	CPX	6	54.14	0.18	1.14	2.08	1.88	ND	16.70	21.45	1.54	ND	99.11	1.984	0.005	0.049	0.060	0.058	0.000	0.912	0.842	0.110	0.000	4.020
RRCM5/33	CPX	6	54.08	0.32	1.83	1.35	2.71	ND	17.50	19.73	1.55	ND	99.07	1.976	0.009	0.079	0.039	0.083	0.000	0.953	0.773	0.110	0.000	4.022
RRCM5/34	CPX	6	53.66	0.08	1.94	1.04	1.72	ND	16.91	23.39	0.93	ND	99.67	1.957	0.002	0.083	0.030	0.052	0.000	0.919	0.914	0.066	0.000	4.023
RRCM5/36	CPX	6	53.89	0.14	1.77	0.94	2.57	ND	16.62	22.57	1.01	ND	99.51	1.971	0.004	0.076	0.027	0.079	0.000	0.906	0.884	0.072	0.000	4.019
RRCM5/37	CPX	6	54.19	0.22	1.97	0.87	2.74	0.14	19.06	18.64	1.36	ND	99.19	1.967	0.006	0.084	0.025	0.083	0.004	1.032	0.725	0.096	0.000	4.022

APPENDIX 5.5 continued

SAMP No.	MINID	OXY	SiO2	TiO2	Al2O3	Cr2O3	FeO	MnO	MgO	CaO	Na2O	K2O	TOTAL	Si	Ti	Al	Cr	Fe2+	Mn	Mg	Ca	Na	K	SUM
RRCM5/38	CPX	6	53.78	ND	1.96	1.11	1.53	0.12	16.76	22.87	0.98	ND	99.14	1.967	0.000	0.085	0.032	0.048	0.004	0.914	0.896	0.069	0.000	4.015
RRCM5/39	CPX	6	54.08	0.19	1.91	1.27	3.45	0.13	19.71	17.31	1.32	0.05	99.43	1.960	0.005	0.081	0.036	0.105	0.004	1.065	0.672	0.093	0.002	4.023
RRCM5/40	CPX	6	53.76	ND	2.19	1.28	1.57	ND	16.67	22.79	1.22	ND	99.48	1.963	0.000	0.094	0.037	0.048	0.000	0.907	0.892	0.086	0.000	4.027
RRCM6/1	CPX	6	54.67	0.22	2.67	0.77	4.93	ND	19.31	15.20	1.65	ND	99.42	1.980	0.005	0.114	0.022	0.149	0.000	1.042	0.590	0.116	0.000	4.019
RRCM6/2	CPX	6	54.64	0.34	2.28	0.89	6.61	ND	19.38	16.95	1.45	0.04	98.58	1.973	0.009	0.097	0.025	0.109	0.000	1.043	0.656	0.102	0.002	4.016
RRCM6/3	CPX	6	54.86	0.21	2.55	1.00	4.78	ND	20.30	14.36	1.63	ND	99.69	1.976	0.006	0.108	0.028	0.114	0.000	1.090	0.554	0.114	0.000	4.020
RRCM6/4	CPX	6	54.53	0.17	2.20	1.00	4.18	0.15	20.27	15.56	1.31	0.05	99.42	1.968	0.005	0.094	0.028	0.126	0.005	1.091	0.602	0.092	0.002	4.013
RRCM6/5	CPX	6	54.82	0.21	2.40	1.06	4.50	0.14	20.26	15.08	1.56	ND	100.03	1.968	0.006	0.102	0.030	0.135	0.004	1.084	0.580	0.109	0.000	4.018
RRCM6/6	CPX	6	54.26	0.21	2.22	0.80	4.73	ND	19.40	16.69	1.37	ND	99.68	1.968	0.006	0.095	0.023	0.144	0.000	1.049	0.649	0.097	0.000	4.031
RRCM6/7	CPX	6	54.69	0.29	2.32	0.77	3.49	0.14	19.46	17.02	1.48	ND	99.66	1.971	0.008	0.099	0.022	0.105	0.004	1.045	0.657	0.104	0.000	4.015
RRCM6/8	CPX	6	54.17	0.35	2.37	0.57	4.98	0.14	18.55	16.70	1.60	ND	99.43	1.969	0.009	0.102	0.016	0.151	0.004	1.005	0.650	0.112	0.000	4.018
RRCM6/9	CPX	6	54.24	0.20	2.44	0.88	4.59	0.13	19.57	15.78	1.46	ND	99.29	1.966	0.005	0.104	0.025	0.139	0.004	1.057	0.613	0.102	0.000	4.015
RRCM6/10	CPX	6	54.20	0.32	2.38	1.30	3.53	ND	19.32	16.41	1.69	ND	99.15	1.968	0.009	0.102	0.037	0.107	0.000	1.046	0.639	0.119	0.000	4.027
RRCM6/11	CPX	6	54.18	0.13	1.05	3.56	1.50	ND	16.00	20.32	2.17	ND	98.91	1.990	0.004	0.045	0.103	0.046	0.000	0.876	0.800	0.155	0.000	4.019
RRCM6/12	CPX	6	54.11	0.33	1.75	1.81	3.45	ND	16.81	19.03	1.88	ND	99.18	1.983	0.009	0.076	0.052	0.106	0.000	0.918	0.747	0.134	0.000	4.025
RRCM6/13	CPX	6	54.17	ND	2.41	2.81	1.83	ND	15.78	19.82	2.26	ND	99.08	1.981	0.000	0.104	0.018	0.056	0.000	0.860	0.777	0.160	0.000	4.019
RRCM6/15	CPX	6	54.60	0.16	0.97	3.41	1.70	ND	16.16	20.58	2.06	ND	99.64	1.990	0.004	0.041	0.098	0.052	0.000	0.878	0.804	0.146	0.000	4.013
RRCM6/16	CPX	6	54.15	ND	2.82	1.65	1.94	ND	16.29	20.64	1.90	ND	99.39	1.970	0.000	0.121	0.047	0.059	0.000	0.883	0.805	0.134	0.000	4.019
RRCM6/17	CPX	6	54.44	0.22	2.44	0.93	5.00	ND	19.69	14.76	1.60	ND	99.08	1.978	0.066	0.105	0.027	0.152	0.000	1.066	0.575	0.113	0.000	4.022
RRCM6/18	CPX	6	53.24	0.21	2.33	0.34	2.54	0.16	16.45	24.15	0.38	ND	99.80	1.944	0.006	0.100	0.010	0.078	0.005	0.895	0.945	0.027	0.000	4.010
RRCM6/20	CPX	6	54.23	0.16	0.95	3.13	1.74	ND	16.62	20.69	1.88	ND	99.40	1.982	0.004	0.041	0.091	0.053	0.000	0.905	0.810	0.134	0.000	4.020

APPENDIX 5.6

RIVER RANCH CONCENTRATE MEGACRYSTS

GARNETS

SAMP No.	MINID	OXY	SiO2	TiO2	Al2O3	Cr2O3	FeO	MnO	MgO	CaO	Na2O	TOTAL	Si	Ti	Al	Cr	Fe2+	Mn	Mg	Ca	Na	SUM
RRMGM1/1	GAR	12	41.70	0.84	21.31	1.88	10.06	0.32	18.49	4.87	0.07	99.54	3.013	0.046	1.814	0.108	0.608	0.019	1.991	0.377	0.009	7.985
RRMGM1/2	GAR	12	41.39	0.78	20.70	2.60	9.34	0.29	18.83	5.20	0.07	99.20	3.003	0.043	1.770	0.149	0.566	0.018	2.037	0.405	0.010	8.001
RRMGM1/3	GAR	12	41.65	1.02	20.53	2.53	9.66	0.29	18.48	5.26	0.07	99.49	3.016	0.055	1.752	0.145	0.585	0.018	1.995	0.408	0.010	7.984
RRMGM1/4	GAR	12	41.63	0.77	20.34	3.10	8.65	0.30	19.19	5.23	0.03	99.57	3.003	0.042	1.754	0.177	0.522	0.018	2.033	0.404	0.009	7.992
RRMGM1/5	GAR	12	41.66	0.68	20.83	2.84	9.10	0.26	18.99	4.89	0.05	99.30	3.012	0.037	1.775	0.162	0.550	0.016	2.047	0.379	0.007	7.985
RRMGM1/6	GAR	12	41.33	0.91	20.61	2.70	9.47	0.29	18.85	5.28	0.07	99.51	2.994	0.050	1.759	0.155	0.574	0.018	2.035	0.410	0.010	8.005
RRMGM1/7	GAR	12	41.64	0.92	20.66	2.31	9.34	0.29	18.55	5.16	0.06	98.93	3.024	0.050	1.769	0.133	0.567	0.018	2.008	0.402	0.008	7.979
RRMGM1/8	GAR	12	41.57	0.73	20.90	2.59	9.34	0.30	18.85	4.90	0.06	99.24	3.010	0.040	1.783	0.148	0.566	0.019	2.034	0.380	0.008	7.988
RRMGM1/9	GAR	12	41.58	0.96	20.94	2.06	9.74	0.28	18.43	5.07	0.08	99.14	3.016	0.052	1.790	0.118	0.591	0.017	0.993	0.394	0.011	7.982
RRMGM1/10	GAR	12	41.28	0.92	20.98	2.09	10.00	0.37	18.39	5.20	0.06	99.29	2.998	0.050	1.796	0.120	0.608	0.023	1.990	0.405	0.008	7.998
RRMGM1/11	GAR	12	41.45	0.88	20.52	2.55	9.21	0.29	18.51	5.23	0.05	98.69	3.019	0.048	1.762	0.147	0.561	0.018	2.010	0.408	0.007	7.980
RRMGM1/12	GAR	12	41.48	0.87	21.75	1.15	10.77	0.33	18.13	4.85	0.06	99.39	3.004	0.048	1.857	0.066	0.652	0.020	1.958	0.376	0.009	7.990
RRMGM1/13	GAR	12	41.49	0.95	20.83	2.15	9.84	0.27	18.19	5.21	0.05	98.97	3.018	0.052	1.785	0.124	0.599	0.017	1.971	0.406	0.006	7.978
RRMGM1/14	GAR	12	41.42	0.49	21.08	1.99	9.79	0.30	18.40	5.11	0.05	99.06	3.008	0.050	1.805	0.114	0.594	0.018	1.992	0.397	0.008	7.986
RRMGM1/15	GAR	12	41.61	0.80	19.95	3.50	8.68	0.34	18.79	5.37	0.00	99.04	3.025	0.044	1.709	0.201	0.527	0.021	2.035	0.418	0.000	7.980

CLINOPYROXENES

SAMP No.	MINID	OXY	SiO2	TiO2	Al2O3	Cr2O3	FeO	MnO	MgO	CaO	Na2O	K2O	TOTAL	Si	Ti	Al	Cr	Fe2+	Mn	Mg	Ca	Na	K	SUM
RRMGM2/1	CPX	6	54.28	0.17	2.10	0.94	4.64	0.14	20.52	15.92	1.22	ND	99.30	1.965	0.005	0.090	0.027	0.140	0.004	1.107	0.593	0.086	0.000	4.017
RRMGM2/2	CPX	6	54.39	0.20	2.98	0.90	5.46	ND	20.37	13.04	1.80	ND	99.19	1.961	0.005	0.127	0.026	0.165	0.000	1.100	0.507	0.126	0.000	4.025
RRMGM2/3	CPX	6	54.79	0.23	2.92	0.92	5.05	ND	20.18	13.54	1.73	ND	99.36	1.977	0.006	0.124	0.026	0.152	0.000	1.085	0.523	0.121	0.000	4.014
RRMGM2/4	CPX	6	54.34	0.17	2.17	1.01	4.52	0.14	20.28	15.42	1.28	ND	99.33	1.966	0.005	0.092	0.029	0.137	0.004	1.094	0.598	0.090	0.000	4.015
RRMGM2/5	CPX	6	54.89	0.18	2.30	1.02	4.55	0.13	20.19	14.91	1.47	ND	99.64	1.976	0.005	0.098	0.029	0.137	0.004	1.084	0.575	0.103	0.000	4.011
RRMGM2/6	CPX	6	54.44	0.14	2.31	1.03	4.54	0.13	20.18	14.95	1.47	ND	99.19	1.970	0.004	0.098	0.030	0.137	0.004	1.089	0.580	0.103	0.000	4.015
RRMGM2/7	CPX	6	54.18	0.20	2.59	0.99	4.97	0.15	19.71	13.99	1.65	ND	98.41	1.975	0.006	0.111	0.028	0.152	0.005	1.071	0.547	0.115	0.000	4.010
RRMGM2/8	CPX	6	54.14	0.23	2.83	0.89	5.32	0.16	20.00	13.64	1.74	ND	98.95	1.964	0.006	0.121	0.025	0.162	0.005	1.082	0.530	0.122	0.000	4.017
RRMGM2/9	CPX	6	54.35	0.28	2.58	0.92	5.27	ND	20.08	13.78	1.33	ND	98.89	1.974	0.008	0.110	0.026	0.160	0.000	1.087	0.536	0.115	0.000	4.016
RRMGM2/10	CPX	6	54.22	0.21	2.22	0.78	4.69	0.13	19.39	16.24	1.31	ND	99.19	1.969	0.006	0.095	0.022	0.142	0.004	1.050	0.662	0.092	0.000	4.012
RRMGM2/11	CPX	6	54.33	0.20	2.52	0.80	4.60	0.13	20.24	14.67	1.54	ND	99.03	1.968	0.006	0.108	0.023	0.139	0.004	1.096	0.569	0.108	0.000	4.018
RRMGM2/12	CPX	6	54.11	0.24	2.75	0.90	5.15	0.07	19.77	14.32	1.67	ND	99.08	1.963	0.006	1.118	0.026	0.156	0.005	1.069	0.557	0.117	0.000	4.017
RRMGM2/13	CPX	6	54.00	0.22	2.05	1.09	4.59	ND	20.80	15.19	1.30	ND	99.24	1.961	0.006	0.088	0.031	0.139	0.000	1.126	0.591	0.091	0.000	4.033
RRMGM2/14	CPX	6	54.35	0.27	2.41	0.96	4.99	ND	20.38	14.91	1.45	ND	99.72	1.964	0.007	0.103	0.027	0.151	0.000	1.098	0.577	0.102	0.000	4.029
RRMGM2/15	CPX	6	53.93	0.18	2.25	1.04	4.52	ND	20.38	15.31	1.36	ND	98.97	1.962	0.005	0.096	0.030	0.137	0.000	1.105	0.597	0.096	0.000	4.028

6. RIVER RANCH XENOLITHS

6.1 INTRODUCTION

Kimberlites sample mantle rocks on their way up to the surface. Thus kimberlites are an important source of samples from the continental mantle, which is otherwise inaccessible. The typical kimberlite mantle sample can be sub-divided into three major components, namely peridotite, eclogite and megacrysts (Gurney and Harte, 1980). The macrocryst minerals described in the previous chapter are disaggregated components of these three major components. Pyroxenites can be found as a minor component of the mantle sample and can occur as discrete xenoliths or as intrusive veins in peridotites. Peridotites and eclogites can both be extensively altered by metasomatic processes. Intrusive veins of entirely metasomatic minerals may sometimes cut through peridotites.

The peridotites may be further sub-divided into dunites, harzburgites and lherzolites. Eclogites classify into variants of essentially garnet-clinopyroxene assemblages, modified by the presence of accessory phases such as rutile, kyanite, corundum, ilmenite, phlogopite, sulphides and aluminous spinel. Pyroxenites classify into wehrlite and websterite mineralogies that can have olivine or not. A full megacryst mineral suite would comprise olivine, orthopyroxene, garnet, clinopyroxene, ilmenite, zircon, phlogopite and possibly carbonate (Gurney et al, 1991).

The above suites of mantle rocks is seldom represented at any single kimberlite locality. Wide variations in xenolith abundance and composition can occur even at geographically closely spaced localities. A typical example is the Leicester kimberlite and the Newlands kimberlite which are both close to Barkly West, Northern Cape in South Africa. The former has abundant megacrysts and peridotites whilst the latter has abundant websterites and eclogites together with some peridotites but hardly any megacrysts. Another example is the Roberts Victor kimberlite near Boshoff which has abundant eclogite and scarce peridotites whilst the Kimberly pipes have abundant peridotites and scarce eclogites.

Occasionally xenoliths are found to contain diamonds. Most commonly these are eclogite, less

frequently peridotite and rarely websterite. Diamond inclusion studies broadly confirm this association except that on the basis of diamond inclusion studies, peridotitic diamonds are more common than eclogitic ones world-wide (Gurney, 1989). Diamond inclusion studies at River Ranch (Kopylova et al, 1995) have indicated that 99.3% of those diamonds observed and analysed have compositions indicating an origin from a garnet or chromite harzburgite peridotite. Eclogitic diamond inclusions are very rare indeed at River Ranch. Metasomatic veins or megacryst minerals have never been found to be associated with diamonds word-wide.

In this study focused on economic aspects of the River Ranch kimberlite pipe, it is of interest to study the xenoliths from the aspect of their relevance to the diamond content of the pipe. The source of the River Ranch diamonds has been established as primarily from harzburgite (Kopylova et al, 1995). Furthermore, garnet and chromite macrocrysts derived from harzburgite are a fairly abundant component of the River Ranch kimberlite as evidenced by the study of the concentrate minerals in the previous chapter. The macrocrysts and the diamonds are both presumed to be derived from disaggregated harzburgite and liberated into the kimberlite.

6.2 MANTLE XENOLITH COMPOSITIONS AND GEOTHERMOMETRY

Mantle xenoliths have been found at River Ranch. They are particularly common in the mantle xenolith rich tuffisitic kimberlite breccia in the northern side of the diatreme (Figure 2.4). However all the xenoliths seen so far have been extensively altered by secondary processes to such an extent that no olivine or orthopyroxene has survived. Even the more resistant garnet and clinopyroxene have been altered although remnants have survived in most xenoliths. Chromite also survives but is never more than an accessory mineral.

The majority of the mantle rocks seen in the River Ranch pit are garnet lherzolites. No mantle derived eclogites or websterites have been found. Eight garnet lherzolites were carefully extracted from the weathered kimberlite host rock with the aim of carrying out a preliminary investigation of the equilibration temperature of the rocks to ascertain whether or not they fall within the normal "diamond window" and to compare with the equilibration temperatures of similar rocks from the Kaapvaal Craton. No garnet harzburgites suitable for similar study have

yet been found.

Garnets, clinopyroxenes and where available, chromites were prised from the altered rocks and mounted for electron probe analysis. The results are presented in Appendix 6.1. All the rocks were coarse grained and have abundant pseudomorphs after olivine and orthopyroxene. Five contain garnet, clinopyroxene and chromite, two had chromite only and one had garnet and clinopyroxene only.

It is immediately apparent from Appendix 6.1 that some of the extracted grains of the same mineral in the same rock had different compositions. This is particularly noticeable in the spinels. Chrome-spinels are known to form as secondary breakdown products of mantle peridotites, particularly garnet. The suggestion that some of the analysed chromites have a secondary origin is consistent with the fact that they have TiO_2 contents greater than 0.6 wt%, and ranging up to 3.21 wt%. Differences in compositions can also be seen for clinopyroxene, especially RRXM2 and garnet (RRXM8 and RRXM2). The analysed minerals therefore do not represent equilibrium assemblages in their entirety. In some cases (eg. RRXM2 garnet) where most of the compositions are similar and the most different compositions are in the isolated minority, it can reasonably be expected that an average value, rejecting the outliers, will approximate the equilibrium composition for that mineral in that rock.

Such an approach allows an estimation of equilibration temperature to be made using Mg-Fe exchange between garnet and clinopyroxene (eg. Ellis and Green, 1979), or by virtue of the Ca/(Ca+Mg) ratio of the clinopyroxene (Finnerty and Boyd, 1987), assuming the presence of orthopyroxene in the xenolith. The latter gives a temperature uncorrected for other mineral components such as iron and chromium. This approach is somewhat subjective and imprecise and can only be regarded as a pilot study giving an indication of equilibration temperatures with considerable lack of precision, probably of the order of +/-100°C. Within these limitations, the Mg-Fe exchange reaction at 50kb using Ellis and Green (1979) further depends greatly on whether or not any correction to the total iron determined by electron probe is made to allow for the presence of Fe^{3+}. The Ellis and Green (1979) geothermometer only uses Fe^{2+}.

An attempt to estimate the equilibration temperature, both with and without an Fe^{3+} correction revealed that there are large differences in the two approaches. Using total iron as FeO, the xenolith tempeartures are in the range +/- 1200 - 1300°C at 50kb whilst attempting to make a stoichiometric correction for ferric iron brings the range down to less than 1200°C, and two xenoliths have calculated negative ferric iron contents.

The Ca/(Ca+Mg) ratios in contrast fall very consistently and closely around a value of 0.39 +/- 0.2. This corresponds to a temperature of 1200°C +/- 50°C on the diopside solvus (Finnerty and Boyd, 1987). This is considered to be the least temperature estimate for xenoliths, which are indistinguishable one from the other within the limitations of the data. Temperatures of equilibration of 1200°C for coarse grained garnet lherzolite are unusual for kimberlites of southern Africa but are not unknown. If they sit on a 40mW/m^2 geotherm they would be derived from pressures of +/- 60kb and depths approaching 200km. Alternatively and more probably they are associated with a slightly higher geothermal gradient and derived from shallower depths. Kopylova et al (1995) have reported an archean geotherm of 47mW/m^2 on the basis of diamond inclusion studies. Some relict of this may be evident in the xenolith record at the time of eruption, which would account for the relatively high (1200°C) equilibration temperature reported here.

APPENDIX 6.1

RIVER RANCH XENOLITHS

SAMP.No	MINID	OXY	SiO2	TiO2	Al2O3	Cr2O3	FeO	MnO	MgO	CaO	Na2O	K2O	TOTAL	Si	Ti	Al	Cr	Fe2+	Mn	Mg	Ca	Na	K	SUM
RRXM2/1	GAR	12	40.87	0.37	18.08	7.17	5.70	0.19	20.60	5.92	NA	NA	98.90	2.977	0.020	1.522	0.413	0.347	0.012	2.236	0.462	NA	NA	8.019
RRXM2/2	GAR	12	41.01	0.36	18.02	7.16	5.92	0.24	20.44	5.88	NA	NA	99.03	2.986	0.020	1.546	0.412	0.360	0.015	2.218	0.459	NA	NA	8.016
RRXM2/3	GAR	12	40.73	0.36	18.21	7.10	5.89	0.31	20.46	6.01	NA	NA	99.07	2.966	0.020	1.564	0.409	0.359	0.019	2.221	0.469	NA	NA	8.027
RRXM2/4	GAR	12	40.70	0.38	18.10	7.22	5.89	0.27	20.64	6.09	NA	NA	99.29	2.960	0.021	1.551	0.415	0.358	0.017	2.238	0.474	NA	NA	8.034
RRXM2/5	GAR	12	40.88	0.35	18.08	7.18	5.38	0.23	20.47	5.97	NA	NA	98.99	2.977	0.019	1.552	0.430	0.355	0.014	2.222	0.466	NA	NA	8.018
RRXM2/6	GAR	12	41.14	0.40	18.15	7.27	5.99	0.20	20.49	6.05	NA	NA	99.69	2.978	0.022	1.548	0.416	0.333	0.013	2.210	0.469	NA	NA	8.019
RRXM2/7	GAR	12	40.73	0.39	18.17	7.10	6.03	0.24	20.56	6.02	NA	NA	99.42	2.963	0.021	1.558	0.408	0.367	0.015	2.229	0.469	NA	NA	8.030
RRXM2/8	GAR	12	40.29	0.38	18.42	7.10	6.01	0.22	20.56	6.01	NA	NA	99.62	2.963	0.021	1.572	0.406	0.346	0.013	2.219	0.466	NA	NA	8.024
RRXM2/9	GAR	12	40.84	0.35	18.30	6.88	6.01	0.23	20.48	5.91	NA	NA	99.00	2.974	0.019	1.571	0.396	0.366	0.014	2.222	0.461	NA	NA	8.023
RRXM2/10	GAR	12	41.01	0.36	18.09	7.37	6.07	0.25	20.38	5.99	NA	NA	99.52	5.976	0.020	1.547	0.423	0.368	0.016	2.204	0.466	NA	NA	8.020
RRXM2/11	GAR	12	41.13	0.40	19.78	4.72	6.61	0.23	20.78	5.53	NA	NA	99.24	2.972	0.022	1.684	0.269	0.403	0.014	2.237	0.428	NA	NA	8.029
RRXM2/12	CPX	6	54.33	ND	1.34	0.76	2.73	ND	20.08	19.08	0.66	0.09	99.07	1.975	0.000	0.058	0.022	0.083	0.000	1.088	0.743	0.047	0.004	4.020
RRXM2/13	CPX	6	53.94	0.29	2.36	0.65	5.04	ND	19.24	16.08	1.54	ND	99.14	1.965	0.008	0.101	0.019	0.153	0.000	1.045	0.628	0.109	0.000	4.028
RRXM2/14	CPX	6	54.09	0.30	2.37	1.66	3.33	0.14	19.31	15.81	1.87	ND	98.88	1.964	0.008	0.102	0.048	0.101	0.004	1.045	0.615	0.132	0.000	4.019
RRXM2/15	CHR	4	ND	3.26	7.61	54.27	21.63	0.31	13.29	ND	NA	NA	100.87	0.000	0.081	0.295	1.412	0.595	0.009	0.652	0.000	NA	NA	3.056
RRXM2/16	CHR	4	ND	ND	17.41	54.26	13.42	ND	15.26	ND	NA	NA	100.64	0.000	0.000	0.639	1.331	0.348	0.000	0.706	0.000	NA	NA	3.029
RRXM2/17	CHR	4	ND	0.75	7.91	62.21	15.81	0.29	13.76	ND	NA	NA	101.07	0.000	0.018	0.302	1.596	0.429	0.008	0.665	0.000	NA	NA	3.025
RRXM7/1	GAR	12	41.52	0.26	17.78	7.55	5.68	0.25	20.40	6.31	NA	NA	99.75	3.002	0.014	1.515	0.432	0.343	0.016	2.199	0.489	NA	NA	8.010
RRXM7/2	GAR	12	41.58	0.25	17.93	7.36	5.55	0.26	20.57	6.26	NA	NA	99.73	3.003	0.013	1.526	0.420	0.335	0.014	2.214	0.484	NA	NA	8.009
RRXM7/3	GAR	12	41.55	0.27	18.20	7.35	5.71	0.31	20.51	6.28	NA	NA	100.18	2.990	0.015	1.544	0.418	0.344	0.019	2.200	0.485	NA	NA	8.015
RRXM7/4	GAR	12	41.15	0.24	17.55	7.86	5.60	0.24	20.30	6.31	NA	NA	99.25	2.994	0.013	1.505	0.452	0.341	0.015	2.201	0.492	NA	NA	8.013
RRXM7/5	GAR	12	41.66	0.28	17.67	7.90	5.58	0.31	20.56	6.31	NA	NA	100.72	2.999	0.015	1.499	0.450	0.336	0.019	2.206	0.487	NA	NA	8.011
RRXM7/6	GAR	12	41.09	0.25	17.14	8.34	5.64	0.31	20.54	6.57	NA	NA	99.88	2.982	0.014	1.466	0.478	0.342	0.019	2.221	0.511	NA	NA	8.033
RRXM7/7	GAR	12	41.35	0.28	17.44	8.05	5.35	0.26	20.39	6.41	NA	NA	99.82	2.994	0.015	1.489	0.461	0.342	0.016	2.201	0.497	NA	NA	8.015
RRXM7/8	CPX	6	54.69	ND	1.46	1.54	2.33	ND	19.40	19.09	1.14	ND	99.65	1.981	0.000	0.062	0.044	0.070	0.000	1.047	0.741	0.080	0.000	4.025
RRXM7/9	CPX	6	54.69	ND	1.41	1.60	2.41	ND	19.38	18.90	1.11	ND	99.50	1.983	0.000	0.060	0.046	0.073	0.000	1.047	0.734	0.078	0.000	4.021
RRXM7/10	CPX	6	54.42	ND	1.47	1.47	2.38	0.13	19.66	18.79	0.08	ND	99.40	1.972	0.000	0.063	0.042	0.072	0.004	1.062	0.730	0.076	0.000	4.021
RRXM7/11	CPX	6	54.76	ND	1.42	1.56	2.18	ND	19.45	18.72	1.11	ND	99.20	1.986	0.000	0.061	0.054	0.066	0.000	1.052	0.728	0.078	0.000	4.016
RRXM8/1	GAR	12	41.38	ND	17.48	7.98	6.86	0.31	19.55	6.43	NA	NA	99.99	3.008	0.000	1.498	0.459	0.417	0.019	2.118	0.501	NA	NA	8.020
RRXM8/2	GAR	12	41.16	0.08	17.47	8.40	7.02	0.34	19.57	6.58	NA	NA	100.62	2.981	0.004	1.491	0.481	0.425	0.021	2.113	0.511	NA	NA	8.027
RRXM8/3	GAR	12	41.11	0.08	16.99	8.66	6.70	0.32	19.57	6.74	NA	NA	100.17	2.991	0.004	1.457	0.498	0.407	0.020	2.123	0.526	NA	NA	8.026
RRXM8/4	GAR	12	41.27	0.96	17.78	6.61	7.09	0.28	20.32	5.78	NA	NA	100.32	2.981	0.051	1.513	0.381	0.428	0.017	2.187	0.462	NA	NA	8.020
RRXM8/5	GAR	12	41.01	0.77	17.62	7.01	6.91	0.30	20.29	6.10	NA	NA	100.08	2.972	0.042	1.511	0.402	0.419	0.019	2.192	0.473	NA	NA	8.030
RRXM8/6	GAR	12	41.23	0.92	17.43	6.91	7.06	0.28	20.18	5.96	NA	NA	100.00	2.989	0.050	1.490	0.400	0.428	0.017	2.181	0.460	NA	NA	8.015
RRXM8/7	GAR	12	41.23	ND	16.80	9.07	6.74	0.30	19.24	6.91	NA	NA	100.29	3.002	0.000	1.441	0.522	0.410	0.018	2.088	0.539	NA	NA	8.020
RRXM8/8	CPX	6	54.30	0.30	1.99	1.59	3.20	ND	19.10	17.25	1.65	ND	99.38	1.970	0.008	0.085	0.046	0.097	0.000	1.033	0.670	0.116	0.000	4.025
RRXM8/9	CPX	6	53.92	0.32	2.03	1.61	3.21	ND	19.19	17.13	1.64	ND	99.05	1.965	0.009	0.087	0.046	0.098	0.000	1.042	0.669	0.116	0.000	4.032
RRXM8/10	CPX	6	54.18	0.29	1.85	1.53	3.32	0.15	19.20	17.68	1.58	ND	99.78	1.961	0.008	0.079	0.044	0.101	0.005	1.035	0.686	0.111	0.000	4.030

NA = Not analysed

APPENDIX 6.1 continued

SAMP.No	MINID	OXY	SiO2	TiO2	Al2O3	Cr2O3	FeO	MnO	MgO	CaO	Na2O	K2O	TOTAL	Si	Ti	Al	Cr	Fe2+	Mn	Mg	Ca	Na	K	SUM
RRXM8/11	CPX	6	54.50	0.35	2.10	1.69	3.32	ND	19.11	16.74	1.71	ND	99.52	1.973	0.010	0.090	0.048	0.100	0.000	1.031	0.649	0.120	0.000	4.021
RRXM8/12	CHR	4	ND	2.32	7.33	57.53	19.41	0.24	13.25	ND	0.15	0.39	100.62	0.000	0.057	0.234	1.496	0.534	0.007	0.649	0.000	0.004	0.008	3.039
RRXM8/13	CHR	4	ND	ND	8.52	63.03	14.36	0.25	13.73	ND	NA	NA	100.30	0.000	0.000	0.327	1.621	0.391	0.007	0.666	0.000	NA	NA	3.022
RRXM9/1	GAR	12	40.99	0.08	17.82	7.80	6.63	0.26	19.32	6.19	NA	NA	99.09	2.998	0.004	1.536	0.451	0.406	0.016	2.106	0.485	NA	NA	8.002
RRXM9/2	GAR	12	41.34	0.08	18.00	7.81	6.72	0.32	19.35	6.31	NA	NA	99.93	2.999	0.004	1.540	0.448	0.408	0.002	2.093	0.490	NA	NA	8.002
RRXM9/3	GAR	12	41.44	0.07	18.09	7.70	6.53	0.29	19.67	6.23	NA	NA	100.02	2.999	0.004	1.543	0.441	0.395	0.018	2.122	0.483	NA	NA	8.005
RRXM9/4	GAR	12	41.05	ND	18.16	7.68	6.85	0.30	19.65	6.27	NA	NA	99.94	2.982	0.000	1.555	0.441	0.416	0.018	2.129	0.488	NA	NA	8.029
RRXM9/5	GAR	12	41.55	0.08	18.07	7.78	6.68	0.32	19.41	6.20	NA	NA	100.09	3.006	0.004	1.541	0.445	0.404	0.020	2.094	0.481	NA	NA	7.995
RRXM9/6	GAR	12	41.26	ND	17.97	7.75	6.73	0.35	19.38	6.30	NA	NA	99.77	3.001	0.000	1.541	0.446	0.411	0.022	2.101	0.491	NA	NA	8.013
RRXM9/7	GAR	12	41.20	ND	18.15	7.62	6.71	0.29	19.51	6.37	NA	NA	99.85	2.994	0.000	1.555	0.438	0.408	0.018	2.113	0.496	NA	NA	8.022
RRXM9/8	CPX	6	54.66	ND	1.42	1.19	3.10	0.12	19.78	18.78	0.87	ND	99.62	1.968	0.000	0.060	0.034	0.094	0.004	1.068	0.729	0.061	0.000	4.018
RRXM9/9	CPX	6	55.06	ND	1.37	1.21	2.94	0.13	19.83	18.73	0.88	ND	100.15	1.978	0.000	0.058	0.034	0.088	0.004	1.062	0.721	0.061	0.000	4.006
RRXM9/10	CPX	6	54.50	ND	1.37	1.10	3.00	ND	19.79	18.60	0.85	0.05	99.26	1.978	0.000	0.059	0.032	0.091	0.000	1.070	0.723	0.060	0.002	4.015
RRXM9/11	CPX	6	54.55	ND	1.35	1.15	3.03	0.14	19.71	18.69	0.87	0.05	99.54	1.974	0.000	0.058	0.033	0.092	0.004	1.063	0.725	0.061	0.002	4.012
RRXM9/12	CPX	6	54.77	ND	1.33	1.23	2.89	ND	19.69	18.74	0.83	ND	99.48	1.984	0.000	0.057	0.035	0.087	0.000	1.063	0.727	0.058	0.000	4.011
RRXM9/13	CPX	6	54.90	ND	1.35	1.22	2.99	ND	19.81	18.64	0.90	ND	99.81	1.982	0.000	0.057	0.035	0.090	0.000	1.066	0.721	0.063	0.000	4.014
RRXM9/14	CHR	4	ND	3.21	3.33	57.16	25.76	0.33	10.19	ND	0.14	0.39	100.51	0.000	0.083	0.135	1.555	0.741	0.010	0.522	0.000	0.004	0.009	3.059
RRXM9/15	CHR	4	ND	0.25	6.82	65.49	13.92	0.25	13.50	ND	ND	0.23	100.46	0.000	0.006	0.263	1.695	0.381	0.007	0.659	0.000	0.000	0.005	3.016
RRXM9/16	CHR	4	ND	0.52	12.41	54.43	22.43	0.35	10.19	ND	ND	0.29	100.62	0.000	0.013	0.481	1.414	0.616	0.010	0.499	0.000	0.000	0.006	3.039
RRXM11/1	GAR	12	42.32	0.26	21.23	3.18	6.74	0.25	20.94	5.06	NA	NA	99.92	3.010	0.012	1.779	0.179	0.401	0.015	2.219	0.384	NA	NA	7.999
RRXM11/2	GAR	12	42.07	0.23	21.05	3.14	6.58	0.28	20.37	4.98	NA	NA	99.20	3.012	0.012	1.776	0.177	0.394	0.017	2.227	0.382	NA	NA	7.997
RRXM11/3	GAR	12	42.63	0.20	21.26	3.10	6.62	0.26	21.19	5.01	NA	NA	100.27	3.017	0.011	1.774	0.173	0.392	0.016	2.235	0.380	NA	NA	7.998
RRXM11/4	GAR	12	42.37	0.25	21.21	3.17	6.74	0.29	21.50	4.90	NA	NA	100.43	2.999	0.013	1.769	0.177	0.399	0.017	2.268	0.372	NA	NA	8.014
RRXM11/5	GAR	12	42.36	0.25	21.31	3.19	6.63	0.25	21.38	4.83	NA	NA	100.20	3.001	0.013	1.779	0.179	0.393	0.015	2.258	0.367	NA	NA	8.005
RRXM11/6	GAR	12	42.34	0.24	21.10	3.27	6.73	0.26	21.41	5.01	NA	NA	100.36	3.000	0.013	1.761	0.183	0.399	0.016	2.261	0.381	NA	NA	8.014
RRXM11/7	GAR	12	42.20	0.26	21.12	3.26	6.64	0.62	21.69	4.88	NA	NA	100.01	2.999	0.014	1.769	0.183	0.394	0.016	2.265	0.371	NA	NA	8.011
RRXM11/8	CPX	6	54.40	ND	1.91	0.71	3.14	ND	19.95	17.66	1.06	0.08	98.91	1.978	0.000	0.082	0.020	0.096	0.000	1.082	0.688	0.075	0.004	4.025
RRXM11/9	CPX	6	54.56	0.09	1.92	0.74	3.26	ND	20.11	17.62	1.06	0.06	99.42	1.973	0.002	0.082	0.021	0.099	0.000	1.084	0.683	0.075	0.003	4.022
RRXM11/10	CPX	6	54.66	ND	1.89	0.75	3.30	0.14	19.95	17.72	1.09	0.07	99.57	1.974	0.000	0.080	0.022	0.100	0.004	1.074	0.686	0.076	0.003	4.019
RRXM11/11	CPX	6	54.83	ND	1.90	0.74	3.24	ND	20.04	17.79	1.08	0.07	99.69	1.978	0.000	0.081	0.021	0.098	0.000	1.078	0.688	0.076	0.003	4.023
RRXM11/12	CPX	6	54.57	0.07	1.91	0.70	3.26	ND	19.84	17.85	1.08	0.06	99.34	1.975	0.002	0.081	0.020	0.099	0.000	1.070	0.692	0.076	0.003	4.018
RRXM11/13	CPX	6	54.83	ND	1.83	0.74	3.18	0.14	19.88	17.81	1.07	0.07	99.55	1.979	0.000	0.078	0.021	0.096	0.004	1.070	0.689	0.075	0.003	4.015
RRXM11/14	CPX	6	54.85	ND	1.92	0.71	3.21	ND	19.86	17.77	1.08	0.04	99.44	1.984	0.000	0.082	0.020	0.097	0.000	1.070	0.688	0.076	0.002	4.019
RRXM11/15	CHR	4	ND	ND	9.81	60.89	14.45	0.23	14.35	ND	NA	NA	100.04	0.000	0.000	0.375	1.562	0.392	0.006	0.694	0.000	NA	NA	3.036
RRXM11/16	CHR	4	ND	1.49	7.57	60.92	16.15	0.21	13.68	ND	NA	NA	100.27	0.000	0.037	0.292	0.443	0.006	0.668	0.000	0.000	NA	NA	3.029
RRXM11/17	CHR	4	ND	0.08	9.88	61.56	13.85	0.27	13.74	ND	NA	NA	99.66	0.002	0.379	1.582	0.377	0.007	0.666	0.000	0.000	NA	NA	3.019
RRXM11/18	CHR	4	ND	1.76	9.28	58.07	16.33	0.31	13.97	ND	NA	NA	100.21	0.000	0.043	0.355	1.489	0.443	0.009	0.675	0.000	NA	NA	3.025
RRXM11/19	CHR	4	ND	1.55	2.33	64.63	20.30	0.30	11.66	ND	NA	NA	101.01	0.000	0.040	0.093	1.735	0.576	0.009	0.590	0.000	NA	NA	3.048
RRXM11/20	CHR	4	ND	0.36	8.50	61.80	14.83	0.20	14.08	ND	NA	NA	100.13	0.000	0.009	0.327	1.593	0.404	0.005	0.684	0.000	NA	NA	3.030
RRXM12/14	CHR	4	ND	ND	9.12	61.83	14.38	0.27	13.63	ND	0.10	0.34	99.67	0.000	0.000	0.351	1.596	0.393	0.007	0.663	0.000	0.003	0.007	3.020
RRXM12/15	CHR	4	ND	0.16	11.81	52.54	22.87	0.30	12.12	ND	0.14	0.20	100.14	0.000	0.004	0.459	1.370	0.631	0.009	0.596	0.000	0.004	0.004	3.077
RRXM12/16	CHR	4	ND	0.20	8.86	52.35	13.84	0.29	14.14	ND	0.15	0.24	100.07	0.000	0.005	0.339	1.599	0.375	0.008	0.684	0.000	0.004	0.005	3.019

NA = Not analysed

APPENDIX 6.1 continued

SAMP.No	MINID	OXY	SiO2	TiO2	Al2O3	Cr2O3	FeO	MnO	MgO	CaO	Na2O	K2O	TOTAL	Si	Ti	Al	Cr	Fe2+	Mn	Mg	Ca	Na	K	SUM
RRXM12/17	CHR	4	ND	0.24	8.94	62.73	13.99	0.24	13.73	ND	0.11	0.24	100.22	0.000	0.006	0.342	1.608	0.379	0.007	0.663	0.000	0.003	0.005	3.013
RRXM13/23	CHR	4	ND	2.53	7.50	58.51	16.70	0.28	14.04	ND	NA	NA	99.93	0.000	0.062	0.290	1.516	0.458	0.008	0.868	0.000	NA	NA	3.028
RRXM13/24	CHR	4	ND	0.71	12.38	55.25	18.41	0.17	12.68	ND	NA	NA	100.04	0.000	0.017	0.472	1.414	0.498	0.005	0.612	0.000	NA	NA	3.028
RRXM13/25	CHR	4	ND	ND	13.57	58.31	15.16	0.22	13.67	ND	NA	NA	101.18	0.000	0.000	0.506	1.459	0.401	0.006	0.645	0.000	NA	NA	3.022
RRXM13/26	CHR	4	ND	ND	11.82	58.76	16.21	0.22	12.31	ND	NA	NA	99.73	0.000	0.000	0.453	1.510	0.441	0.006	0.600	0.000	NA	NA	3.017
RRXM14/1	GAR	12	42.48	0.24	21.31	3.09	7.02	0.29	21.08	5.00	NA	NA	100.51	3.006	0.013	1.778	0.173	0.416	0.017	2.223	0.379	NA	NA	8.005
RRXM14/2	GAR	12	42.53	0.24	21.47	3.12	7.10	0.25	21.25	4.99	NA	NA	100.95	2.998	0.013	1.783	0.174	0.418	0.015	2.233	0.377	NA	NA	8.011
RRXM14/3	GAR	12	42.57	0.20	21.47	2.96	6.84	0.29	21.18	4.84	NA	NA	100.35	3.011	0.011	1.790	0.166	0.405	0.017	2.233	0.367	NA	NA	8.000
RRXM14/4	GAR	12	42.53	0.25	21.13	3.62	7.00	0.34	21.07	5.09	NA	NA	101.03	3.001	0.013	1.757	0.202	0.413	2.020	2.216	0.385	NA	NA	8.007
RRXM14/5	GAR	12	42.32	0.19	21.42	3.18	6.83	0.92	21.18	4.99	NA	NA	100.40	2.997	0.010	1.788	0.178	0.404	0.017	2.236	0.379	NA	NA	8.009
RRXM14/6	GAR	12	42.13	0.22	21.39	3.22	7.06	0.23	21.11	4.95	NA	NA	100.40	2.988	0.012	1.788	0.181	0.419	0.019	2.232	0.376	NA	NA	8.015
RRXM14/7	GAR	12	42.01	0.25	21.19	3.39	6.77	0.28	21.10	5.10	NA	NA	100.09	2.988	0.013	1.773	0.190	0.403	0.017	2.238	0.388	NA	NA	8.013
RRXM14/8	CPX	6	54.20	0.32	1.94	0.83	3.19	0.13	19.25	18.28	1.40	ND	99.54	1.963	0.009	0.083	0.024	0.097	0.004	1.039	0.709	0.098	0.000	4.026
RRXM14/9	CPX	6	54.54	0.34	2.34	0.91	3.51	0.14	19.46	17.18	1.59	ND	100.01	1.962	0.009	0.099	0.026	0.106	0.004	1.043	0.662	0.111	0.000	4.022
RRXM14/10	CPX	6	54.36	0.34	2.53	0.92	3.47	0.13	19.37	16.68	1.31	ND	99.44	1.964	0.009	0.109	0.026	0.105	0.004	1.043	0.645	0.113	0.000	4.018
RRXM14/11	CPX	6	54.25	0.37	2.31	0.80	3.36	0.13	19.38	17.45	1.52	ND	99.57	1.961	0.010	0.098	0.023	0.101	0.004	1.044	0.676	0.107	0.000	4.024
RRXM14/12	CPX	6	54.63	0.36	2.49	0.98	3.70	0.15	19.36	16.81	1.60	ND	100.09	1.962	0.010	0.106	0.028	0.111	0.004	1.037	0.647	0.112	0.000	4.017
RRXM14/13	CPX	6	54.26	0.34	2.18	0.79	3.41	ND	19.21	17.67	1.43	ND	99.29	1.968	0.009	0.093	0.023	0.103	0.000	1.039	0.687	0.101	0.000	4.023
RRXM14/14	CPX	6	54.75	0.33	2.08	0.83	3.41	ND	19.31	17.82	1.43	ND	99.96	1.974	0.009	0.088	0.024	0.105	0.000	1.038	0.689	0.100	0.000	4.025
RRXM14/15	CPX	6	54.57	0.33	2.41	0.96	3.67	ND	19.46	16.91	1.60	ND	99.91	1.967	0.009	0.103	0.027	0.111	0.000	1.045	0.530	0.112	0.000	4.027
RRXM14/16	CPX	6	54.30	0.37	2.16	0.81	3.40	ND	19.36	17.45	1.51	ND	99.36	1.968	0.010	0.092	0.023	0.103	0.000	1.046	0.678	0.106	0.000	4.026
RRXM14/17	CHR	4	ND	2.31	7.87	59.54	15.60	0.28	14.61	ND	0.15	0.26	100.62	0.000	0.056	0.300	1.524	0.422	0.008	0.705	0.000	0.004	0.006	3.025
RRXM14/18	CHR	4	ND	0.23	23.98	44.54	16.29	0.30	14.71	ND	0.12	0.29	100.46	0.000	0.005	0.857	1.068	0.413	0.008	0.665	0.000	0.003	0.006	3.025

NA = Not analysed

7. DISCUSSION

7.1 KIMBERLITE PHASES

The main phases of kimberlite at River Ranch are diatreme facies material, within which are preserved isolated blocks of crater facies rocks and late stage hypabyssal intrusive material. The crater facies blocks are concentrated in the eastern and western portions of the diatreme and are not found in the central section at the current level of mining. This is interpreted to support the suggestion that two separate venting episodes are represented, as also a likely consideration from the lobate section of the diatreme at surface (see Figure 2.4).

The sequence of intrusion of the different phases can be summarised as follows:

1. The mantle xenolith-rich phase is interpreted as the oldest. This is so because only relics of it still remain on the edges of the diatreme. It has been replaced by younger phases in the central section of the pipe.

2. The eastern tuffisitic kimberlite was the next intrusive phase. The contact of the eastern tuffisitic kimberlite with the rest of the western phases is curvilinear, (Figure 2.4) suggesting that the western tuffisitic kimberlite and the tuffisitic kimberlite breccia are intrusive into the eastern tuffisitic kimberlite.

3. It is not easy to distinguish the age relationship between the western tuffisitic kimberlite and the tuffisitic kimberlite breccia. The two phases have different groundmass compositions (sections 3.2.1.2 and 3.2.2.2) but their relationship to each other has not been established.

4. The tuff-bearing breccia is younger than both the tuffisitic kimberlite breccia and the western tuffisitic kimberlite. The tuff-bearing breccia is a tuffisitic kimberlite breccia that contains fragments of the sandy/crystal tuff, older kimberlite phases and crustal fragments. The sandy/crystal tuff xenoliths are absent in all of the older intrusive phases.

5. The hypabyssal kimberlite is interpreted as a late stage intrusive phase from the root zone (see Figure 2.5).

7.2 TYPE OF KIMBERLITE (GROUP I OR GROUP II)

Skinner (1988) distinguished Group I and Group II kimberlites by the following mineralogical characteristics:

Group I kimberlites have olivine, monticellite, phlogopite, calcite and serpentine commonly volumetrically abundant. Groundmass spinels and perovskites are typical and primary ilmenite is usually present. Diopside is rare in the matrix of hypabyssal facies kimberlite and where present, it can be attributed to reaction processes associated with inclusions of crustal xenoliths.

Group II kimberlites on the other hand are commonly dominated by primary phlogopite occuring as phenocrysts or within the groundmass. Phenocrysts and/or groundmass diopside may also be present. Groundmass spinels and perovskite if present, are rare and very fine grained. Groundmass ilmenite is not common and monticellite is a rare constituent.

The primary mineralogy characterising the River Ranch kimberlite is olivine (pseudomorphed), monticelllite (also pseudomorphed by calcite), diopside, perovskite, rare phlogopite and groundmass spinels. Diopside is abundant especially in the hypabyssal kimberlite and the eastern tuffisitic kimberlite while ilmenite is absent. This mineralogy is consistent with Group I kimberlites, except that the abundance of diopside in some of the phases is not conformable with Group I mineralogy. The diopside observed is not due to crustal contamination because the diopside laths are matrix minerals and not associated with any crustal xenoliths. Ilmenite is conspicuously absent but the presence of monticellite in reasonable quantities is interpreted to indicate that the River Ranch kimberlite is an ilmenite-free Group I kimberlite.

7.3 DIAMOND CHARACTERISTICS AND GRADE CONTROL

It has been established in this study that there are large quantities of brown diamonds (50.9%) and a lesser proportion of white (26.1%) at River Ranch. The remaining diamonds are mainly grey (21.2%). It has also been established that there are 47.8% fragments in the diamond population. A significant percentage of these are of inferior quality. All these factors when combined, make the River Ranch diamond population of lower than average value. This accentuates grade control as an important function of mine planning if profits are to be realised. A bulk sampling exercise has already been carried out to establish the variation of diamond grades amongst the different kimberlite phases. It has been experienced elsewhere that there is consistency in grade in the diatreme section of kimberlite pipes with depth. This is attributed to considerable mixing of the components during fluidization on emplacement of the kimberlite (Clement, 1982). Changes are only anticipated between the different phases in the diatreme facies rocks. The work that has been done to characterise the phases through surface mapping and petrographic studies will enable physical recognition of these phases as mining progresses. Blending in accordance with different grades can be done. Increasing plant head grade by stockpiling very low grade phases like the sandy/crystal tuff can also be considered as a possibility of maximising returns, when as at present diamond prices are very low.

Pre-production sampling is a necessary function for grade monitoring/control. However large bulk samples are expensive and time consuming to handle. Micro-diamond counts can be used for grade estimation provided there is relationship between the micro-diamond population and the macro-diamonds. It has already been established that more than 99% of the diamonds are of peridotitic paragenesis. The diamonds can therefore probably be treated as a single population. In this case there is a greater likelihood that there is a relationship between the micro-diamonds and the macro-diamond population. If micro-diamonds can be used for grade estimation of macro-diamonds at River Ranch, this would be of major significance in mine planning. A similar exercise proved successful for the Argyle diamond mine (Deakin and Boxer, 1989). In this case microdiamonds were recovered from large diameter core drill samples. Results of this study suggest that investigations of a similar possible relationship at River Ranch is fully justified.

The River Ranch recovery plant consists of a heavy media separation and a rotary pan section. The rotary pan section recovers diamonds from material less than 2mm in size. The operation of the pan section is largely dependent on the availability of fine grained particles and clay in the kimberlite to generate puddle for gravity concentration. As mining progresses, the kimberlite will become fresh and more competent. The result is that less and less fine particles and clay will be liberated from the kimberlite. This gives rise to operational problems for the pan section and may force this section to be made redundant. The available database from this work can be used to decide a cut-off screen for the recovery of economic diamonds in such an eventuality. Terrac plots the amount of stones, of carats and of dollar value per size interval on lognormal graph paper (Figure 4.1, for the River Ranch database). The distribution of the number of stones and of carats, plot as parallel lines as they are moment distributions (Rombouts, 1990). The distribution of the value has a different logarithmic variance and this lognormal curve will not be parallel to the stones and carats distributions. The effect of varying the lower cut-off screen on the quantity and value of the recovered and unrecovered diamonds can easily be assessed on a Terrac lognormal plot. For a given cut-off screen, one can read from the lognormal graphs, how large a proportion of respectively stones, carats and dollars are lost. This can be compared with the ore particle analysis after crushing. For instance the fraction below 2mm can represent up to 80% by volume of the ore, but contains only a negligible part of the diamond value.

7.4 MANTLE MINERAL GEOCHEMISTRY

The River Ranch garnet population is predominantly peridotitic with a very minor eclogitic population. Diamond inclusion studies by Kopylova et al (1995) have also confirmed that eclogite is not a major diamond source at River Ranch. Within the chromite population, both xenocrysts and phenocrysts have been observed. The unusual elevated titanium content in some of the xenocrysts may be attributed to metasomatic effects. In terms of semi-quantitative estimates of the amount of diamonds sampled by the River Ranch kimberlite, the chemistry and proportion of garnets and chromites within the 'diamond in' field or 'diamond inclusion' field is consistent with a medium grade diatreme.

A full chrome-poor megacryst suite as recorded at locations like Monastery (eg. Moore, 1986) does not exist at River Ranch. Ilmenite is absent from the River Ranch megacryst suite and orthopyroxene and olivine, if present, would not have survived the pervasive alteration on the current level of mining. However the River Ranch megacryst clinopyroxene are unlikely to have equilibrated with orthopyroxene due to their unusual correlation shown in Figure 5.8. Estimates of temperatures of equilibration could therefore not be made from the Ca/(Ca+Mg) ratios of the clinopyroxenes. The thickness of the mantle sampled by the River Ranch kimberlite could not be made due to lack of information on temperature and pressure from the megacrysts. As megacryst clinopyroxene are difficult to separate out from the peridotitic clinopyroxene in the concentrate, no temperature estimates could be made from the concentrate clinopyroxene either.

Within the transporting kimberlite magma, redox conditions of the melt can be estimated by analysis of the ilmenite composition. The River Ranch kimberlite is devoid of any ilmenites and this therefore precludes estimation of the degree of resorbtion of the diamonds. Diamond resorbtion can affect the overall grade of any kimberlite in that more than 50% of the original size of the diamond can be lost (Robinson et al, 1989).

7.5 MANTLE XENOLITHS

Mantle xenoliths in kimberlites do not always give representative mineralogy, chemistry and equilibration pressure-temperature conditions within the mantle in which they are derived. This is so because reaction processes between the xenoliths and fluids in the transporting kimberlite magma tend to alter the original chemistry of the rocks. Such effects have been observed in some of the grains from the River Ranch xenoliths. The extent of such alteration depends largely on the duration of the contact between the xenoliths and the magma and the rate of transportation from the mantle to the surface. The transportation rate determines the rate at which pressure and temperature are reduced which in turn will have an effect on mineral reactions in the xenoliths.

Peridotite xenoliths from southern Africa have been divided on the basis of temperature of

equilibration into high and low temperature groups (Harte, 1983, Finnerty and Boyd, 1987). The diving temperature for most peridotite suites is around 1100°C for a geotherm of 40mW/m^2. The majority of high temperature peridotites for kimberlites of southern Africa are deformed although coarse grained examples have been found at Frank Smith, Louwrencia and East Griqualand (Boyd and Nixon, 1979) and at Jagersfontein (Hops et al, 1988). The coarse grained peridotites at River Ranch, although having equilibration temperatures of around 1200°C are unlikely to be high temperature peridotites on the basis of the above mentioned division. They are more likely to be associated with a higher geothermal gradient associated with the Limpopo Mobile Belt than the one associated with the Kaapvaal craton. The higher geotherm has been established at 47mW/m^2 on the basis of diamond inclusion studies by Kopylova et al (1995).

8. CONCLUSIONS

The River Ranch kimberlite is associated with a number of different intrusive episodes which sampled varying quantities of diamonds on their way to the surface. Six intrusive phases have been identified in the diatreme. The phases can be distinguished on the basis of their texture, quantity of xenoliths, type of xenoliths and colour. Petrographic observations, particularly the groundmass mineralogy, confirmed the different phases. The kimberlite is an unusual Group I, which is characterised by the absence of megacrystic and groundmass ilmenite and the presence of groundmass diopside.

Brown diamonds are the most predominant. White and grey diamonds constitute more or less equal proportions. Yellow diamonds are scarce. Pink and green diamonds are extremely rare. There is a high proportion of diamond fragments in the whole population. It is highly unlikely that the fragments are a result of the mining process. Dodecahedral diamonds far outnumber the octahedrals. The overall diamond population has a lower than average value.

The predominance of peridotitic mantle mineral macrocrysts in the kimberlite and the results of diamond inclusion studies by Kopylova et al (1995), all confirm that the kimberlite sampled a predominantly peridotite diamond source. Very little of eclogite diamond source was sampled. The estimated equilibration temperature obtained from the course grained lherzolitic xenoliths is about 1200°C. The high temperatures are most likely to be associated with high geothermal gradients.

ACKNOWLEDGEMENTS

I am grateful to many people for the help, love and encouragement they gave at various stages throughout the duration of this project.

Auridiam Zimbabwe (Pvt) Ltd is thanked for the generous sponsorship of this project. Special thanks go to the senior management, Mr Patrick Harford (Managing Director) and Mr Kevin Dabinett (General Manager) for allowing me the opportunity to carry out this study on River Ranch Diamond Mine. Patrick and Kevin took a special interest in this project and Kevin always generously gave me time off to go to Cape Town.

The Foundation for Research and Development (FRD) is acknowledged for meeting part of my school fees and all my laboratory expenses.

I am really indebted to my supervisor, Prof. John Gurney, for the guidance he gave me throughout the long and tedious, but sometimes enjoyable, course of this project. It was such a privilege to study under John and I leant quite a lot from his wide knowledge and experience related to kimberlites and diamonds. Thanks John.

Dr. Leon Daniels (The DOG) is thanked for helping initiate the project and for his field supervision, useful comments and encouragement.

I am extremely grateful to the Horwood family (my family too!) for the love and encouragement they have always been willing to give. To my special friend, Steve Horwood, thanks for all the good times shared and the numerous things you were always willing to assist me with. To Ingrid Horwood , thank you `mom' and to Tansy , you are wonderful. To the late Reg Horwood, who passed away during the course of my study, I will always miss you.

Paul Zweistra and Dr. Melissa Kirkley introduced me to kimberlite petrography. I leant a great deal from Paul's in-depth knowledge and experience.

A number of staff members in the Geological Sciences Department at UCT gave me assistance in a number of ways. Dick Rckard introduced me to the probe machine, Dave Wilson prepared the petrographic and probe slides, Charles Basson organised the photomicrographs, Neville Buchanan did the copies, Jean Lamb and Nicky Wilson-Harris helped with the administration work and Wolfgang Berg made useful comments and edited the petrography section.

Back home, Lawrence Shumbayaonda helped with digitising the diagrams for the first draft, Irene Mohadi typed the initial draft and Melissa Wray helped organise my data on the computer.

Staff members at Mineral Services, Mike Baumgartner, Mark Buntzen and Anne Westoby are thanked for doing the final maps on the GIS. John Gurney is once again thanked for making the GIS facility available for me.

Lastly but not the least, I thank my mom and dad for the support they gave me throughout my study life. Special thanks to my wife, Cherrie, for the love and for being so patient.

REFERENCES

Allsopp, H.L. , Smith, C.B. , Seggie, A.G. , Skinner, E.M.W. and Colgan, E.A. , 1995. The emplacement age and geochemical character of the Venetia kimberlite bodies, Limpopo Belt, northern Transvaal. *S. Afr. J. Geol.*, **98(3)**: 239-244.

Barton, J.M. Jr , Van Reenen, D.D. and Roering, C. , 1990. The significance of 3000 Ma mafic dykes in the Central Zone of the Limpopo Belt, southern Africa. *Precambrian Res.*, **48**: 299-308.

Bence, A.E. and Albee, A.L. , 1968. Empirical correlation factors for the micro-analysis of silicates and oxides. *J. Geol.* , **76**: 382-403.

Boyd, F.R. and Nixon, P.H. , 1979. Garnet lhezolite xenoliths from the kimberlites of East Griqualand, South Africa. Carnegie Inst. Wash. Yearbook **78**: 488-492.

Clement, C.R. , 1982. A comparative geological study of some major kimberlite pipes in the Northern Cape and Orange Free State. Unpubl. Ph.D. thesis, Univ. of Cape Town. 432pp.

Clement, C.R. and Skinner, E.M.W. , 1985. A textural-genetic classification of kimberlites. *Trans. geol. Soc. South Africa*, **88**: 403-409.

Clifford, T.N. , 1966. Tectono-metallogenic units and metallogenic provinces of Africa. *Earth Planet. Sci. Lett.* , **1**: 421-434.

Coward, M.P. , 1983. Some thoughts on the tectonics of the Limpopo Belt. *Spec. Publ. Geol. Soc. South Africa*, **8**: 75-180.

Cox, K.G. , Johnson R.L. , Monkman, C.J. , Stilman, C.J. , Vail, J.R. , and Wood, D.N. , 1965. The geology of the Nuanetsi Igneous Province. *Philos. Trans. Geol. Soc.*

Daniels, L.R.M. , 1991. Diamonds and associated minerals from the Dokolwayo kimberlite, Kingdom of Swaziland.Unpubl. Ph.D. thesis, Univ. Cape Town, South Africa: 108pp.

Daniels, L.R.M. , 1994. Kimberlite characteristics for exploration in Sub-Saharan Africa. *In*: P. Tromp and T.G. Blenkinsop (Eds). Proceedings of Conference on Sub-Saharan Economic Geology, Harare, Zimbabwe. Spec. Publ. Geol. Soc. Zimbabwe, no. 3. A.A. Balkema, Rotterdam.

Deakin, A.S. and Boxer, G.L. , 1989. Argyle AK1 diamond size distribution: the use of fine diamonds to predict the occurrence of commercial sized diamonds. *In*: Ross, J. (Ed). *Kimberlites and Related Rocks*. Geol. Soc. Austr. Spec. Publ. **14(2):** 1117-1122.

Ellis, D.J. and Green, D.H. , 1979. An experimental study of the effect of Ca upon garnet - clinopyroxene Fe - Mg exchange equilibria. *Contrib. Mineral. Petrol.* , **71**: 13-22.

Finnerty, A.A. and Boyd, F.R. , 1987. Thermobarometry for garnet peridotites: basis for the determination of thermal and compositional structure of the upper mantle. *In*: Nixon, P.H. (Ed), *Mantle Xenoliths*. Wiley and Sons, Chichester: 381-402.

Griffin, W.L. , Gurney, J.J. , Ryan, C.G. , Cousens, D.R. , Sie, S.H. , and Suter, G.F. , 1989. Trapping temperatures and trace elements in P-type garnets in diamonds: a proton microprobe study. Extended Abstract, workshop on Diamonds, 28th Int. Geol.Congr. Washington D.C. : 23-25.

Griffin, W.L. and Ryan, C.G. , 1993. Trace elements in garnets and chromites: Evaluation of diamond exploration targets. *In*: Diamonds: *Exploration, Sampling and Evaluation.* Prospectors and Developers Assoc. Canada, Short course notes: 187-211.

Gurney, J.J. , 1984. A correlation between garnets and diamonds in kimberlites. *In*: Glover, J.E. and Harris, P.G. (Eds.), *Kimberlite occurrence and origin: a basis for conceptual models in exploration.* Univ. Australia, Publication no.*8*: 143-166.

Gurney, J.J. , 1989. Kimberlites and Related Rocks: Their Crust Mantle Setting, Diamonds and Exploration. *In*: Ross, J.R. et al (Eds), *Geol. Soc. Aust. Spec. Publ.* Vol 2, **14:** 935-965.

Gurney, J.J. , Harris, J.W. and Rickard, R.S. , 1979. Silicate and oxide inclusions in diamonds from the Finsch kimberlite pipe 1-15. *In*: Boyd, F.R. and Meyer, H.O.A. (Eds.), *Kimberlites, Diatremes and Diamonds: Their geology, petrology and geochemistry.* A.G.U. , Washington D.C. 399pp.

Gurney, J.J. , Helmstaedt, H. , and Moore, R.O. , 1993. A review of the use and application of mantle mineral geochemistry in diamond exploration. *Pure and Appl. Chem.*, **(65)12**: 2423-2442.

Gurney, J.J. , Moore, R.O. , Otter, M.L. , Kirkley, M.B. , Hops, J.J. and McCandless, T.E. , 1991. Southern African kimberlites and their xenoliths. *In*: Kampunzu, A.B. and Lubala, R.T. (Eds.), *Magmatism in Extensional Structural Settings - the Phanerozoic African Plate.* Springer - Verlag Berlin Heidelberg: 495-536.

Gurney, J.J. and Harte, B. , 1980. Chemical variations in upper mantle nodules from southern African kimberlites. *Philos Trans. R. Soc. Lond.* **A297**: 273-293.

Gurney, J.J. and Switzer, G.S. , 1973. The discovery of garnets closely related to diamonds in the Finsch Pipe, South Africa. *Contrib. Mineral. Petrol.*, **39**: 103-116.

Gurney, J.J. and Zweistra, P. , 1995. The interpretation of major element compositions of mantle minerals in diamond exploration. *Jour. Geochem. Explorat.*, **53**: 293-309.

Harris, J.W. , Hawthorne, J.B. , Oosterveld, M.M. , Wehmeyer, E. , 1975. A classification scheme for diamond and a comparitive study of South African diamond characteristics. *In*: Ahrens, L.H. , Dawson, J.B. , Duncan, A.R. , Erlank, A.J. , (Eds.), *Phys. Chem. Earth.*, **9**. Pergamon, Oxford. 765-783.

Harte, B. , 1983. Mantle peridotites and processes - the kimberlite sample. *In*: Hawkesworth, C.J. and Norry, M.J. (Eds.). *Continental basalts and mantle xenoliths*. Shiva, Cheshire, England: 46-91

Hatton, C.J. , 1978. The geochemistry and origin of xenoliths from the Roberts Victor Mine. Unpubl. Ph.D. thesis, Univ of Cape Town, South Africa. 179pp.

Hawthorne, J.B. , 1975. Model of a kimberlite pipe. *Phys. Chem. Earth,* **9:** 16pp.

Hops, J.J. , Gurney, J.J. , Harte, B. and Winterburn, P. , 1988. Megacrysts and high-temperature nodules from the Jagersfontein kimberlite pipe. *In*: Proc. 4th Int. Kimb. Conf., Perth. Geol. Soc. Australia.

Kopylova, M.G. , Gurney, J.J. and Daniels, L.R.M. , 1995. Mineral inclusions in diamonds from the River Ranch kimberlite (abs). *In*: 6th Int. Kimberlite Conference, Novosibirsk, Russia. Extended Abstr. vol: 289-291.

Kramers, J.O. and Smith, C.B. , 1983. A feasibility study of U-Pb and Pb-Pb dating of kimberlites using groundmass mineral fractions and whole rock samples. *Isotope Geoscience,* **1**: 23-38.

Lawless, P.J. , 1974. Some aspects of the geochemistry of kimberlite xenocrysts. Unpubl. Msc thesis, Univ of Cape Town, South Africa.
London., **A 257**: 71-218

MacGregor, A.M. , 1953. Precambrian formations of tropical Africa. 19th Int. geol. Congr. Algeria Sect., **1**: 39-52

Mason, R. , 1973. The Limpopo Mobile Belt - southern Africa. *Philos. Trans. R. Soc. London.*, **A 273**: 463-485.

McCourt, S. and Vearncombe, J.R. , 1987. Shear zones bounding the Central Zone of the Limpopo Mobile Belt, southern Africa. *J. Struct. Geol.,* **9**: 127-137.

McCourt, S. and Vearncombe, J.R., 1992. Shear zones of the Limpopo Mobile Belt and adjacent granitoid-greenstone terranes: Implications for late Archean collision tectonics in southern Africa. *Precambrian Res.* **55**: 553-569.

Mitchell, R.H. , 1991. Kimberlites and lamproites: Primary sources of diamond. *Geoscience Canada. Vol 18,* **1**: 1-16.

Moore, R.O. , 1986. A study of the kimberlites, diamonds and associated rocks and minerals from the Monastery mine, South Africa. Unpubl. Ph.D. thesis, Univ Cape Town, South Africa. 251pp.

Richardson, S.H. , Gurney, J.J. , Erlank, A.J. and Harris, J.W. , 1984. Origin of diamond in old enriched mantle. *Nature*, **366**: 198-202.

Richardson, S.H. , Harris, J.W. and Gurney, J.J. , 1993. Three generations of diamonds from old continental mantle. *Nature*, **366**: 256-258.

Robinson, D.N. , 1979. Surface textures and other features of diamonds. Unpubl. Ph.D. thesis, Univ. of Cape Town, South Africa.

Robinson, D.N. , Scott, J.A. , Van Niekerk, A. and Anderson, V.G. , 1989. The sequence of events reflected in the diamonds of some southern African kimberlites. In: *Kimberlites and Related Rocks, Vol. 2. Their Mantle/Crust Setting, Diamonds and Diamond Exploration.* Geol. Soc. Aust. , Spec. Publ. no. **14**, Blackwell: 990-1000.

Roering, C. , Van Reen, D.D. , Smit, C.A. , Barton, J.M. Jr , De Beer, J.H. , De Wit, M.J. , Stettler, E.H. , Van Schalkwyk, J.F. , Stevens, G. and Pretorious, S. , 1992. Tectonic model for the evolution of the Limpopo Belt. *Precambrian Res.* , **55**: 539-552.

Rombouts, L. , 1990. Terrac valuation of rough diamonds: A Terraconsult handbook for Terrac software. Terraconsult BVBA, Belgium: 27pp.

Rombouts, L. , 1995. Sampling and statistical evaluation of diamond deposits. *Journal of Geochem. Exp.* **53**: 351-367.

Skinner, E.M.W. , 1988. Contrasting Group II and Group I kimberlite petrology: towards a genetic model for kimberlites. *In*: Proc. 4th Int. Kimb. Conf., Perth. Geol. Soc. Australia. 528-544.

Skinner, E.M.W. and Clement, C.R. , 1979. Mineralogical classification of southern African kimberlites. 129-139. *In*: Boyd, F.R. and Meyer, H.O.A., (Eds.), *Kimberlites, Diatremes and Diamonds: Their geology, petrology and geochemistry.* A.G.U., Washington D.C. 399pp.

Sobolev, N.V. , 1974. Deep seated inclusions in kimberlites and the problem of the composition of the upper mantle. English translation by Brown, D.A. , 1977. A.G.U. Washinton D.C.

Sobolev, N.V. , Lavrent'ev YuG. , Pokhilenko, N.P. and Usova, L.V. , 1973. Chrome-rich garnets from kimberlites of Yakutia and their paragenesis. *Contrib. Mineral. Petrol.* , **40**: 39-52

Treloar, P.J. , Coward, M.P. and Harris, N.B.W. , 1992. Himalayan-Tibetan analogies for the evolution of the Zimbabwean Craton and Limpopo Belt. *Precambrian Res.* , **55**: 571-587.

Wagner, P.A. , 1914. The diamond fields of southern Africa. *Transvaal Leader. Johannesburg.* 355pp.

Watkeys, M.K. , 1979. Explanation of the geological map of the country west of BeitBrige. *Rhodesia Geological Survey Short Report* no. **45**: 96pp.

Watkeys, M.K. , 1984. The Precambrian geology of the Limpopo Mobile Belt north and west of Messina. Unpubl. Ph.D. thesis, Univ. of Witwatersrand, Johannesburg. 349pp.